SHEAR BEHAVIOUR OF BFRP STRENGTHENED RC T-BEAMS

A THESIS SUBMITTED IN PARTIAL FULFILMENT
OF THE REQUIREMENTS FOR THE DEGREE OF

Master of Technology (Research)

in

Structural Engineering

by

SHARMILI ROUTRAY

(Roll No. 612CE3006)

DEPARTMENT OF CIVIL ENGINEERING
NATIONAL INSTITUTE OF TECHNOLOGY, ROURKELA
ROURKELA – 769 008, ODISHA, INDIA
June 2015

SHEAR BEHAVIOUR OF BFRP STRENGTHENED RC T-BEAMS

A THESIS SUBMITTED IN PARTIAL FULFILMENT
OF THE REQUIREMENTS FOR THE DEGREE OF

Master of Technology (Research)

in

Structural Engineering

by

SHARMILI ROUTRAY

Under the guidance of

Prof. K. C. BISWAL
&
Prof. M. R. BARIK

DEPARTMENT OF CIVIL ENGINEERING
NATIONAL INSTITUTE OF TECHNOLOGY, ROURKELA
ROURKELA – 769 008, ODISHA, INDIA
June 2015

DEDICATED
TO MY PARENTS
THE REASON OF WHAT I AM TODAY.
THANKS FOR YOUR GREAT SUPPORT AND CONTINUOUS CARE

Department of Civil Engineering

National Institute of Technology, Rourkela

Rourkela – 769 008, Odisha, India

CERTIFICATE

This is to certify that the thesis entitled, **"SHEAR BEHAVIOUR OF BFRP STRENGTHENED RC T-BEAMS"** *submitted by* ***SHARMILI ROUTRAY*** *bearing Roll No.* ***612CE3006*** *in partial fulfillment of the requirements for the award of* ***Master of Technology (Research)*** *Degree in* ***Civil Engineering*** *with specialization in* ***"Structural Engineering"*** *during 2014-15 session at National Institute of Technology, Rourkela is an authentic work carried out by her under our supervision and guidance.*

To the best of our knowledge, the matter embodied in the thesis has not been submitted to any other University/Institute for the award of any Degree or Diploma.

Prof. K. C. Biswal ***Prof. M. R. Barik***

Date:

Place: Rourkela

ABSTRACT

Deterioration in reinforced concrete structures is a major issue faced by the infrastructures and bridge industries all over the world. Since complete replacement of these structures requires high investment, strengthening has become the suitable solution to modify and improve the performance of the structures. Previously steel plates were used as external reinforcement to strengthen deficient RC structures, but in the last fifteen years or so on, FRP composites have been used to replace steel because of their superior properties. RC T-section is the most common shape of beams and girders in buildings and bridges. Shear failure of RC T-beams is identified as the most disastrous failure mode as it does not give any advance warning before failure. The shear strengthening of RC T-beams using externally bonded (EB) FRP composites has become a popular structural strengthening technique, due to the well-known advantages of FRP composites such as their high strength-to-weight ratio and excellent corrosion resistance.

This study explores the result of an experimental investigation for enhancing the shear capacity of reinforced concrete (RC) T-beams with shear deficiencies, strengthened with Basalt Fiber Reinforced Polymer (BFRP) sheets which are a relatively new and economic alternative to more expensive fibers commonly used in strengthening of RC beams. A total of 22 numbers of concrete T-beams are tested and various sheet configurations and layouts are studied to determine their effects on the shear capacity of the beams. One beam of the beams is considered as control beam, while other beams are strengthened with externally bonded BFRP sheets/strips. To accommodate essential services like electricity cables, natural gas pipes, water and drainage pipes, air-conditioning, telephone lines, and computer network transverse web opening are necessary in modern building construction. Hence, the present study investigates the shear behaviour of RC T-beams with different types of transverse web openings. The various parameters investigated in this study included BFRP amount and distribution, bonded surface, number of layers of BFRP, fiber orientation, transverse web openings of different shape (i.e., circular versus square versus rectangular) and end anchor. The experimental results demonstrated that the use of the new mechanical anchorage scheme comprising of laminated composite plates increases the shear capacity of the beams significantly by preventing the debonding of BFRP sheets, so that the full strength of the BFRP sheets get utilized. An analytical study is also carried out to validate the experimental findings.

ACKNOWLEDGEMENT

First and foremost, praises and thanks to the God, the Almighty, for His showers of blessings throughout my research work to complete the research successfully.

The satisfaction and euphoria on the successful completion of any task would be incomplete without the mention of the people who made it possible whose constant guidance and encouragement crowned out effort with success.

I would like to express my heartfelt gratitude to my esteemed supervisor, Prof. K. C. Biswal for his technical guidance, valuable suggestions, and encouragement throughout the experimental and theoretical study and in preparing this thesis.

Also, I am highly grateful to my esteemed co-supervisor, Prof. Manoranjan Barik who has afforded me continuous encouragement and support to carry out research. His enthusiasm and consistent notation in my works has motivated me to work for excellence.

I express my honest thankfulness to honorable Prof. Sunil Kumar Sarangi, Director, NIT Rourkela, Prof. S.K Sahu, Professor and HOD, Dept. of Civil Engineering, NIT, Rourkela for stimulating me for the best with essential facilities in the department.

I am grateful to the **Dept. of Civil Engineering, NIT ROURKELA,** for giving me the opportunity to execute this project, which is an integral part of the curriculum in M.Tech program at the National Institute of Technology, Rourkela

Many special thanks to my dearest friends Mr. Biswajit Jena, Mr. Raghav Ravi Teja & Miss B. Rohini for their generous contribution towards enriching the quality of the work and in elevating the shape of this thesis.

I would also express my obligations to Mr. R. Lugun & Mr. Sushil, Laboratory team members of Department of Civil Engineering, NIT, Rourkela and academic staffs of this department for their extended cooperation.

This acknowledgement would not be complete without expressing my sincere gratitude to my parents for their love, patience, encouragement, and understanding which are the source of my motivation and inspiration throughout my work.

Lastly, I would like to dedicate my work and this thesis to my beloved parents.

SHARMILI ROUTRAY

TABLE OF CONTENTS

		Page No.
Abstract		i
Acknowledgments		ii
Table of Contents		iii
List of Tables		vii
List of Figures		viii
Abbreviations		xiv
Notations		xv
CHAPTER 1	**Introduction**	**1-5**
1.1	Preamble	1
1.2	Fiber Reinforced Polymer (FRP)	1
1.3	Strengthening using FRP	3
1.4	Objective	5
1.5	Thesis Layout	5
CHAPTER 2	**Review of Literature**	**6-23**
2.1	Brief Review	6
2.2	Strengthening of Reinforced Concrete (RC) Rectangular beams	6
2.3	Strengthening of Reinforced Concrete (RC) T-Beams	16
2.4	Strengthening of Reinforced Concrete (RC) Rectangular and T-Beams with web opening	20
2.5	Critical Observations	22
2.6	Scope of the Present Investigation	23
CHAPTER-3	**Experimental Programme**	**24-56**
3.1	General	24
3.2	Test Specimens	24
3.3	Casting of Specimens	25
3.4	Material Properties	25
3.4.1	Concrete	25
3.4.2	Cement	26
3.4.3	Fine Aggregate	27

3.4.4 Coarse Aggregate 27
3.4.5 Water 27
3.4.6 Reinforcing Steel 28
3.4.7 Detailing of Reinforcement in RC T-beams 28
3.4.8 Fiber Reinforced polymer (FRP) 29
3.4.9 Epoxy Resin 30
3.4.10 Fabrication of BFRP plate for tensile test 30
3.4.11 Determination of Ultimate stress, Ultimate Load & Modulus of Elasticity of BFRP 32
3.4.12 Form Work 33
3.4.13 Mixing of Concrete 34
3.4.14 Compaction of Concrete 34
3.4.15 Curing of Concrete 34
3.4.16 Strengthening of Beams with FRP fabrics 35
3.5 Experimental Set-up For Testing of Beams 37
3.6 Description of Specimens 39
3.6.1 Series A 39
3.6.1.1 BEAM 1 40
3.6.1.2 BEAM 2 40
3.6.1.3 BEAM 3 41
3.6.1.4 BEAM 4 41
3.6.1.5 BEAM 5 42
3.6.1.6 BEAM 6 42
3.6.1.7 BEAM 7 43
3.6.1.8 BEAM 8 43
3.6.1.9 BEAM 9 44
3.6.1.10 BEAM 10 44
3.6.1.11 BEAM 11 45
3.6.1.12 BEAM 12 45
3.6.1.13 BEAM 13 46
3.6.2 Series B 46

3.6.2.1 BEAM 14 46
3.6.2.2 BEAM 15 47
3.6.2.3 BEAM 16 47
3.6.2.4 BEAM 17 48
3.6.2.5 BEAM 18 48
3.6.2.6 BEAM 19 49
3.6.2.7 BEAM 20 49
3.6.2.8 BEAM 21 50
3.6.2.9 BEAM 22 50
3.7 Summary 51
CHAPTER-4 Test Results and Discussions 57-114
4.1 Introduction 57
4.1.1 Series A 57
4.1.2 Series B 58
4.2 Crack Behaviour and Failure Modes 59
4.2.1 Series A 59
4.2.1.1 Control Beam (CB) 59
4.2.1.2 Strengthened Beam 1 (SB1) 60
4.2.1.3 Strengthened Beam 2 (SB2) 61
4.2.1.4 Strengthened Beam 3 (SB3) 63
4.2.1.5 Strengthened Beam 4 (SB4) 64
4.2.1.6 Strengthened Beam 5 (SB5) 65
4.2.1.7 Strengthened Beam 6 (SB6) 66
4.2.1.8 Strengthened Beam 7 (SB7) 67
4.2.1.9 Strengthened Beam 8 (SB8) 68
4.2.1.10 Strengthened Beam 9 (SB9) 69
4.2.1.11 Strengthened Beam 10 (SB10) 70
4.2.1.12 Strengthened Beam 11 (SB11) 71
4.2.1.13 Strengthened Beam 12 (SB12) 72
4.2.2 Series B 73
4.2.2.1 Control Beam 1 (CB1) 73

4.2.2.2 Strengthened Beam 13 (SB13) 74
4.2.2.3 Strengthened Beam 14 (SB14) 75
4.2.2.4 Control Beam 2 (CB2) 76
4.2.2.5 Strengthened Beam 15 (SB15) 77
4.2.2.6 Strengthened Beam 16 (SB16) 78
4.2.2.7 Control Beam 3 (CB3) 79
4.2.2.8 Strengthened Beam 17 (SB17) 80
4.2.2.9 Strengthened Beam 18 (SB18) 81
4.3 Load-deflection history 82
4.3.1 Series A 82
4.3.2 Series B 89
4.4 Load at initial crack 100
4.5 Ultimate Load Carrying Capacity 100
4.5.1 Series A 100
4.5.2 Series B 108
CHAPTER- 5 Analytical Study 115-123
5.1 General 114
5.2 Shear Strength of RC T-Beams Strengthened with FRP Reinforcement using Chen & Teng Model 114
5.2.1 Effective or average stress in the FRP (FRP Debonding) 115
5.2.2 Effective or average stress in the FRP (FRP Rupture) 116
5.3 Analytical Calculations 117
5.4 Comparison of experimental results with analytical predictions 121
CHAPTER- 6 Conclusions 124-126
6.1 Summary 123
6.2 Conclusions 123
6.3 Recommendations for Future Studies 125
References 127-132
Publications 133

LIST OF TABLES

Title of the Table	Page No.
3.1 Nominal Mix Proportions of Concrete	25
3.2 Test Results of Cubes after 28 days	26
3.3 Tensile Yield Strength of Reinforcing Steel bars	28
3.4 Dimension of the Specimens for tensile test	32
3.5 Result of the specimens from tensile test	33
3.6 Beam material properties and test parameters	51
4.1 Ultimate load and nature of failure for various beams	113
5.1 Contribution of FRP to the shear capacity **(V_{FRP})**	121
5.2 Comparisons of experimental and predicted shear strength results	123

LIST OF FIGURES

Title of the Figure	Page No.
1.1 Different Types of FRP	2
1.2 Macroscopic Structure of Fiber & Matrix	3
1.3 Fiber directions in composite materials	4
3.1 Cross-section and reinforcement details of the control beam	29
3.2 Reinforcement Detailing of T- Beam	29
3.3 Specimens for tensile testing of unidirectional BFRP composite	31
3.4 Experimental setup for tensile testing of the specimen in INSTRON universal testing machine	32
3.5 Steel Frame Used For Casting of RC T-Beam	34
3.6 Application of epoxy and hardener on the beam	36
3.7 Fixing of BFRP sheets on the beam	36
3.8 Roller used for the removal of air bubble	37
3.9 Details of the Test setup with location of dial gauges	38
3.10 Experimental Setup for testing of beams	38
3.11 Shear force and bending moment diagram for four point static loading	39
3.12 Model of control beam (CB)	40
3.13 Model of beam with 2 layers of BFRP U-wrap in 0^0 orientation (SB1)	40
3.14 Model of beam with 2 layers of BFRP side-wrap in 0^0 orientation (SB2)	41
3.15 Model of beam with 2 layers of BFRP U-strip in 0^0 orientation (SB3)	41
3.16 Model of beam with 2 layers of BFRP side-strip in 0^0 orientation (SB4)	42
3.17 Model of beam with 2 layers of BFRP U-wrap in 90^0 orientation (SB5)	42
3.18 Model of beam with 2 layers of BFRP side-wrap in 90^0 orientation (SB6)	43
3.19 Model of beam with 2 layers of BFRP U-strip in 90^0 orientation (SB7)	43
3.20 Model of beam with 2 layers of BFRP side-strip in 90^0 orientation (SB8)	44
3.21 Model of beam with 2 layers of BFRP U-strip in 45^0 orientation (SB9)	44
3.22 Model of beam with 2 layers of BFRP U-wrap in 90^0 orientation with end anchorage (SB10)	45

3.23 Model of beam with 4 layers of BFRP U-wrap in 90^0 orientation with end anchorage (SB11) 45
3.24 Model of beam with 2 layers of BFRP U-strip in 90^0 orientation with end anchorage (SB12) 46
3.25 Model of control beam with Circular web openings (CB1) 46
3.26 Model of beam with 4 layers of BFRP U-wrap in 90^0 orientation with Circular web openings (SB13) 47
3.27 Model of beam with 4 layers of BFRP U-wrap in 90^0 orientation with Circular web openings and anchorage system (SB14) 47
3.28 Model of control beam with Rectangular web openings (CB2) 48
3.29 Model of beam with 4 layers of BFRP U-wrap in 90^0 orientation with Rectangular web openings (SB15) 48
3.30 Model of beam with 4 layers of BFRP U-wrap in 90^0 orientation with Rectangular web openings and anchorage system (SB16) 49
3.31 Model of control beam with Square web openings (CB3) 49
3.32 Model of beam with 4 layers of BFRP U-wrap in 90^0 orientation with Square web openings (SB17) 50
3.33 Model of beam with 4 layers of BFRP U-wrap in 90^0 orientation with Square web openings and anchorage system (SB18) 50
4.1 (a) Experimental Setup of CB under four-point loading system 60
(b) Hair line crack started in shear region at a load of 60kN 60
(c) Crack pattern near Right support 60
(d) Crack pattern at ultimate failure 60
4.2 (a) Experimental Setup of beam SB1 under four-point loading system 61
(b) Debonding of BFRP sheet at ultimate load 61
(c) Ultimate failure of beam SB1 by debonding of BFRP sheet followed by diagonal shear crack 61
4.3 (a) Experimental Setup of beam SB2 under four-point loading system 62
(b) Debonding of BFRP sheet at ultimate load 62
(c) Ultimate failure of beam SB2 by debonding of BFRP sheet followed by diagonal shear crack 62

4.4 (a) Experimental Setup of beam SB3 under four-point loading system 63
(b) Hair line crack started in shear region at a load of 75kN 63
(c) Ultimate failure of beam SB3 by debonding of BFRP strip followed by diagonal shear crack 63
4.5 (a) Experimental Setup of beam SB4 under four-point loading system 64
(b) Hair line crack started in shear region at a load of 65kN 64
(c) Ultimate failure of beam SB4 by debonding of BFRP strip followed by diagonal shear crack 64
4.6 (a) Experimental Setup of beam SB5 under four-point loading system 65
(b) Splitting of BFRP sheet started 65
(c) Ultimate failure of beam SB5 by debonding of BFRP sheet followed by diagonal shear crack 65
4.7 (a) Experimental Setup of beam SB6 under four-point loading system 66
(b) Splitting of BFRP sheet started 66
(c) Ultimate failure of beam SB6 by debonding of BFRP sheet followed by diagonal shear crack 66
4.8 (a) Experimental Setup of beam SB7 under four-point loading system 67
(b) Hair line crack started in shear region at a load of 85kN 67
(c) Ultimate failure of beam SB7 by debonding of BFRP strip followed by diagonal shear crack 67
4.9 (a) Experimental Setup of beam SB8 under four-point loading system 68
(b) Hair line crack started in shear region at a load of 70kN 68
(c) Ultimate failure of beam SB8 by debonding of BFRP strip followed by diagonal shear crack 68
4.10 (a) Experimental Setup of beam SB9 under four-point loading system 69
(b) Hair line crack started in shear region at a load of 110kN 69
(c) Ultimate failure of beam SB9 by debonding of BFRP strip followed by diagonal shear crack 69
4.11 (a) Experimental Setup of beam SB10 under four-point loading system 70
(b) Prevention of debonding of BFRP sheet due to Anchoring System 70

(c) Ultimate failure of beam SB10 by tearing of BFRP sheet followed by diagonal shear crack 70
4.12 (a) Experimental Setup of beam SB11 under four-point loading system 71
(b) Prevention of debonding of BFRP sheet due to Anchoring System 71
(c) Ultimate failure of beam SB11 by tearing of BFRP sheet followed by diagonal shear crack 71
4.13 (a) Experimental Setup of beam SB12 under four-point loading system 72
(b) Prevention of debonding of BFRP strip due to Anchoring System 72
(c) Ultimate failure of beam SB12 by tearing of BFRP strip followed by diagonal shear crack 72
4.14 (a) Experimental Setup of CB1 under four-point loading system 73
(b) Hair line crack started in shear region at a load of 50kN 73
(c) Crack pattern at ultimate failure 73
4.15 (a) Experimental Setup of beam SB13 under four-point loading system 74
(b) Initiation of debonding of BFRP sheet 74
(c) Ultimate failure of beam SB13 by debonding of BFRP sheet followed by diagonal shear crack 74
4.16 (a) Experimental Setup of beam SB14 under four-point loading system 75
(b) Initiation of tearing of BFRP sheet 75
(c) Ultimate failure of beam SB14 by tearing of BFRP sheet followed by diagonal shear crack 75
4.17 (a) Experimental Setup of CB2 under four-point loading system 76
(b) Hair line crack started in shear region at a load of 55kN 76
(c) Crack pattern at ultimate failure 76
4.18 (a) Experimental Setup of beam SB15 under four-point loading system 77
(b) Initiation of splitting of BFRP sheet 77
(c) Ultimate failure of beam SB15 by debonding of BFRP sheet followed by diagonal shear crack 77
4.19 (a) Experimental Setup of beam SB16 under four-point loading system 78
(b) Initiation of tearing of BFRP sheet 78
(c) Ultimate failure of beam SB16 by tearing of BFRP sheet 78

4.20 (a) Experimental Setup of CB3 under four-point loading system 79
(b) Hair line crack started in shear region at a load of 58kN 79
(c) Crack pattern at ultimate failure 79
4.21 (a) Experimental Setup of beam SB17 under four-point loading system 80
(b) Initiation of splitting of BFRP sheet 80
(c) Ultimate failure of beam SB17 by debonding of BFRP sheet followed by diagonal shear crack 80
4.22 (a) Experimental Setup of beam SB18 under four-point loading system 81
(b) Initiation of tearing of BFRP sheet 81
(c) Ultimate failure of beam SB18 by tearing of BFRP sheet followed by diagonal shear crack 81
4.23 Load vs. Deflection Curve for CB 82
4.24 Load vs. Deflection Curve for SB1 83
4.25 Load vs. Deflection Curve for SB2 83
4.26 Load vs. Deflection Curve for SB3 84
4.27 Load vs. Deflection Curve for SB4 84
4.28 Load vs. Deflection Curve for SB5 85
4.29 Load vs. Deflection Curve for SB6 85
4.30 Load vs. Deflection Curve for SB7 86
4.31 Load vs. Deflection Curve for SB8 86
4.32 Load vs. Deflection Curve for SB9 87
4.33 Load vs. Deflection Curve for SB10 87
4.34 Load vs. Deflection Curve for SB11 88
4.35 Load vs. Deflection Curve for SB12 88
4.36 Load vs. Deflection Curve for CB1 89
4.37 Load vs. Deflection Curve for SB13 89
4.38 Load vs. Deflection Curve for SB14 90
4.39 Load vs. Deflection Curve for CB2 90
4.40 Load vs. Deflection Curve for SB15 91
4.41 Load vs. Deflection Curve for SB16 91
4.42 Load vs. Deflection Curve for CB3 92

4.43 Load vs. Deflection Curve for SB17 92
4.44 Load vs. Deflection Curve for SB18 93
4.45 Load vs. Deflection Curve for CB vs. SB1 & SB2 & SB3 & SB4 93
4.46 Load vs. Deflection Curve for CB vs. SB5 & SB6 & SB7 & SB8 94
4.47 Load vs. Deflection Curve for CB vs. SB3 & SB7 & SB9 95
4.48 Load vs. Deflection Curve for CB vs. SB1 & SB5 & SB10 95
4.49 Load vs. Deflection Curve for CB vs. SB3 & SB7 & SB12 96
4.50 Load vs. Deflection Curve for CB vs. SB10 & SB11 97
4.51 Load vs. Deflection Curve for CB vs. SB10 & SB11 & SB12 97
4.52 Load vs. Deflection Curve for CB1 vs. SB13 & SB14 98
4.53 Load vs. Deflection Curve for CB2 vs. SB15 & SB16 99
4.54 Load vs. Deflection Curve for CB3 vs. SB17 & SB18 99
4.55 Load at initial crack of beams CB, SB3, SB4, SB7, SB8, SB9 and SB12 100
4.56 Ultimate load carrying capacity of beams CB, SB1 and SB5 101
4.57 Ultimate load carrying capacity of beams CB, SB3 and SB7 101
4.58 Ultimate load carrying capacity of beams CB, SB2 and SB6 102
4.59 Ultimate load carrying capacity of beams CB, SB4 and SB8 103
4.60 Ultimate load carrying capacity of beams CB, SB3, SB7 and SB9 104
4.61 Ultimate load carrying capacity of beams CB, SB5 and SB6 104
4.62 Ultimate load carrying capacity of beams CB, SB7 and SB8 105
4.63 Ultimate load carrying capacity of beams CB, SB5 and SB10 106
4.64 Ultimate load carrying capacity of beams CB, SB10 and SB11 106
4.65 Ultimate load carrying capacity of beams CB, SB7 and SB12 107
4.66 Ultimate load carrying capacity of beams CB, SB10 and SB12 108
4.67 Ultimate load carrying capacity of beams CB1, SB13 and SB14 108
4.68 Ultimate load carrying capacity of beams CB2, SB15 and SB16 109
4.69 Ultimate load carrying capacity of beams CB3, SB17 and SB18 110
4.70 Ultimate load carrying capacity of beams SB13, SB15 and SB17 110
4.71 Ultimate load carrying capacity of beams SB14, SB16 and SB18 111
5.1 Notation for general shear strengthening scheme, Chen and Teng 116

ABBREVIATIONS

ACI	American Concrete Institute
BFRP	Basalt Fiber Reinforced Polymer
CB	Control Beam
CFRP	Carbon Fiber Reinforced Polymer
EB	Externally Bonded
FRP	Fiber Reinforced Polymer
FGPB	Fiber Glass Plate Bonding
GFRP	Glass Fiber Reinforced Polymer
HYSD	High-Yield Strength Deformed
IS	Indian Standard
NSM	Near Surface Mounted
PSC	Portland Slag Cement
RC	Reinforced Concrete
SB	Strengthened Beam

NOTATIONS

A_{st}	Area of Steel
f_{ck}	Characteristic compressive strength of concrete
f_y	Yield strength of steel
V_c	Shear capacity of concrete
V_s	Shear contribution of steel stirrups and bent up bars
V_{frp}	Shear contribution of FRP
V_n	Shear strength of a strengthened RC beam
f_{frp}	Tensile strength of FRP
$\emptyset_{frp}$	Reduction factor for the FRP
β	Angle of fiber orientation with respect to horizontal direction for the left side of the beam
d	Effective depth of beam
S_{frp}	Spacing of FRP strips measured along the longitudinal axis
x_u	Neutral axis depth
f_{cu}	Cube compressive strength of concrete
b	Width of beam
σ_{frp}	Stress in FRP
A_{frp}	Area of FRP
E_{frp}	Modulus of elasticity of FRP
d’	Effective cover
D	Overall depth of the beam
φ	Diameter of the reinforcement
f_y	yield stress of the reinforcement bar
P_u	Ultimate load
λ	Load enhancement ratio
α	Ratio of ultimate load carrying capacity of experimental to analytical results

CHAPTER 1

1 INTRODUCTION

1.1 Preamble

The rapid deterioration of the infrastructures is one of the major issues facing concrete and bridge industry worldwide. The deterioration of these structures are mainly due to ageing, poor maintenance, corrosion, aggressive environmental conditions, poor initial design or construction errors and accidental situations like earthquakes. In the past a large number of structures were constructed using the older design codes which are structurally unsafe according to today's design standards. Since the complete replacement of such deficient structures requires enormous amount of money and time, strengthening has become the suitable way of improving their load carrying capacity and extending their service lives.

The conventional design approaches available are concrete-jacketing and steel-jacketing. The concrete-jacketing makes the existing section large and thus improves the load carrying capacity of the structure. But these techniques have several demerits such as construction of new formworks, additional weight due to enlargement of section, high installation cost etc. The steel-jacketing has proven to be an effective technique to enhance the performance of structures, but this method requires difficult welding work in the field and have potential problem of corrosion which increases the cost of maintenance. Now-a-days, FRP composite materials are an excellent option to be used as external reinforcement because of their high specific stiffness, high specific weight, high tensile strength, light weight, resistance to corrosion, high durability and ease of installation.

1.2 Fiber Reinforced Polymer (FRP)

FRP composites are, as the name proposes, a composition of two or more materials which, when suitably united, form a different material with properties not available from the individual ingredients.

Fiber reinforced composite materials consist of fibers of high tensile strength and adhesive that binds the fibers together to produce the structural material. Commonly used fibers are aramid, basalt, carbon and glass in the civil engineering industry. The adhesive that is commonly used is epoxy which protects the fibers, providing durability and under the loading

condition distributes the load to the fibers. The fibers are oriented in the direction(s) that utilize them most efficiently. The successful application of FRP in different fields like aerospace, sports, recreation and automobile industries is the reason for the increase in demand of FRP. The properties of FRP composites and their versatility have resulted in significant efficiency, reliability and cost effectiveness in rehabilitation.

Figure 1.1 Different Types of FRP

The following are advantages and disadvantages of FRP composite.

Advantages of FRP

1. Corrosion Resistance.
2. Lightweight.
3. Ease of installation.
4. Less Finishing and maintenance.
5. High fatigue resistance.
6. Ductility of FRP wrapped members improves extensively.
7. They are perfect for external application.
8. They are durable both environmentally and from service point of view.
9. They are available in various forms: sheets, plates, fabric, etc.
10. They are available in long lengths that eliminate joints.
11. They cure within 24 hours.
12. Versatile in nature.

Disadvantages of FRP

1. High cost, susceptibility to deformation under long-term loads.
2. Temperature and moisture effects, lack of design standards, and most importantly, lack of awareness.

Among various types of FRPs, mostly used FRP materials are carbon and glass fibers. Though the strength of carbon fiber is very high, but it is more expensive as compared to other types of fibers. Glass fiber is less expensive as compared to carbon fiber, but it was proven to be less effective and less durable against corrosive medium. Hence, to overcome all of these disadvantages basalt fiber have been used in the present research work. The cost of glass and basalt fibers is nearly same. Basalt fiber exhibits high corrosion resistant and chemical durability towards corrosive medium, such as salts, acid solutions and alkalis. It has also higher thermal ability as compared to glass fibers.

1.3 Strengthening using FRP

Concrete beams are the main element in structural engineering which are designed to carry both horizontal loads due to seismic or wind and vertical gravity loads. Like all other concrete elements they are susceptible for situations where there is an increase in structural loads. Generally reinforced concrete (RC) beams fail in two ways: flexure failure and diagonal tension (shear) failure. Flexural failure is generally preferred to shear failure as the former is ductile while the latter is brittle. A ductile failure permits stress redistribution and gives prior notice to occupants, whereas a brittle failure is sudden and thus catastrophic.

The use of external FRP reinforcement may be classified as: flexural and shear strengthening.

Flexural strengthening using FRP

For flexural strengthening the laminates of FRP are used and applied with epoxy to the tension zone of the RCC members which acts as external tension reinforcements to increase the flexural strength of the RCC members.

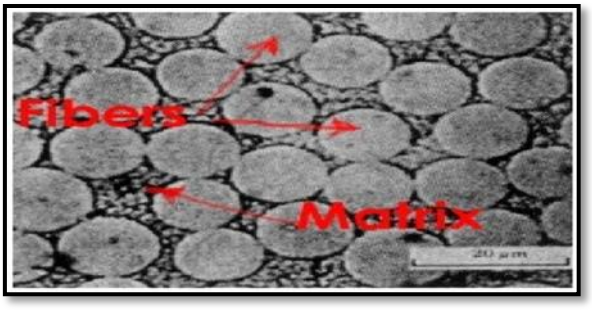

Figure 1.2 Macroscopic Structure of Fiber & Matrix

Structural members like beams, plates and columns can be strengthened in flexure through the use of FRP composites bonded to their tension zone using epoxy as a common adhesive

for this purpose. The direction of fibers is kept parallel to that of the direction of high tensile stresses. Both prefabricated FRP strips and sheets are used.

Shear strengthening using FRP

When the RC beam is deficient in shear, or when its shear capacity is less than the flexural capacity after flexural strengthening, shear strengthening must be considered. It is critically important to assess the shear capacity of RC beams which are proposed to be strengthened.

To enhance the shear capacity of the beams, both composite sheets and plates can be used, but the former one is more appreciable because of their flexible nature and ease of application and handling. Various FRP bonding schemes may be used to improve the shear capacity of RC beams. These include (1) side bonding (bonded to the sides of the beams only) (2) U jacketing (bonded to the sides and tension face of the beam) and (3) wrapping (bonded around the whole cross section of the beam). As RC T-section is the most popular shape of beams and girders in buildings and bridges, complete wrapping is not a feasible alternative.
Fibers may be unidirectional or bidirectional as shown in figure 1.3. The use of fibers in two directions can obviously be favourable with respect to shear resistance even if strengthening for reversed loading is not required, except for unlikely case in which one of the fiber directions is exactly parallel to the shear cracks.

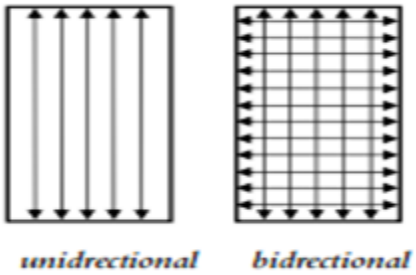

Figure 1.3 Fiber directions in composite materials

In spite of the improved properties of FRP, a structure strengthened with FRP can fail too early causing debonding of the FRP. Therefore, the FRP does not achieve its full strength. In order to prevent the premature failure of the FRP composite, various anchoring systems such as U-jacketing, mechanical fastening, spike anchors and hybrid anchoring techniques are developed. Depending on the application, each type of anchor has caused some improvement in delaying premature debonding, but the problem has not been satisfactorily solved yet.

These drawbacks have opened up a new area of research on development of anchorage system.

1.4 Objective

The main objectives of the present research work may be summarized as follows:

- To analyse the structural behaviour of T-section RC beams under static loading condition.
- To investigate the shear behaviour and modes of failure of shear deficient RC T-beams strengthened with FRP composite sheets.
- To examine the effect of different parameters such as number of layers, bonding surface, different fiber orientation etc. on the shear capacity of the RC T-beams.
- To study the effect of strengthening with externally bonded FRP on the enhancement of strength in RC T-beams with web openings of different cross-section.
- To investigate the effect of an anchorage scheme on the improvement of shear capacity of the RC T-beams.

1.5 Thesis Layout

The current thesis comprises of six chapters.

The general introduction to strengthening of reinforced concrete (RC) beams and its importance in today's construction industry along with the objective of the present research work are reported in chapter 1.

A review of literature on strengthening of reinforced concrete beams are presented in chapter 2. The critical observations on earlier published works are emphasized and the scope of the present research work is reported.

Chapter 3 represents the description of the experimental program. A brief description of test set-up is illustrated and the testing procedure is discussed.

Chapter 4 contains the test results and discussion. The observed crack patterns and failure modes are described.

Chapter 5 discusses the analytical procedure for computing the shear capacity of the strengthened beams.

The significant conclusions and the recommendation for future extension of the present research work are outlined in chapter 6.

A list of important references cited in the present thesis is presented at the end.

CHAPTER 2

2 REVIEW OF LITERATURE

2.1 Brief Review

The rapid deterioration of infrastructure is becoming a principal challenge facing construction industries worldwide. The renewal policies applied to deteriorate structures comprise of complete replacement and rehabilitation. Since the complete replacement of structures involve a huge investment and time, rehabilitation becomes the suitable way for renewal of deteriorated structures. Fiber reinforced polymer (FRP) is the popular retrofitting material which have shown great promise in rehabilitation of the existing reinforced concrete (RC) structures and strengthening of new structural members.

An extensive survey of literature pertaining to the objectives outlined in the previous chapter is presented. The major achievements and results reported in the literature are emphasized. The survey of literature has been partitioned into several sections in order of their relevance to the present study. They are as follows:

- Strengthening of Reinforced Concrete (RC) Rectangular beams
- Strengthening of Reinforced Concrete (RC) T-beams
- Strengthening of Reinforced Concrete (RC) Rectangular and T-beams with web opening

2.2 Strengthening of Reinforced Concrete (RC) Rectangular beams:

Ghazi et al. (1994) examined the shear behaviour of reinforced concrete (RC) beams strengthened using fiber glass plate bonding (FGPB) to study the structural and non-structural cracking behaviour due to various causes. The shear deficient beams were damaged to a certain level (up to the appearance of first shear crack), then they were repaired by using fiber glass plate bonding (FGPB) techniques. To upgrade the shear capacity of the beams different shear repairing schemes were used, such as, FGPB repair by shear strips, by shear wings and by U-jacketing in the shear regions of the beams. The test result illustrated that there is almost identical increase in the shear capacity for both strip and wings shear repairs and these two schemes were not adequate to cause repaired beams to fail in flexure.

Varastehpour and Hamelin (1997) studied the application of composite materials in civil engineering by strengthening of a reinforced concrete beam in situ using externally bonded fiber reinforced polymer (FRP). For design purpose it is very important to study mechanical properties of the interface and the rheological behaviour of composite materials. A new test was suggested to determine experimentally the mechanical properties of the concrete/glue/plate interface. Based on the equilibrium of forces and compatibility of deformation an iterative model capable of simulating the bond slip and material non-linearity was developed to predict the ultimate forces and deflections. A series of large scale beams strengthened with FRP were tested up to failure. To study the efficiency of the externally bonded plate load-deflection values were recorded and compared with the predicted values to verify the test results.

Norris et al. (1997) presented experimental and analytical studies on the behaviour of damaged reinforced concrete beams (RC) strengthened with epoxy bonded carbon fiber reinforced plastic (CFRP) sheets to the tension face of the beams to enhance their flexural capacity. The beams were fabricated, loaded beyond the concrete cracking strength, and strengthened with various CFRP configurations. The effect of different orientations of CFRP with reference to the axis of the beam on the strength and stiffness of the beams was considered. The experimental results showed that there is a considerable increase in strength and stiffness of the existing concrete structures by using CFRP sheets in the tension face and web of the concrete beam depending upon the various orientations of fiber.

A comprehensive design approach complied with Canadian Concrete Standard for slabs and reinforced concrete flexural beams strengthened with externally bonded fiber reinforced plastic (FRP) plates was studied by Chaallal et al. (1998). The design approach was separated into two parts. The first part described the analytical model for flexural strengthening which include two families of failure modes: classical modes (such as tensile failure of laminate and crushing of concrete in compression) and premature modes (such as ripping off of the concrete cover and debonding of the plate). The second part explained the derivation of design equations to enable computation of the required cross-sectional area of shear lateral FRP plates or strips for various plating patterns: vertical strips, inclined strips, U-sheet jackets and wings.

The flexure and shear behaviour of full-scale reinforced concrete (RC) beams retrofitted with fiber reinforced polymer (FRP) laminates was studied by Kachlakev and McCurry (2000).

Out of four numbers of beams, one beam was considered as control beam and the rest three beams were strengthened with various configurations of CFRP and GFRP composites to simulate the retrofit of the existing structure. To enhance the flexural capacity unidirectional CFRP sheets were used and unidirectional GFRP sheets were used to mitigate the shear failure. Load, deflection and strain data were obtained by conducting four-point bending test. The test results showed that there is a significant increase in the static capacity by the use of FRP composites for structural strengthening compared to control section. For all the beams load at first crack and post cracking stiffness were enhanced primarily by using flexural CFRP. The ultimate deflections were found to be 200% higher than the pre-existing shear deficient beam.

An experimental investigation was conducted by Khalifa et al. (2000) to examine the shear behaviour and failure modes of reinforced concrete (RC) beams externally strengthened with carbon fiber reinforced polymer (CFRP) sheets. A total of twenty-seven numbers of full scale RC beams were cast and tested up to failure. Various parameters studied in the experimental programme included steel stirrups, shear span to depth ratio, CFRP amount and distribution, bonded surface, fiber orientation and end anchor. The effectiveness of CFRP reinforcement in the enhancement of the shear capacity of RC beams (both rectangular and T-cross section) in negative and positive moment regions was also studied in this research work. The test result indicated that the use of CFRP sheets as an external reinforcement in enhancing the shear capacity of RC beams is significant and dependent upon the various test parameters investigated.

The effect of shear strengthening of RC beams using different configurations of CFRP on the stress distribution, ultimate strength, initial crack and crack propagation was studied experimentally by Alex et al. (2001). The general and regional behaviour of concrete beams strengthened with CFRP sheets were studied with the help of strain gauges and the appearance of the first crack and the crack propagation in the structure up to failure was monitored.

Duthinh and Starnes (2001) examined seven numbers of concrete beams which were reinforced with steel internally and with CFRP laminate externally applied after the concrete had cracked under four-point bending. The test results illustrated that the use of FRP as external reinforcement was very effective for flexural strengthening. With the increase of amount of steel, there was a decrease in the additional strength provided by CFRP. The

beams reinforced with both steel and carbon had adequate deformation capacity with their brittle mode of failure compared to a beam reinforced heavily with steel only. Clamping or wrapping of the ends of the FRP laminate combined with adhesive bonding was effective in anchoring the laminate.

Sheikh et al. (2002) examined the behaviour of damaged specimens which were repaired with glass and carbon fiber reinforced polymer (GFRP and CFRP) sheets and wraps, tested upto failure. The experimental programme consisted of testing of three wall-slab specimens and two beams. From the experimental work it was observed that fiber reinforced polymers (FRP) were found to be more effective in strengthening for flexure as well as shear. Various analytical models were used to simulate experimental behaviour of the specimens.

Sheikh (2002) studied the effectiveness of the application of FRP in damaged concrete structures in enhancing their structural performance both in terms of strength and ductility. The structural components considered for the experiment include slabs, beams, columns and bridge culverts. Research on columns mainly focused on enhancing their seismic resistance by confining them with FRP. All the tested specimens were considered as full-scale to two-third scale models of the structural components. The test results showed that retrofitting with FRP can be a suitable alternative to the traditional techniques.

The shear behaviour and failure modes of the rectangular simply supported reinforced concrete (RC) beams with shear deficiencies was investigated by Khalifa and Antonio (2002). A total of twelve numbers of RC beams were tested to fail in shear and the parameters considered throughout the experimental programme included steel stirrups, shear span to effective depth ratio as well as amount and distribution of CFRP. The test results illustrated that there is a significant enhancement in the shear capacity of beams by using externally bonded CFRP composite. The contribution of CFRP to the shear capacity was found to be more effective for beams without shear reinforcement than for beams with adequate shear reinforcement and also the contribution of externally bonded CFRP to the shear capacity was influenced by shear span-to-depth ratio.

Chen and Teng (2003) studied about the shear capacity of FRP strengthened RC beams which illustrated that the strengthened beams fail in shear mainly in one of the two modes, i.e., FRP debonding and FRP rupture. A simple, accurate and rational design proposal was developed in this study for the shear capacity of FRP strengthened beams which fail by FRP debonding.

Existing strength proposals were revised with their highlighted deficiencies and based on a rational bond strength model between FRP and concrete, a new shear strength model was established for debonding failures in FRP shear strengthed RC beams. This new model clearly identifies the non-uniform stress distribution in the FRP with a shear crack as determined by the bond strength between the FRP strips and the concrete.

Hadi (2003) carried out an experimental investigation to examine the enhancement in the strength and load carrying capacity of reinforced concrete (RC) beams, those had been failed in shear. The experimental programme consisted of sixteen beam specimens which were retrofitted with different types of fiber reinforced polymer (FRP) and then retested. Load, deflection and strain data were obtained during the four point static loading testing of the wrapped beam specimens up to failure. The test results indicated that the use of FRP composites for shear strengthening enhances the static capacity significantly and there are various parameters which influence the strength of the beams.

Taljsten (2003) examined the method of shear strengthening of concrete structures by unidirectional CFRP composite sheets. Various traditional strengthening techniques were briefly studied then the design procedure for shear strengthening using CFRP composite was described along with the tests on beams strengthened in shear using CFRP sheets. The test results revealed the importance of considering the principal directions of the shear crack in relation to the unidirectional fiber and also the field application indicated that it is easy to use CFRP fabrics to strengthen existing structures for shear.

Rabinovitch and Frostig (2003) carried out an experimental and analytical investigation to study about the strengthening, upgrading and rehabilitation of existing reinforced concrete structures using externally bonded composite materials. The stress concentration that arises near the edge of the fiber reinforced plastic strips, the failure modes caused by these edge effects and the means for the prevention of such modes of failure were mainly emphasised. Out of five beams, three beams were tested with different edge configurations which include wrapping the edge region with vertical composite straps and special form of the adhesive layer at its edge. The remaining two beams were preloaded upto failure before strengthening and the ability to rehabilitate members that endured progressive or even total damage was studied. The test results indicated that there is a significant enhancement in the strength and serviceability of the tested beams and also established that this method is appropriate for the rehabilitation of severly damaged structural members.

The shear strengthening of reinforced concrete (RC) beams using FRP composites was studied by Teng et al. (2004). Externally bonding of FRP sheets/strips is new technique for the shear strengthening of RC beams which deliver extra FRP web reinforcement. A large amount of research works have been conducted on this new technique over the last decades, which has established its effectiveness and has led to a good understanding of the behaviour and strength of shear strengthened beams. In this study the methods of strengthening were described along with a summary of experimental observations of failure modes. By comparing the test results the accuracy of existing design provisions was investigated and the limitations of existing experimental and theoretical studies were highlighted.

Santhakumar et al. (2004) presented a numerical study by using ANSYS sortware to simulate the performance of retrofitted reinforced concrete (RC) shear beams. The study was carried out on the unretrofitted RC beam designated as control beam and RC beams retrofitted with carbon fiber reinforced plastic (CFRP) composites in $\pm 45^{o}$ and 90^{0} fiber orientations. A quarter of the beam was used for modelling by taking advantage of the symmetry of the beam and loadings. The effect of retrofitting on uncracked and precracked beams was studied and the load-deflection plots were also obtained. The numerical results obtained were validated with the experimental findings reported by Tom Norris et al. (1997) and the numerical results showed a good agreement with the experimental values. The crack formation and propagation in case of retrofitted beams in which the crack patterns cannot be seen by the experimental study due to wrapping of CFRP composites can be tracked with the help of this numerical modelling.

Cao et al. (2005) examined the shear behaviour of reinforced concrete (RC) beams with bonded fiber reinforced polymer strips. The beam can be strengthened using various configurations: complete wrapping, U jacketing and side bonding. The strengthened beams generally failed in shear in one of the two modes: FRP debonding and rupture. The FRP debonding mode governs in almost all beams with side strips and U jackets, while FRP rupture mode governs in all beams with complete FRP wraps and some beams with U jackets. This study presented an experimental inveastigation on the debonding failure state by testing eighteen number of beams. The distribution of strains in the FRP strips intersected by the critical shear crack along with the shear capacity of debonding was focused and a simple model was proposed to predict the contribution of FRP to the shear capacity of the beam at the complete debonding of the critical FRP strip.

The shear strengthening of RC deep beams with externally bonded FRP systems was investigated by Islam et al. (2005). Six identical beams were fabricated, out of which one beam was tested in its virgin condition to serve as reference and the remaining beams were strengthened with carbon fiber wrap, strip or grids and tested up to failure. The test results indicated that by the use of a bonded FRP system there is a much slower growth of the critical diagonal cracks and enhancement in the load carrying capacity of the beam. FRP grids placed in normal orientation were found to be the most effective system as long as the material used in strengthening is concerned and the other systems were also found to be almost equally effective.

The coupling of shear-flexural strengthening of RC beams using CFRP sheets was investigated experimentally by Al-Amery and Al-Mahaidi (2006). Six number of RC beams were tested with various combinations of CFRP sheets and straps in addition to a strengthened beam as control test. The instrumentation used for the strain measurements in different CFRP layers and for the slip measurements occurring between the CFRP sheets and concrete are located along the span. Test results and observations revealed that due to the coupling of CFRP sheets and straps, there is a significant enhancement in the beam strength and a more ductile behaviour was obtained due to the prevention of debonding failure.

Saafan (2006) investigated experimentally the efficiency of GFRP composites in strengthening simply supported reinforced concrete (RC) beams designed with deficiency in shear. Using the hand lay-up technique, successive layers of a woven fiber glass fabric were bonded along the shear span to enhance the shear capacity and to avoid catastrophic premature failure modes. Eighteen number of beams were tested to study the influence of various shear strengthening schemes and variable longitudinal reinforcement ratios on the structural behaviour of RC beams. The test results revealed that by proper application of GFRP wraps considerable increase in the shear strength and enhancements in the overall structural behaviour could be achieved for the beams with shear deficiency.

Mosallam and Banerjee (2007) carried out an experimental investigation to study the shear strength enhancement of reinforced concrete (RC) beams strengthened externally with FRP composites. Nine full scale RC beam specimens of three different classes: unstrengthened, repaired and retrofitted were tested along with three composite systems namely, carbon/epoxy wet layup, E-glass/epoxy wet layup and carbon/epoxy procured strips. Experimental results revealed that the composite systems caused substaintial enhancement in

ultimate strength of repaired and strengthed beams as compared to the pre-cracked and unstrengthened beam specimens. In order to evaluate different analytical models and recognize the influence factors on the shear behaviour of FRP strengthened RC beams, the experimental results were compared with analytical models and it was observed that the shear span-to-depth ratio is an imoptant factor for shear strength enhancement and shear failure modes.

Esfahani et al. (2007) examined the effect of reinforcing bar ratio (ρ) on the flexural behaviour of reinforced concrete (RC) beams strengthened with carbon fiber reinforced polymer (CFRP) sheets. Twelve number of RC beam specimens were cast, out of which three specimens were treated as control specimens and remaining nine specimens were strengthened in flexure using CFRP sheets. Beam sections with three varying reinforcing ratios, ρ, were used as longitudinal tensile reinforcement in specimens. It was observed that the flexural strength and stiffness of the strengthened beams increased compared to the control specimens. The test results concluded that the design guidelines of ACI 440.2R-02 and ISIS Canada overestimate the influence of CFRP sheets in enhancing the flexural strength of beams with small value of ρ compared to the maximum value (ρmax) specified in the above guidelines and with the increase in ρ value in the beams, the ratios of test load to the load computed using two design guidelines also increased.

Kim et al. (2008) examined the shear strength models for RC beams strengthened using FRP material which consists of a plasticity model for web crushing, a truss model for diagonal tension and a simple flexural theory based on the ultimate strength method. The model considered the interfacial shear-bonding stress between base concrete and the fiber to analyse the shear strengthening influence of the fiber which reflects that the main cause of shear failure in RC strengthened beams is quick loss of load capacity due to departure of the fibers from the base material. The experiment data were compared with the model concerning load carrying capacity and failure modes and also to evaluate its application the experimental results of other reported data were compared to the predictive model which show a good adaptability and high accuracy.

Serbescu et al. (2008) studied about the appropriateness of relatively new basalt fiber as an commercial substitute to the most expensive carbon fiber normally used in the strengthening of RC beams. A set of design models for anchorage debonding were compared against an extensive selection of experimental data and it was revealed that the basalt can be a effective

substitute to carbon fibres when the strengthening necessities are adequate. Even a small amount of U-shaped shear basalt strips was capable to deliver substantial anchorage, delaying plate end debonding and decreasing the brittleness of the failure.

Siddiqui (2009) investigated the flexure and shear behaviour of RC beams strengthened with externally bonded fiber reinforced polymer (FRP) composites. Six RC beams were cast and divided into two groups, each group containing three beams. The specimens of the first group were designed to be weak in flexure and strong in shear; whereas the specimens of the second groups were designed to be weak in shear and strong in flexure. In each group out of three beams one beam was taken as control beam and remaining beams were strengthened using different CFRP strengthening schemes. Test results revealed that the bonding of CFRP sheets with U-shape end anchorage bonded to the tension side is most effective in flexural strengthening; whereas bonding of inclined CFRP strips to the side faces RC beams is very efficient in enhancing the shear capacity of beams.

Balamuralikrishnan (2009) studied the flexural strengthening of RC beams strengthened using carbon fiber reinforced polymer (CFRP) fabrics. A total of ten number of beams were cast, out of which two beams were treated as control specimens and the remaining eight beams were strengthened using CFRP fabric in single and double layers which are parallel to beam axis at the bottom under virgin condition. All the beams were designed as under reinforced section and tested up to failure under monotonic and cyclic loads. Static and cyclic responses of all the beams were estimated in terms of strength, stiffness, ductility ratio, energy absorption capacity factor, bonding between CFRP fabric and concrete and the related modes of failures. The theoretical moment-curvature relationship and the load-displacement responses were predicted for all the strengthened beams and control beams by using ANSYS software and compared with the experimental results. The comparison revealed that the strengthened beams exhibit enhanced flexural strength and stiffness and composite action until failure.

Sundarraja and Rajamohan (2009) studied experimentally the strengthening of shear deficient reinforced concrete (RC) beams with glass fiber reinforced polymer (GFRP) inclined strips. The effectiveness in terms of spacing and width of inclined GFRP strips, spacing of internal steel stirrups and longitudinal steel rebar section on the shear capacity of the RC beams were examined. The effect of GFRP inclined strips externally bonded in the shear region of the beam on the modes of failures, ultimate load and deflection behaviour were studied along

with the shear contribution of GFRP strips. Test results indicated that the strengthened beams using inclined U-wrap GFRP strips is an efficient configuration compared to the side strips and the use of inclined GFRP strips avoid the brittle failure of the beams.

Pannirselvam et al. (2009) evaluated the structural behaviour of reinforced concrete (RC) beams using externally bonded FRP reinforcement. A total of five rectangular beams were cast, out of which one beam was taken as reference beam and the remaining beams were strengthened with GFRP laminates on their soffit. The test results revealed that the strengthened beams with GFRP laminates shows enhanced performance than the unstrengthened beams.

Martinola et al. (2010) studied the strengthening and repair of RC beams by using a jacket made of fiber reinforced polymer (FRP) with tensile hardening behaviour. For repairing of RC beams, the beams were initially damaged and then eventually repaired. A numerical analysis was also carried out to study the reinforcement behaviour. The experimental and numerical results revealed the effectiveness of the proposed technique both at ultimate and serviceability limit states.

Bukhari et al. (2010) evaluated the contribution of CFRP sheets on the shear capacity of continuous reinforced concrete beams and reviewed the existing design guidelines for shear strengthening of beams using CFRP sheets and proposed a modification to Concrete Society Technical Report TR55. A total of seven, two span continuous concrete beams were cast with rectangular cross-section. Out of these beams one beam was taken as control beam and the remaining beams were strengthened using various configurations of CFRP sheets. The experimental results indicated that the shear capacity of the beams was substaintially enhanced by using CFRP sheets and 45^0 fiber orientation to the axis of the beam was found to be more effective. Ceroni (2010) investigated experimentally on the RC beams externally bonded using carbon fiber reinforced plastic (CFRP) laminates and Near Surface Mounted (NSM) bars under monotonic and cyclic loads.

Obaidat et al. (2011) carried out an experimental programme to study the flexure and shear behaviour of the structurally damaged full-scale reinforced concrete (RC) beams retrofitted using CFRP laminates. The principal parameters considered were internal reinforcement ratio, position of retrofitting and the length of CFRP. The experimental results indicated that the beams retrofitted using CFRP laminates are structurally effective and are restored to

stiffness and strength values nearly equal to or more than those of the control beams. The results also revealed that retrofitting shifts the mode of failure to be brittle and the effectiveness of the strengthening technique using CFRP in flexure diversed depending on the length.

Gang et al. (2013a) presented an experimental study on the flexural behaviour of RC beams reinforced with steel-wire continuous basalt fiber composite plates. This work explored a method for flexurally strengthening reinforced concrete (RC) beams using newly developed steel-wire continuous basalt fiber composite plates (SBFCPs) that consists of steel wires and continuous basalt-fiber-reinforced polymer (BFRP) composites. The test results revealed that the SBFCP strengthened specimens performed superior than the unstrengthened specimen with respect to load capacity and member stiffness. A parametric study confirmed that the volumetric ratio of steel wires in the SBFCPs influence the load capacity and stiffness of specimens strengthened with SBFCPs. The results also indicated that anchorage by steel plates and bolts improves the load capacity and ductility of strengthened specimens.

Gang et al. (2013b) reported a work on the pre-stressed fiber-reinforced polymer (FRP) strengthening system which can be an efficient method to enhance the efficiency of FRP materials and the behaviour of the strengthened members under service conditions. A method using partially impregnated carbon-basalt hybrid fiber sheets (CBHFS) was proposed to improve the tensile capacity of dry fiber sheets. The test results indicated that the tensile capacity of dry fiber sheets can be enhanced effectively and that it is not influenced by the specimen length when fiber hybridization and partial impregnation are applied together.

2.3 Strengthening of Reinforced Concrete (RC) T-Beams:

The shear strength of RC beams strengthened by using epoxy bonded glass fiber reinforced polymer (GFRP) plates to the tension flanges of the beams was studied experimentally by Saadatmanesh and Ehsani (1992). Six numbers of RC beams were cast and tested up to failure under four-point static loading. The load versus strain in GFRP plate, steel rebar, extreme compression fiber of concrete and the load versus deflection at the mid-span of the beams were plotted and then compared to the predicted values. The test results indicated that there is a considerable enhancement in the flexural strength of the strengthened beams by using epoxy bonded GFRP plates to the tension face and the cracking behaviour of the beams

were improved by delaying in the formation of visible cracks and reduction in the crack widths at higher loads.

The effectiveness of RC beams using externally bonded composite fabrics for enhancing beam shear capacity was studied by Chajes et al. (1995). Twelve numbers of under-reinforced T-beams were cast, out of which four beams were taken as control beams and the remaining eight beams were strengthened by using various types of woven composite fabrics namely: aramid, E-glass and graphite composites bonded to the web of the T-beams using epoxy. All the beams were tested under flexure and the results of the strengthened beams were compared with the performance of the control beams which indicated that the beams strengthened using external composite reinforcement exhibited admirable bond characteristics.

The shear behaviour and the failure modes of simply supported RC T-beams externally strengthened in shear with FRP composites by using two different strengthening systems namely; externally bonded FRP sheets and Near Surface Mounted (NSM) FRP rods was studied by Khalifa et al. (2000). Eleven numbers of RC T-beams were cast and divided into three series. The first series was tested to study the effect of the concrete surface roughness on the shear capacity and axial rigidity of the CFRP sheets. The second series examined the ability of externally bonded CFRP reinforcement to enhance the ultimate capacity of beams with internal steel reinforcement. The third series focused on the innovative shear strengthening system using NSM CFRP rods. The test results revealed that the shear capacity can be substaintially enhanced by using externally bonded CFRP sheets and NSM CFRP rods and the contribution of CFRP sheets to the shear capacity also increases as CFRP axial rigidity increases.

The improvement in shear capacity of existing reinforced concrete (RC) T-beams strengthened using externally bonded CFRP composites with different configurations was investigated by Khalifa and Nanni (2000). Six full scale, RC T-beams were cast, out of which one beam was taken as reference and the remaining beams were strengthened with different configurations of CFRP sheets considering various parametres, such as; wrapping schemes, CFRP amount, 90º/0º ply combination and CFRP end anchorage. The experimental results indicated that the shear capacity of the beams can be considerably enhanced by using externally bonded CFRP composites and U-wrap with end anchorage was found to be most effective configuration among all. To predict the capacity of the tested beams, design

algorithims in ACI code format and Euro code format were proposed and the results showed that the proposed design approach is conservative and acceptable.

The behaviour of reinforced concrete (RC) T-beams strengthened in shear using externally bonded carbon fiber reinforced polymer (CFRP) was analyzed experimentally by Bousselham and Chaallal (2006). Twentytwo number of RC T-beams were tested considering various test parameters, such as; CFRP ratio, internal shear steel reinforcement ratio, shear length to the beam depth ratio (a/d ratio). The test result indicated that the contribution of CFRP composites to the shear capacity is not in proportion to the CFRP thickness and depends on the internal transverse steel reinforcement and a/d ratio. The test results were compared to the shear resistance value obtained from the ACI 440.2R-02 guidelines, which revealed that the guideline fail to define the effect of a/d ratio and presence of shear steel reinforcements and overestimates the shear resistance for high FRP thickness.

Ozgur (2008) carried out a research work to study the strengthening of shear deficient RC T-beams with low strength concrete using CFRP composites subjected to cyclic loads. Six RC T-beams were tested up to failure under cyclic loading considering different test variables, such as; width of the CFRP straps, arrangements of straps along the shear span and anchorage techniques applied to the ends of the straps. To obtain ductile flexural behaviour, shear deficient beams with low strength concrete were strengthened using CFRP straps. The test results concluded that all CFRP configurations enhanced the strength, stiffness and energy dissipation capacity of the specimens substaintially and the failure modes and ductility of the specimens varied along with the CFRP strap width and arrangement.

An experimental investigation was carried out by Tanarslan and Altin (2009) on the shear deficient RC T-beams strengthened with externally bonded CFRP strips subjected to cyclic loading. Six shear deficient RC T-beam specimens were tested under cyclic loading, out of which one specimen was tested in its virgin condition without strengthening and the rest beams were tested after strengthening with side bonded and U-jacketed CFRP strips. The test results concluded that the premature debonding of the CFRP strips is the principal failure mode for externally strengthened RC beams, hence the effect of anchorage usage on shear behaviour and strength is to be studied.

Deifalla and Ghobarah (2010) studied the behaviour of RC T-beams strengthened with FRP fabrics subjected to combined shear and torsion. Six half-scale beams, two control specimens

and four strengthened beams using four configurations of CFRP were tested using a specially designed test setup that subjects the beam to combined shear and torsion with different ratios. The extended U-jacketing configuration was found to be most effective in terms of strength and ductility while being relatively realistic for strengthening and also caused increase in the stiffness of the beams after cracking as compared to that of the control beam.

Heyden et al. (2010) carried out an experimental study on the behaviour of structurally damaged full-scale reinforced concrete beams retrofitted with CFRP laminates in shear and flexure. The experimental results indicated that beams retrofitted in shear and flexure by using CFRP laminates are structurally efficient and are restored to stiffness and strength values nearly equal to or greater than those of the control beams. It was found that the efficiency of the strengthening technique by CFRP in flexure varied depending on the length. The main failure mode in the retrofitted beams was plate debonding.

The effectiveness of the Near Surface Mounted (NSM) technique with CFRP laminates for the shear strengthening of RC T-beams was studied experimentally by Dias and Barros (2010). The test programme considered three inclinations (45º, 60º and 90º) of the laminate and for each one, three percentage of CFRP were considered. The test results indicated that inclined laminates were more effective than the vertical laminates, with the increase of percentage of laminates the shear capacity of the beams increases, the contribution of the laminates for the shear resistance of the beam was restricted by the concrete tensile strength. The failure modes of the beams were varied with the percentage of the laminates. Test results also revealed that NSM is the most effective in the better ultilization of the tensile strength of the CFRP material and in enhancing the beam shear resistance. The ACI and FIB (Federation International du Beton) analytical formulations were anticipated a greater contribution of the EBR shear strengthening systems than the values recorded experimentally.

The behaviour and performance of reinforced concrete deep beams having T-section strengthened in shear using CFRP sheets was investigated by Lee et al. (2010). A total of fourteen number of shear deficient RC T-section deep beams were cast with a shear span-to-effective depth ratio of 1.22 and tested under four-point loading system considering various key parameters, such as; strengthening length, fiber direction combination of CFRP sheets and an anchorage using U-wrapped CFRP sheets. The test results indicated that almost all the strengthened deep beams exhibited a shear–compression due to partial delamination of the

CFRP sheets and the key parameters of strengthening length, fiber direction combination, and anchorage have substantial effect on the shear behaviour of strengthened deep beams.

Panda et al. (2011,2012) carried out an experimental investigation to study the shear behaviour of RC T-beams strengthened in shear using epoxy bonded GFRP fabric. Nine beams were treated as control beams with three different stirrup spacings and the remaining beams were strengthened in shear using one, two and three layers of GFRP sheets bonded to the side of the web and in the form of U-jacket around the web of T-beams for each type of stirrup spacing. The effectiveness, shear behaviour, cracking pattern and modes of failures of the strengthened RC T-beams were evaluated and the test results illustrated that RC T-beams strengthened with side bonded and U-jacketed GFRP sheets in shear enhances the load carrying capacity of the beams significantly and the design approach proposed by ACI guidelines shows conservative results as compared with the experimental data. Panigrahi et al. (2014) studied the behaviour of shear deficient RC T-beams strengthened with epoxy bonded bi-directional GFRP fabrics. Test results indicated that the external strengthening with GFRP composites can be used to increase the shear capacity of RC T-beams, but the efficiency varies depending on the test variables considered.

2.4 Strengthening of Reinforced Concrete (RC) Rectangular and T-Beams with web opening:

Now-a-days it is very essential to provide passage for important services like water supply, ventilating, electricity, air-conditioning, telephone and sewage through a network of pipes and ducts. Openings in concrete beams facilitate the connection of these services.

Shanmugamt and Swaddiwudhipongt (1988) examined the behaviour of steel fiber reinforced concrete deep beams with rectangular openings. Nine simply supported beams with two rectangular openings, one in each shear span, were placed symmetrically about the vertical axis in each of the beams and were tested up to failure. Steel fiber content in all the beams was kept the same which equals to 1% by volume. The experimental results concluded that the effect of opening on the behaviour and ultimate shear strength of deep beams depends mainly on the degree to which it intercepts the natural load path and the location at which this interception occurs.

The behaviour of RC beams having transverse openings under predominant shear was studied by Mansur (1998). On the basis of the structural response of the beam, appropriate guidelines were proposed for the classification of an opening as small or large. A design method using the existing design philosophy for shear was recommended for small openings and explained by a numerical design example. In the recommended design method, the maximum shear permitted in the section to avoid diagonal compression failure was supposed to be the same as that for solid beam excluding for considering the entire section through the opening. Mansur (2006) studied the behaviour of reinforced concrete beams with circular and large rectangular web openings. The study focused on the main outcomes related to the analysis and design of beams under bending and shear. It was concluded that the design method for beams with large openings can be further simplified without losing rationality and having irrational extra cost.

Chen et al. (2008) investigated the behaviour of steel reinforced concrete beams with various opening shapes and different moment to shear ratios. Thirteen full-scale steel reinforced concrete (SRC) beams were cast and tested up to failure. The test results illustrated that specimens with high moment to shear ratio established ductile behaviour because of the confinement attributed to the stirrup and structural steel and specimens with low moment to shear ratio failed due to the shear cracking. An interaction between bending and shear was studied for tested SRC beams.

Maaddawy and Sherif (2009) examined the potential use of upgrade reinforced concrete (RC) deep beams with square openings. Thirteen number of deep beams with two square openings, one in each shear span, were placed symmetrically about the mid-point of the beam were cast and tested under four-point bending. Test variables considered were opening size, location and the presence of the CFRP sheets. It was observed that the use of externally bonded CFRP sheets around the openings was found to be very efficient in upgrading the shear strength of RC deep beams. The test results indicated that the CFRP shear-strengthened RC deep beams with openings failed suddenly due to a formation of diagonal shear cracks in the top and bottom chords of the opening. In all strengthened beams, the concrete was pulled out from the U-shaped CFRP jacket wrapped around the top chord of the opening.

Pimanmas (2010) studied on the strengthening of RC beams with circular and square openings by FRP rods. Thirteen numbers of beams with circular and square openings were tested by considering two patterns of strengthening by FRP rod: one is to place FRP rods

enclosing the opening and the other is to place FRP rods diagonally throughout the entire depth of the beam. The test results indicated that placing of FRP rods throughout the entire beam's depth caused a considerable enhancement in loading capacity and ductility. A nonlinear finite element analysis, based on smeared crack approach, was proposed for numerical verification and investigative the effect of length, position and inclination of FRP rods. The numerical result demonastrated that the inclined rods are more efficient than vertical ones.

Ahmed et al. (2012) studied the behaviour, analysis and design of Reinforced Concrete (RC) beams with transverse web openings. Different features were emphasized and the classification of openings were described, guidelines for opening location, and the structural behaviour of RC beams with web openings. Numerous design methodologies were also described, for example the American Concrete Institute (ACI) approach, the Architectural Institute of Japan (AIJ) approach and the strut and tie method. Furthermore, the strengthening of RC beams with openings using Fibre Reinforced Polymer (FRP) material and steel plates were also carried out.

2.5 Critical Observations

The critical observations made from the survey of the existing literature regarding the strengthening of reinforced concrete (RC) beams using epoxy bonded FRP are summarized as follows:

- Most of the research works have been made to investigate flexural and shear behaviour of RC rectangular beams strengthened with fiber reinforced polymer (FRP) composites.
- Till date no work has been reported to study the shear behaviour of RC T-beams using externally bonded Basalt fiber reinforced polymer (BFRP) composites.
- A limited work has been reported on the strengthening of RC T-beams with web openings and no study has been reported on the strengthening of beams with transverse opening using BFRP composites.
- The debonding of FRP sheets from main concrete surface due to improper anchorage is a major issue which needs further attention from research community.
- Study on the prevention of debonding of FRP from the concrete surface using mechanical anchorage scheme is scanty.

- Many researchers are of the opinion that the previous design approaches do not have comprehensive understanding of the shear behaviour of RC T-beams.

2.6 Scope of the Present Investigation

Based on the critical observations made from the survey of existing literatures and to achieve the objective outlined in the previous chapter, the scope of the present research study is summarized as follows:

- To analyse the shear behaviour of T-section RC beams under static loading condition.
- To examine the shear behaviour and modes of failure of RC shear deficient T-beams externally strengthened with basalt fiber reinforced polymer (BFRP) sheets.
- To investigate the effect of different test parameters such as fiber amount and distribution, bonded surface, number of layers, fiber orientation and end anchorage system on the shear capacity of RC T-beams strengthened with externally bonded BFRP composites.
- To study the behaviour of shear deficient RC T-beams with transverse openings of circular, square and rectangular shapes in web portion.
- To investigate the effect of a new anchorage scheme on the shear behaviour of the RC T-beams.
- To compute analytically the shear capacity of the RC T-beams.

CHAPTER 3

3 EXPERIMENTAL PROGRAMME

3.1 General

The purpose of the present research work is to study the effect of the externally bonded fiber reinforced polymer sheets on the shear capacity of the RC T-beams with and without transverse openings under static loading conditions. In this experimental programme a total of twenty two numbers of beams are cast and tested by applying symmetrical four point static loading system up to failure. The beams are grouped into two series designated as A and B. The first series of tests, series A, dealt with the shear strengthening of the RC beams with T-shaped cross-section without transverse openings. The second series B, focused on the shear strengthening of the RC T-beams with transverse openings of different shapes. In each series, one of the beams is not strengthened with FRP and considered as control beam whereas other beams are strengthened with externally bonded unidirectional BFRP sheets in the shear zone of the beams.

The variables selected for the experimental works are BFRP amount and distribution (i.e., continuous wrap versus strips), bonded surface (i.e., lateral sides versus U-wrap), number of layers of BFRP, fiber orientation (i.e., 0° direction versus 90° direction versus 45^0 direction), Transverse web openings of different shape (i.e., circular versus square versus rectangular) and end anchor (i.e., U-wrap with and without end anchor).

3.2 Test Specimens

Twenty two reinforced concrete T-beams are considered in this study with dimensions as follows:

Span= 1300mm
Width of web= 150mm
Depth of web= 125mm
Depth of flange= 50mm
Effective depth= 125mm

The steel reinforcement in the beams consists of 2 numbers of 16 mm φ and 1 number of 12 mm φ HYSD bars as tension reinforcement. Four numbers of 10 mm φ bars are provided as hanger bars.

The length and depth of the beam have been taken as 1300 mm and 175mm, respectively due to the limitation of the loading system available in the Structural Engineering laboratory, NIT Rourkela. The beams are overdesigned in flexure as per Indian code IS: 456-2000 in order to guarantee a shear failure. The effect of length parameter on the load carrying of beam has not been studied due to above limitation.

3.3 Casting of Specimens

The beam specimens are made from the nominal mix of the concrete of grade M20 with mix proportions as per IS: 456-2000 [30] and presented in Table 3.1. For mixing purpose, the concrete mixer is used and the water cement ratio is fixed at 0.55. Three numbers of 150x150x150 mm concrete cube specimens are cast along with each beam and cured for 28 days to determine the compressive strength of concrete.

Table 3.1 Nominal Mix Proportions of Concrete

Description	Cement	Sand (Fine Aggregate)	Coarse Aggregate	Water Cement Ratio
Mix proportioning (By weight)	1	1.67	3.33	0.55
Quantities of materials for one specimen beam (kg)	19.64	32.79	65.38	10.8

3.4 Material Properties

3.4.1 Concrete

Concrete is a material which is made from the combination of cement, water combined with sand (fine aggregate) and coarse aggregate. Due to the chemical reaction of cement and water a tough stone like mass is formed. The concrete paste formed can be moulded into any shape to get a smooth surface. Hardening of the paste starts immediately after mixing. The presence

of water is essential for the chemical reaction and to increase the strength, so proper care should be taken to avoid the rapid loss of water after mixing. Excess water makes the concrete more permeable and weaker.

The compression test is conducted for the cube specimens at the end of 28 days of curing and the test results are tabulated in Table 3.2.

Table 3.2 Test Results of Cubes after 28 days of curing

Specimen Name	Specimen ID	Average Cube Compressive Strength (MPa)
Control Beam	CB	23.1
Strengthened Beam 1	SB1	25.27
Strengthened Beam 2	SB2	24.67
Strengthened Beam 3	SB3	24.33
Strengthened Beam 4	SB4	23.36
Strengthened Beam 5	SB5	28
Strengthened Beam 6	SB6	26.81
Strengthened Beam 7	SB7	26.07
Strengthened Beam 8	SB8	24.45
Strengthened Beam 9	SB9	26.34
Strengthened Beam 10	SB10	28.33
Strengthened Beam 11	SB11	28.89
Strengthened Beam 12	SB12	28
Control Beam 1	CB1	23.55
Strengthened Beam 13	SB13	26.22
Strengthened Beam 14	SB14	28.65
Control Beam 2	CB2	26.14
Strengthened Beam 15	SB15	28.14
Strengthened Beam 16	SB16	27.26
Control Beam 3	CB3	23.26
Strengthened Beam 17	SB17	29.04
Strengthened Beam 18	SB18	25.18

3.4.2 Cement

Cement is a construction material which is generally found in powder form, obtained by burning and crushing the stone containing clay carbonate of lime and some amount of carbonate of magnesia (called natural cement) or obtained by burning at a very high temperature a mixture of calcareous and argillaceous materials (called artificial cement). For construction purposes most commonly used cement is Portland cement. It is manufactured by finely grinding the clinkers made by burning mixture of calcareous and argillaceous materials at a very high temperature and is bluish-grey in colour. Throughout this experimental program Portland Slag Cement (PSC) of Konark Brand is used with a specific gravity of 2.96.

3.4.3 Fine Aggregate

Fine aggregate/sand is composed of small mineral grains obtained from decomposition of rocks. It is differentiated from gravel only by the means of the size of the mineral grains, but is dissimilar from clays by means of containing organic materials. Sand is a major component for making concrete and mortar and also used widely for polishing and sand blasting purpose. The fine aggregate/sand passing through a 4.75 mm sieve, with a specific gravity of 2.64 is used throughout this experimental program. As per Indian Standard specification IS: 383-1970 the fine aggregate used is classified as zone III.

3.4.4 Coarse Aggregate

Coarse aggregates are the major component for making concrete. These are the crushed stone of limestone, trap rock and granite. The coarse aggregates, one retained on 20 mm size sieve and another retained on 10 mm size sieve are used in 50:50 proportions by weight for this investigation. The coarse aggregate with a specific gravity of 2.88 is used, grading confirming to IS: 383-1970.

3.4.5 Water

Generally, for mixing of concrete water fit for drinking is used. It should be free from alkalis, acids, vegetables, oils or other organic impurities. Water serves two main functions in concrete mix. It reacts with cement to form a cement paste which gets hardened with time and in the mixture of sand and cement it serves as a lubricant. Throughout this experimental program, for all concrete mix ordinary clean potable tap water is used.

3.4.6 Reinforcing Steel

High-Yield Strength Deformed (HYSD) bars confirming to IS 1786:1985 are used as reinforcing bars. The bars of 16 mm and 12 mm diameter are used as tension reinforcement and 10mm diameter bars are used for hang-up bars. Three identical samples of each diameter are tested under uniaxial tension to determine the yield strength of the bars. The average of three samples is considered as the proof stress or yield strength of the bars and is given in Table 3.3. The Young's modulus of steel bars is $2x10^5$ MPa.

Table 3.3 Tensile Yield Strength of Reinforcing Steel bars

Sl. no. of sample	Diameter of bar tested (mm)	0.2% Proof stress (N/mm^2)	Avg. Proof Stress (N/mm^2)
1	16	506	494
2	16	495	
3	16	480	
4	12	595	578
5	12	560	
6	12	579	
7	10	535	529
8	10	521	
9	10	530	
10	8	527	523
11	8	520	
12	8	521	

3.4.7 Detailing of Reinforcement in RC T-beams

The arrangement of reinforcement is same for all the beams. Two numbers of 16 mm φ and one number of 12 mm φ HYSD bars are provided as tension reinforcements and four numbers of 10 mm φ steel bars are used as hang-up bars. The cross-section and reinforcement details of the control beam are depicted in Figure 3.1. All the strengthened beams have same cross-section and reinforcement details as that of the control beam.

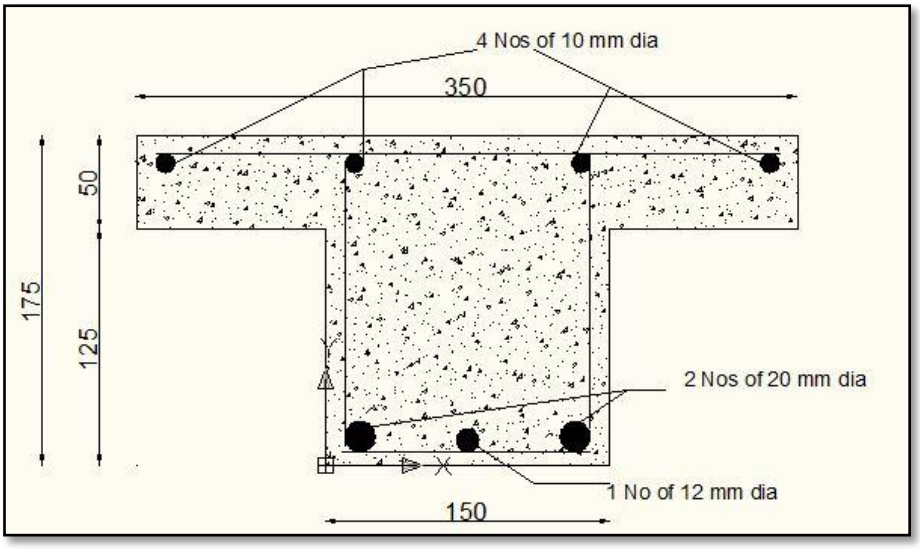

Figure 3.1 Cross-section and reinforcement details of the control beam

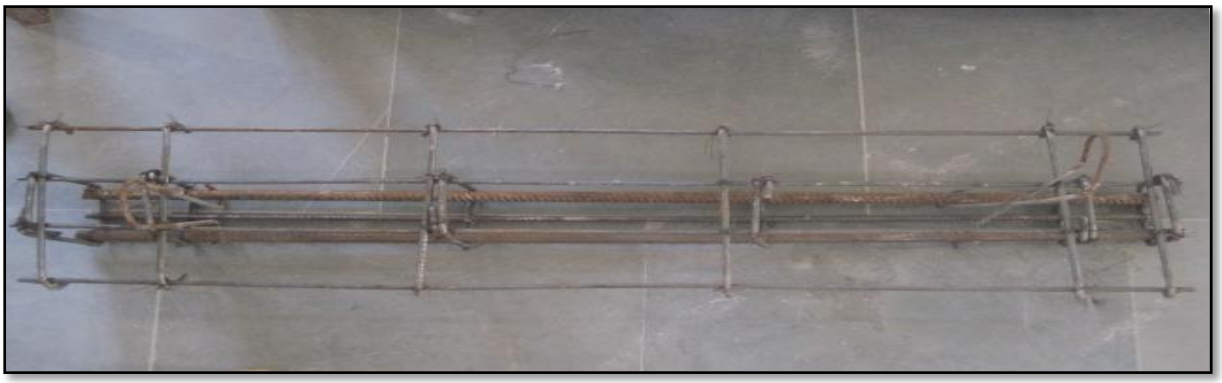

Figure 3.2 Reinforcement Detailing of T- Beam

3.4.8 Fiber Reinforced polymer (FRP)

Fiber reinforced polymers embedded in matrix is considered as composite which is a heterogeneous and anisotropic material having linear elastic behaviour. Generally, carbon and glass fibers are used as the strengthening materials. For bonding of fiber layers, epoxy is used as the binding material.

Basalt fiber is a relatively new fiber introduced in the construction industry. Among different types of fibers, carbon fiber is the most expensive one. Glass fiber can be used as an alternative to carbon fiber which is cheaper, but it is proven to be less effective and less durable against corrosive medium. The cost of glass and basalt fibers is nearly same. From the literature [51, 53], it is found that the strength to weight ratio of a basalt fiber exceeds that of glass by 1.5 times. Basalt fiber also exhibits high corrosion resistant and chemical

durability towards corrosive medium, such as salts, acid solutions and alkalis. It has also higher thermal ability as compared to glass fibers. The production procedure of basalt fiber from basalt rock is very simple and involves very less expenditure. Due to its advantageous properties over the glass fibers, it can be effectively used in place of glass fiber. Hence, it can be said that basalt fiber is an economic alternative with reference to more expensive fibers commonly used in practice.

3.4.9 Epoxy Resin

Fiber composites used in the strengthening technique contain an adhesive of thermosetting resins that can be epoxy, vinyl ester or polyester. Epoxy resin is the widely used matrix in the construction industry. Epoxy resin is prepared from two dissimilar chemicals, an epoxide "resin" with polyamine "hardener". The resin and hardener used in this study are Araldite LY 556 and hardener HY 951 respectively.

3.4.10 Fabrication of BFRP plate for tensile test

There are two basic processes for fabrication of plate, that is, hand lay-up and spray-up. The most common method for fabrication process is the hand lay-up process. In hand lay-up process liquefied resin is laid along with reinforcement (unidirectional basalt fibre) against the finished surface of an open mould. The resin was used for hardening the material to a durable, lightweight product due to chemical reaction. The resin acts as the matrix for the reinforcing basalt fibers, just like concrete acts as the matrix for steel reinforcing rods. The volume fraction of fiber and matrix is 45:55.

The following component materials are used for fabricating the BFRP plate:

I. Unidirectional basalt FRP (BFRP)
II. Resin (Epoxy)
III. Catalyst (Hardener)
IV. Releasing agent (Polyvinyl alcohol)

A flat plywood rigid platform is used to fabricate the plies of unidirectional basalt fiber in the prescribed sequence using hand lay-up process. On the plywood platform a releasing sheet is placed and polyvinyl alcohol is used as a releasing agent. The fabrication starts by applying the resin (epoxy and hardener) on the mould by brush, which provide an even peripheral surface and protect the fibers from straight contact with the environment. The first layer of reinforcement is placed on the mould over the resin and is spread uniformly over the

reinforcement by using brush. A steel roller is used to eliminate the entangled air gurgle. The above process of hand lay-up is repeated till all the fibers (reinforcements) are placed. Again, the top of the plate is covered with a releasing sheet which is applied with polyvinyl alcohol. Then, for compressing purpose a heavyweight rigid platform is placed on the uppermost surface of the plate. A curing process for a minimum of 48 hours is maintained before being cut to the required shape for testing.

Plates of 2 layers, 4 layers, 6 layers and 8 layers of 0^0 and 90^0 fiber directions are cast and three specimens from each are prepared as per ASTM standards (D3039) and are tested .

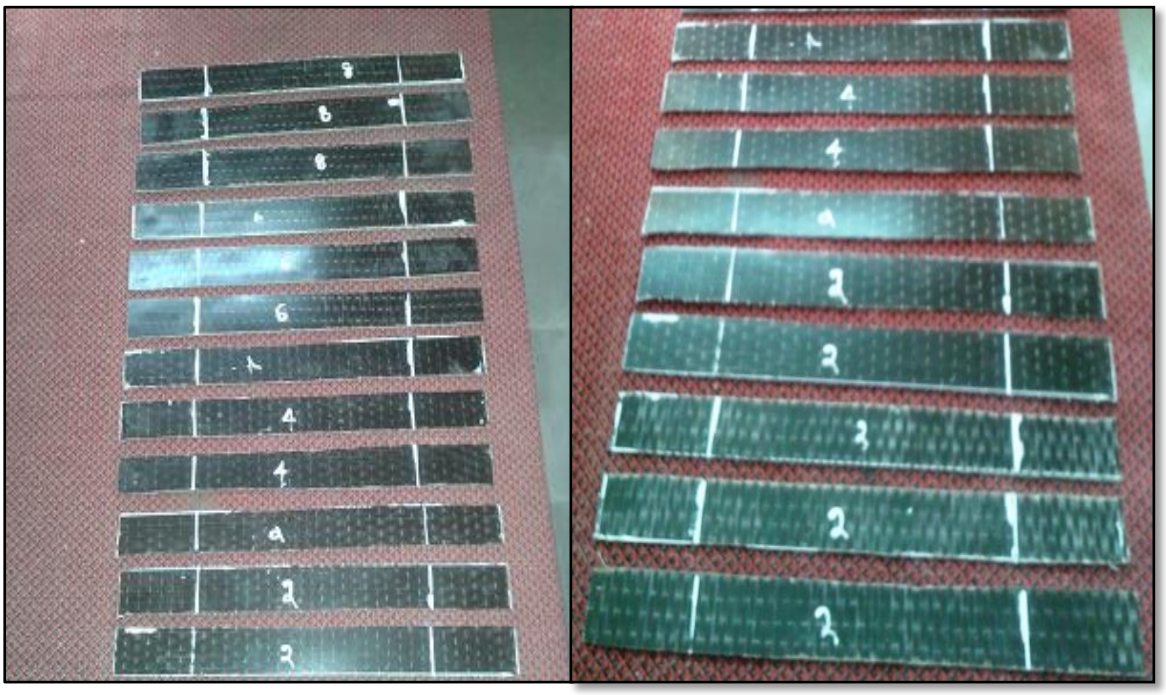

Figure 3.3 Specimens for tensile testing of unidirectional BFRP composite

Figure 3.4 Experimental setup for tensile testing of the specimen in INSTRON universal testing machine

3.4.11 Determination of Ultimate stress, Ultimate Load & Modulus of Elasticity of BFRP

The unidirectional tensile test is conducted to determine the ultimate stress, ultimate load and modulus of elasticity of the specimens. By using diamond cutter or hex saw the specimens are cut from the plates and is polished with the help of polishing machine. The mean of the three specimens is considered. The dimensions of the tested specimens are tabulated in Table 3.4.

Table 3.4 Dimension of the Specimens for tensile test

Orientation	No. of layers	Length of sample (cm)	Width of sample (cm)	Thickness of sample (cm)
0^0 orientation	2 Layers	25	2.5	0.56
	4 Layers	25	2.5	1.07
	6 Layers	25	2.5	1.53
	8 Layers	25	2.5	2.03
90^0 orientation	2 Layers	25	2.5	0.56
	4 Layers	25	2.5	1.07
	6 Layers	25	2.5	1.53
	8 Layers	25	2.5	2.03

The tensile strength and modulus of elasticity of the specimens are determined in the Production Engineering Lab, NIT, Rourkela using INSTRON 100kN. First, specimens are gripped in the fixed upper jaw and then gripped in the movable lower jaw. To prevent the slippage, gripping of the specimen should be proper. In this study, the gripping is taken as 50 mm from each side. The load, as well as the extension, is recorded digitally with the help of a load cell and an extensometer respectively. The stress versus strain graph is plotted from the results obtained and the initial slope of it gives the modulus of elasticity. The ultimate stress and ultimate load are obtained at the failure of the specimen. The mean value of the three specimens of each layer of 0^0 and 90^0 orientations is given in Table 3.5.

Table 3.5 Result of the specimens from tensile test

Orientation	No. of layers	Ultimate Stress (MPa)	Ultimate Load (N)	Young's Modulus (MPa)
0^0 orientation	2 Layers	13.86	202	4588
	4 Layers	14.07	577	5561
	6 Layers	19.53	883	5607
	8 Layers	23.57	1010	6395
90^0 orientation	2 Layers	328	5808	11920
	4 Layers	391	11870	12870
	6 Layers	421	22110	13130
	8 Layers	469	25480	13920

3.4.12 Form Work

A rigid and strong form work is necessary to hold the fresh concrete, plastic in nature and to mould it to the required shape and size. To avoid the leakage of cement slurry the joints of the form work are sealed properly. Then a thick polythene sheet is laid over the rigid floor after applying machine oil to the inner faces of the former. The reinforcement cage is then placed in position inside the form work carefully by placing concrete cover blocks at the bottom and with a cover of 20mm on the sides.

Figure 3.5 Steel Frame Used For Casting of RC T-Beam

3.4.13 Mixing of Concrete

The mixing of concrete is done thoroughly using a standard concrete mixer, to obtain a uniform concrete mix. First coarse and fine aggregates are mixed thoroughly followed by cement. To make the concrete workable required amount of water is added gradually in to the mixer till a uniform colour is attained. The mixing is continued for two minutes after all the materials are mixed properly inside the mixer.

The aggregate size generally used for casting of reinforced concrete beam is 20mm down. . In the present research work, both 20 mm down and 10 mm down aggregates are used in 50:50 proportions by weight. Any sort of problems related to the homogeneity of the mix and composite action of concrete and steel reinforcement is not observed in the present experimentation.

3.4.14 Compaction of Concrete

For proper compaction of concrete, a needle vibrator of 30 mm size is used. Proper care is taken to avoid the dislocation of the reinforcement cage inside the form work during compaction. By using a trowel and wooden float the upper surface of the concrete is smoothed, finished. The date of concreting and specimen detail is written on the upper surface after six hours to recognize it correctly.

3.4.15 Curing of Concrete

Curing is essential to prevent the loss of water necessary for the process of hydration and hence for hardening. After 24 hours, the specimens are taken out from the mould and covered

with wet jute bags for curing purpose. To keep the jute bags wet, potable water is sprinkled 3 times per day to allow perfect curing of concrete. The curing is continued for 28 days.

3.4.16 strengthening of Beams with FRP fabrics

During the process of strengthening, the FRP fabrics are bonded to the concrete surface using a suitable resin and hardener. First the bottom surface of the beam is cleaned by removing all the loose particles. Then by means of coarse sand paper, the necessary part of the concrete surface is made uneven and all the dirt and debris particles are removed with an air blower. The epoxy resin is mixed and applied on the required part of the concrete surface after the preparation of the concrete surface. The mixing is done in a plastic container by taking 10 percent of hardener (HY 951) with respect to the epoxy resin (Araldite LY 556) and is continued for some time to obtain a uniform mixture. Then the fabrics are cut as per the required size and the epoxy resin is applied to the concrete surface. After the application of epoxy resin coating, the BFRP fabric is employed at the top of the coating and a steel roller is used to eliminate the entrapped air bubbles at the interface of concrete/epoxy or fabric/epoxy for perfect bonding. Then over the first layer of BFRP the second layer of epoxy resin is applied and BFRP fabric is employed over the epoxy resin coating. Again a steel roller is used for eliminating the entrapped air and the above process is repeated until the required number of BFRP fabrics is obtained on the concrete surface. To avoid hardening of epoxy resin hardener mix this operation must be done very quickly. The excess epoxy resin is extruded by applying a constant uniform pressure on the composite fabric surface to achieve a good adherence between the concrete, the epoxy and the fabric. The operation is carried out at room temperature, cured for minimum 3 days before testing.

Figure 3.6 Application of epoxy and hardener on the beam

Figure 3.7 Fixing of BFRP sheets on the beam

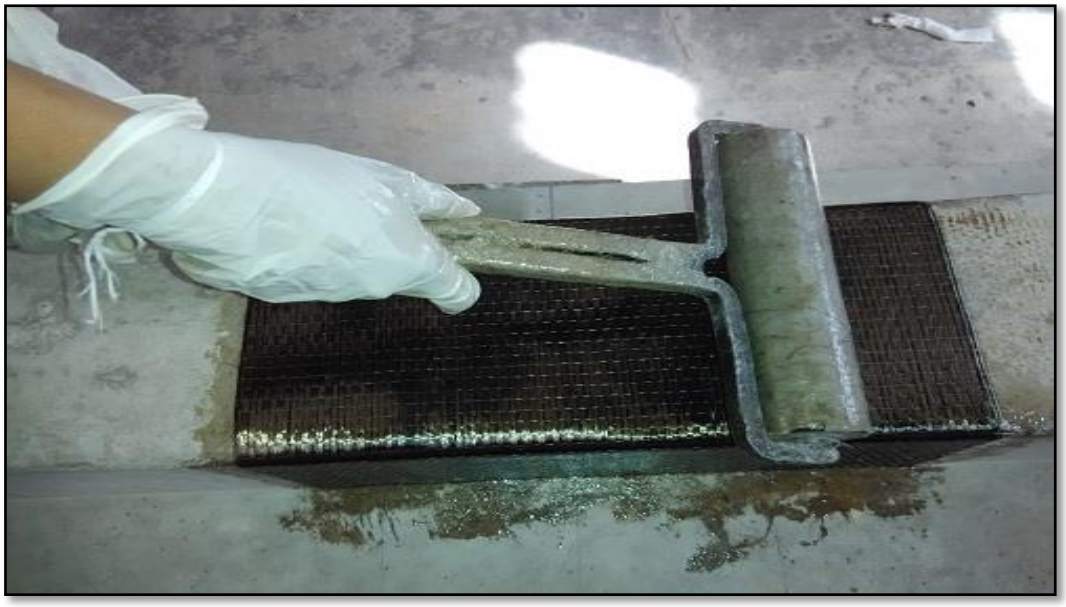

Figure 3.8 Roller used for the removal of air bubble

3.5 Experimental Set-up for Testing of Beams

All the beam specimens are tested by means of a four-point static loading system at the 'Structural Engineering' Laboratory of Department Civil Engineering, National Institute of Technology, Rourkela. At the end of the curing period of 28 days, control beams of both the series are tested by applying load gradually up to failure. Similarly, after the curing period of 28 days, the strengthen beams are strengthened by bonding the BFRP fabrics to the concrete surface, cured for minimum of 3 days and then tested by applying load gradually up to failure. The details of the test setup are displayed in Figure 3.9. To measure the load during testing a load cell of 500kN capacity provided with a hydraulic jack is used.

The arrangement of the four point static loading system is given in Figure 3.9. The load is transferred to a spreader beam by means of a load cell. The spreader beam is placed above the test specimen by means of steel rollers placed on steel plates bedded on cement to afford an even levelled surface. The expected test loads should be carried by the loading frame for all the specimens without any distortion The beam specimen to be tested is placed on steel rollers placed between two steel plates bearing leaving 150mm from the ends of the specimen. The remaining 1000mm is separated into three identical parts of 333mm as presented in the Figure 3.9. The lines are drawn on the specimens to be tested at distances of L/3, L/2, & 2L/3 from the left support (L=1300mm). The deflection of the specimens is recorded with the help of three dial gauges. Two dial gauges are positioned under two

concentrated loads, i.e. at L/3 and 2L/3 distances and the other dial gauge is positioned under the centre of the specimen, i.e. at L/2 distance to measure the deflections.

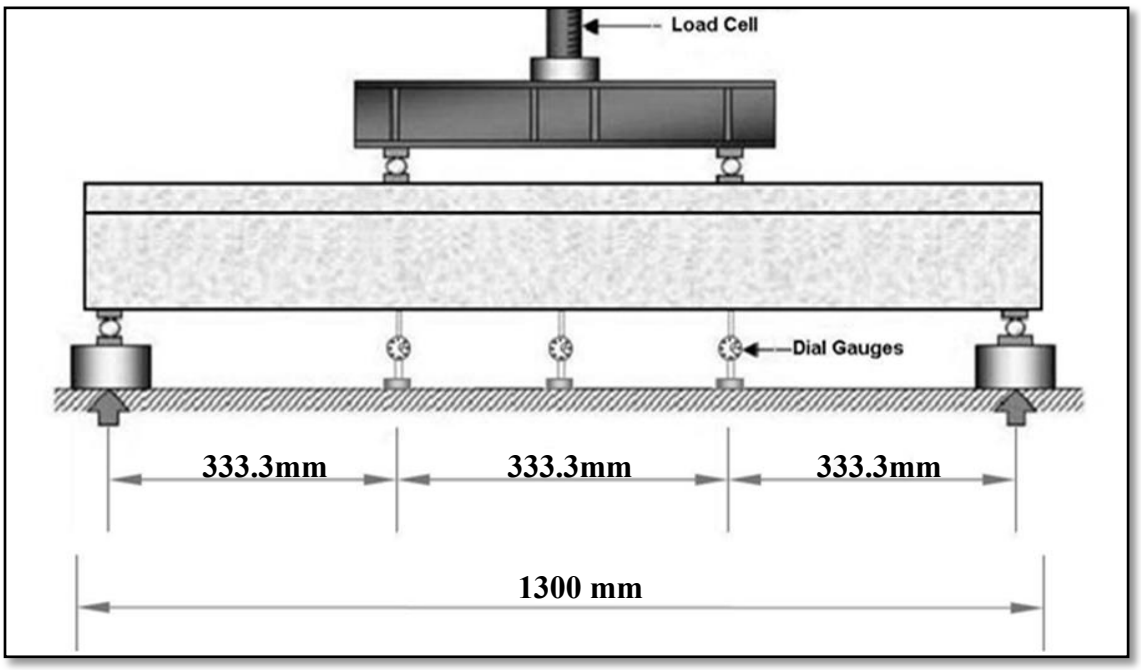

Figure 3.9 Details of the Test setup with location of dial gauges

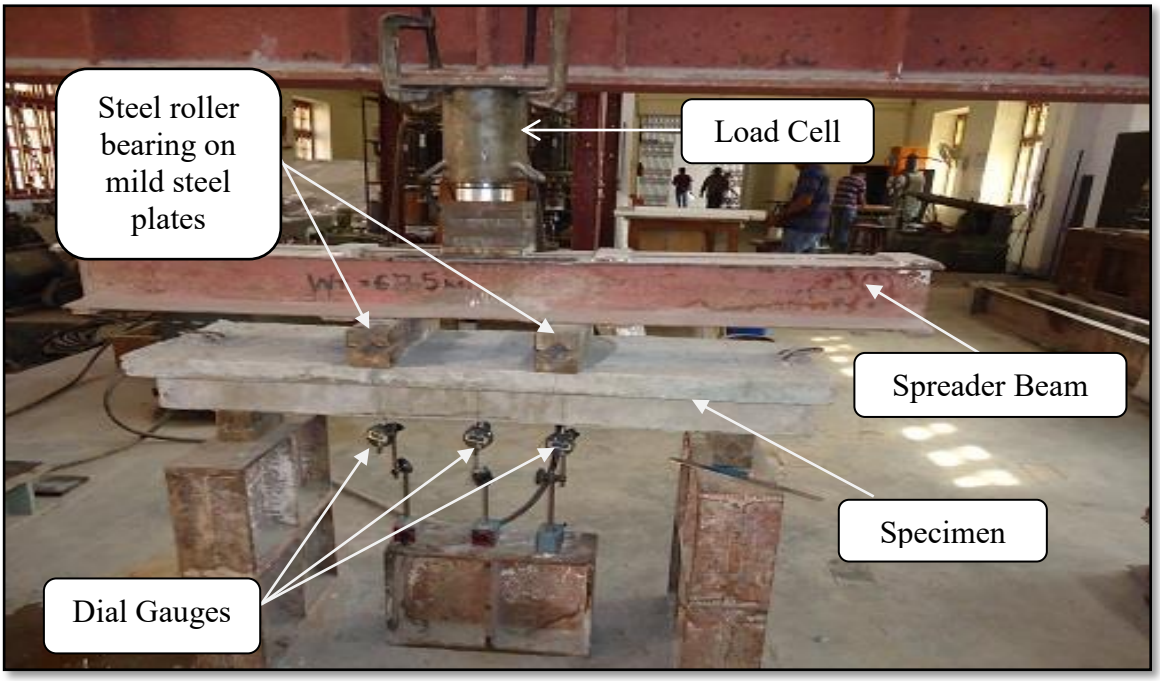

Figure 3.10 Experimental Setup for testing of beams

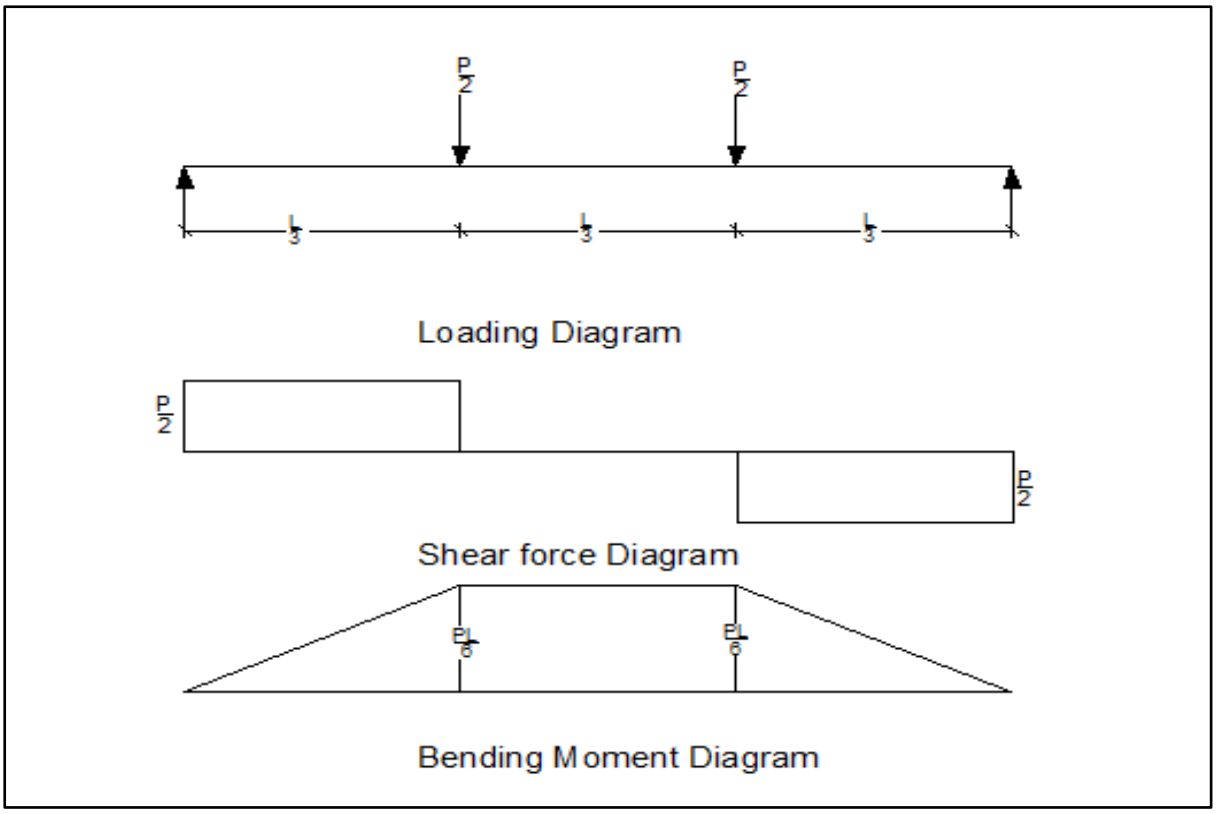

Figure 3.11 Shear force and bending moment diagram for four point static loading

3.6 Description of Specimens

The experimental study comprises of 22 numbers of simply supported RC T-beams divided into two series as described earlier. The longitudinal reinforcement provided at bottom is same for all the beams of two series and consists of 2 numbers of 16 mm φ and 1 number of 12 mm φ bars.

3.6.1 Series A

Series A consists of 13 numbers of RC beams with T-shaped cross-section without transverse openings.

3.6.1.1 BEAM 1

Control Beam (CB)

The control beam (CB) is weak in shear, i.e. shear deficient beam given in Figure 3.12 and is designed to know the behaviour of the shear failure under four point static loading system.

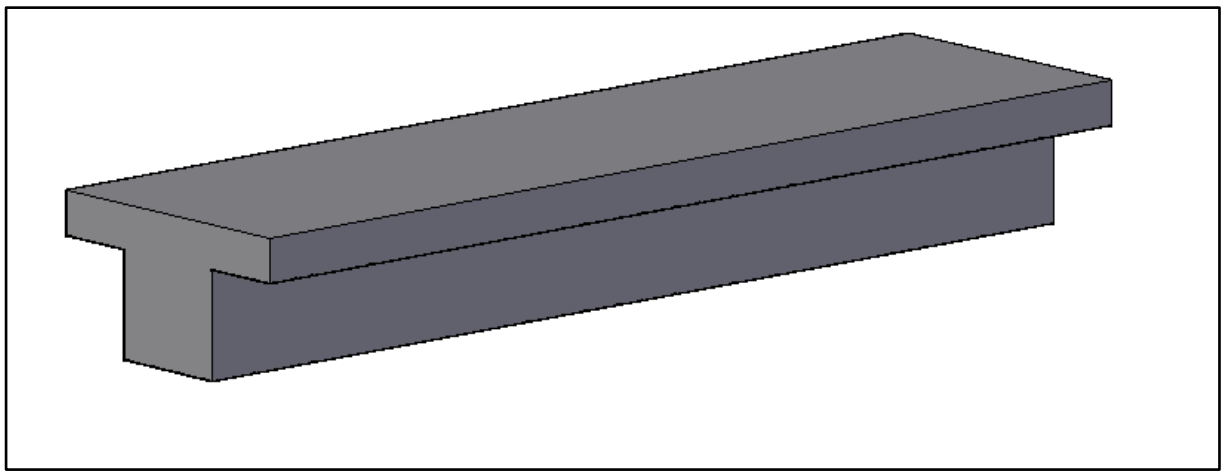

Figure 3.12 Model of control beam (CB)

3.6.1.2 BEAM 2

Strengthened Beam 1 (SB1)

The beam SB1 is strengthened by applying 2 layers of BFRP in 0^0 orientation having U-wrap on the bottommost and web portions in the shear region (i.e. a length of 0 to L/3 and 2L/3 to L from the left support) shown in Figure 3.13. The beam is tested under the same four point static loading system.

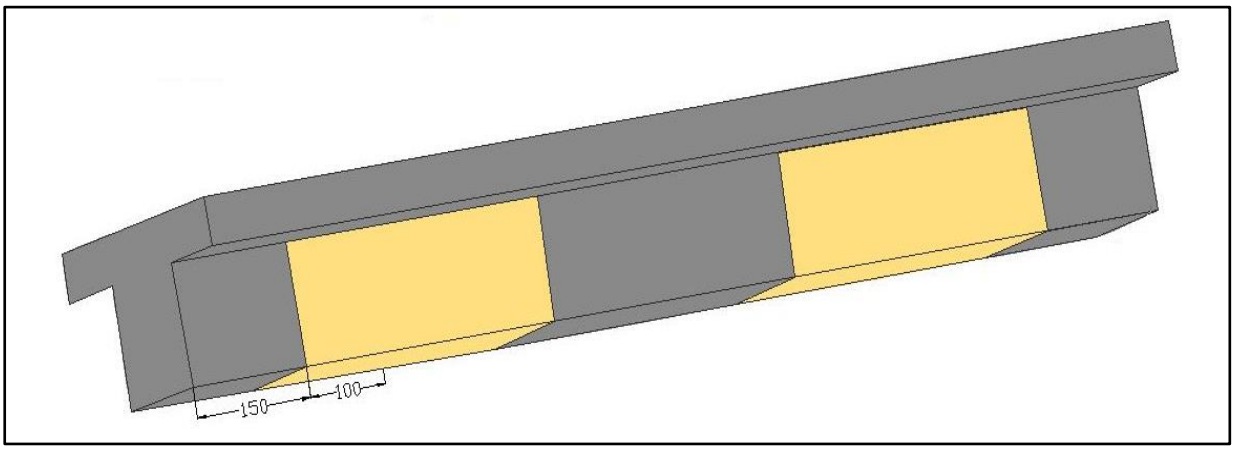

Figure 3.13 Model of beam with 2 layers of BFRP U-wrap in 0^0 orientation (SB1)

3.6.1.3 BEAM 3

Strengthened Beam 2 (SB2)

The beam SB2 is strengthened with 2 layers of BFRP in 0^0 orientation bonded only on the sides of the beam (i.e. on web portions) in the shear region (i.e. a length of 0 to L/3 and 2L/3 to L from the left support) as given in Figure 3.14.

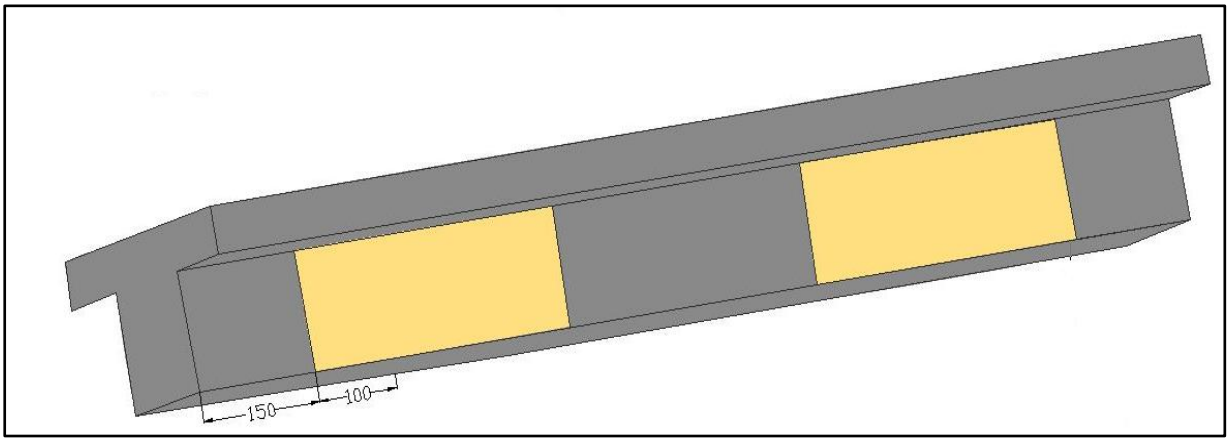

Figure 3.14 Model of beam with 2 layers of BFRP side-wrap in 0^0 orientation (SB2)

3.6.1.4 BEAM 4

Strengthened Beam 3 (SB3)

The beam SB3 is strengthened with BFRP U-strips of 2 layers in 0^0 orientation bonded to the bottommost and web portions in the shear region (i.e. a length of 0 to L/3 and 2L/3 to L from the left support) with 3 strips of equal thickness of 50 mm and spacing between the strips is 50 mm bonded to both the shear spans of the beam as given in Figure 3.15.

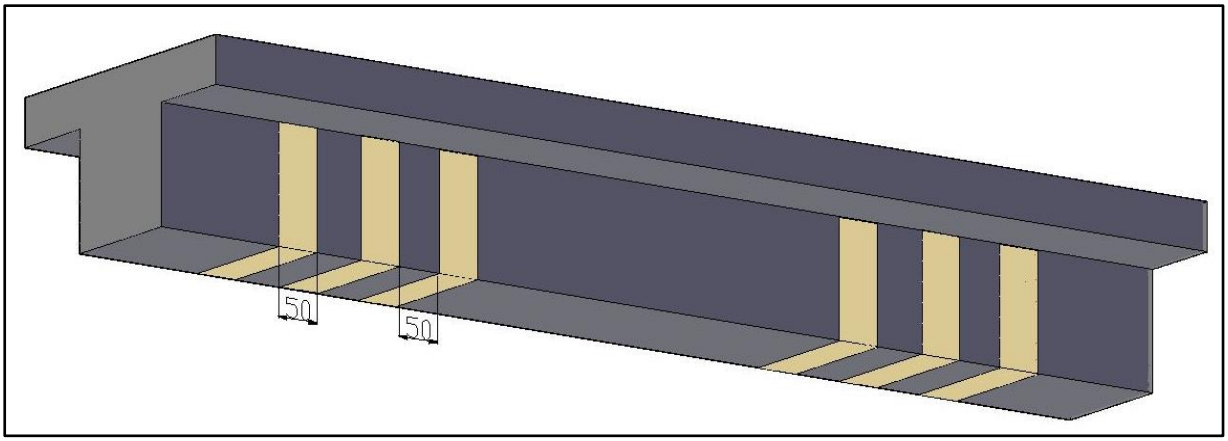

Figure 3.15 Model of beam with 2 layers of BFRP U-strip in 0^0 orientation (SB3)

3.6.1.5 BEAM 5

Strengthened Beam 4 (SB4)

The beam SB4 is strengthened with 2 layers of BFRP strips in 0^0 orientation bonded only on the sides of the beam (i.e. on web portions) in the shear region (i.e. a length of 0 to L/3 and 2L/3 to L from the left support) with 3 strips of equal thickness of 50 mm and spacing between the strips is 50 mm bonded to both the shear spans of the beam as given in Figure 3.16.

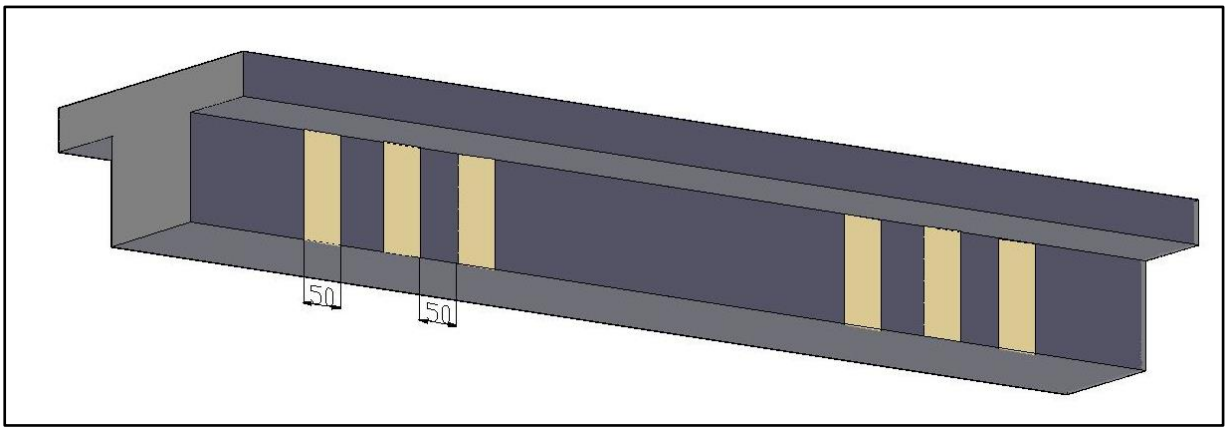

Figure 3.16 Model of beam with 2 layers of BFRP side-strip in 0^0 orientation (SB4)

3.6.1.6 BEAM 6

Strengthened Beam 5 (SB5)

The beam SB5 is strengthened by applying 2 layers of BFRP in 90^0 orientation having U-wrap on the bottommost and web portions in the shear region (i.e. a length of 0 to L/3 and 2L/3 to L from the left support) shown in Figure 3.17.

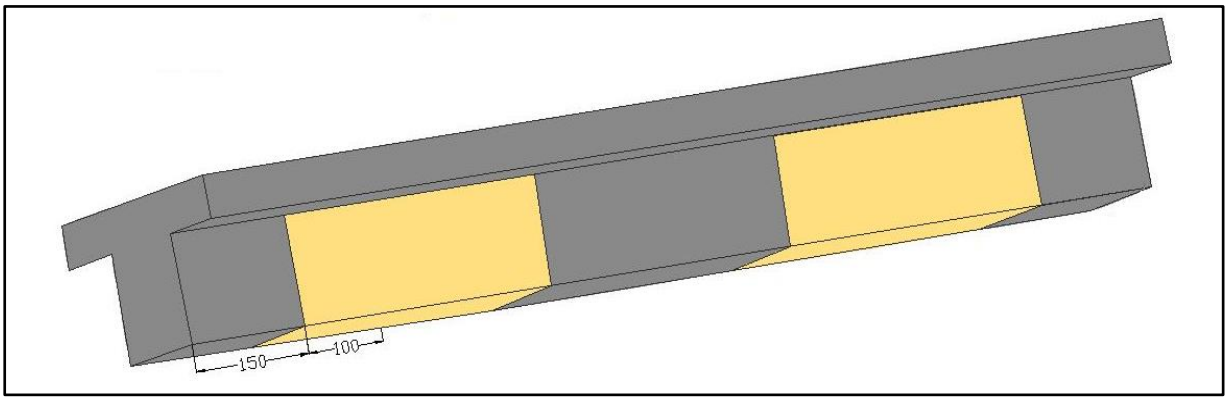

Figure 3.17 Model of beam with 2 layers of BFRP U-wrap in 90^0 orientation (SB5)

3.6.1.7 BEAM 7

Strengthened Beam 6 (SB6)

The beam SB6 is strengthened with 2 layers of BFRP in 90^0 orientation bonded only on the sides of the beam (i.e. on web portions) in the shear region (i.e. a length of 0 to L/3 and 2L/3 to L from the left support) as given in Figure 3.18.

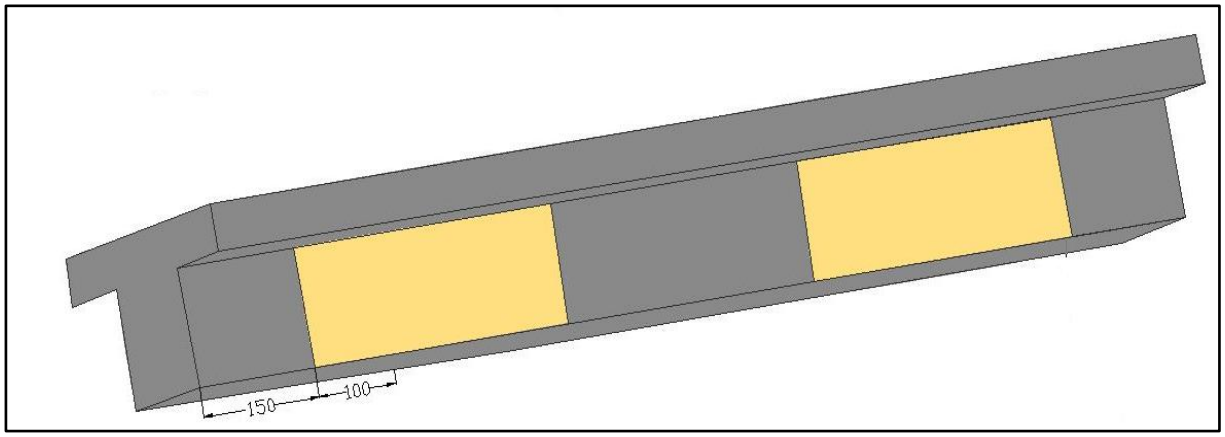

Figure 3.18 Model of beam with 2 layers of BFRP side-wrap in 90^0 orientation (SB6)

3.6.1.8 BEAM 8

Strengthened Beam 7 (SB7)

The beam SB7 is strengthened with BFRP U-strips of 2 layers in 90^0 orientation bonded to the bottommost and web portions in the shear region (i.e. a length of 0 to L/3 and 2L/3 to L from the left support) with 3 strips of equal thickness of 50 mm and spacing between the strips is 50 mm bonded to both the shear spans of the beam as given in Figure 3.19.

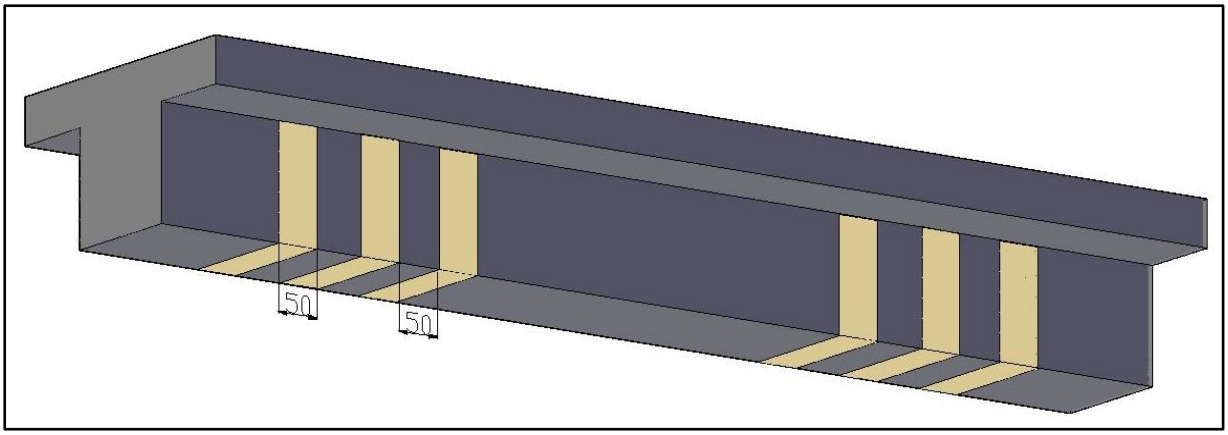

Figure 3.19 Model of beam with 2 layers of BFRP U-strip in 90^0 orientation (SB7)

3.6.1.9 BEAM 9

Strengthened Beam 8 (SB8)

The beam SB8 is strengthened with 2 layers of BFRP strips in 90^0 orientation bonded only on the sides of the beam (i.e. on web portions) in the shear region (i.e. a length of 0 to L/3 and 2L/3 to L from the left support) with 3 strips of equal thickness of 50 mm and spacing between the strips is 50 mm bonded to both the shear spans of the beam as given in Figure 3.20.

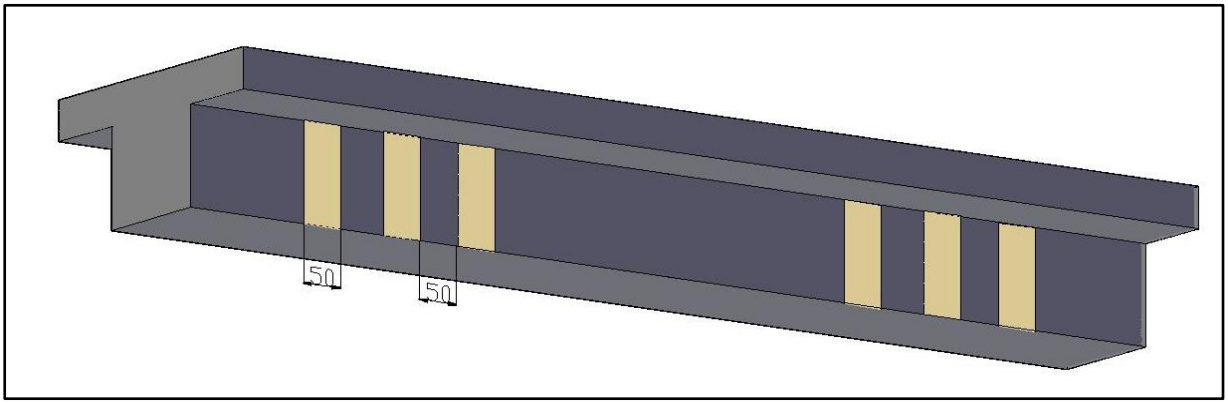

Figure 3.20 Model of beam with 2 layers of BFRP side-strip in 90^0 orientation (SB8)

3.6.1.10 BEAM 10

Strengthened Beam 9 (SB9)

The beam SB9 is strengthened with BFRP U-strips of 2 layers inclined with 45^0 bonded to the bottommost and web portions in the shear region (i.e. a length of 0 to L/3 and 2L/3 to L from the left support) with 3 strips of equal thickness of 50 mm and spacing between the strips is 50 mm bonded to both the shear spans of the beam as given in Figure 3.21.

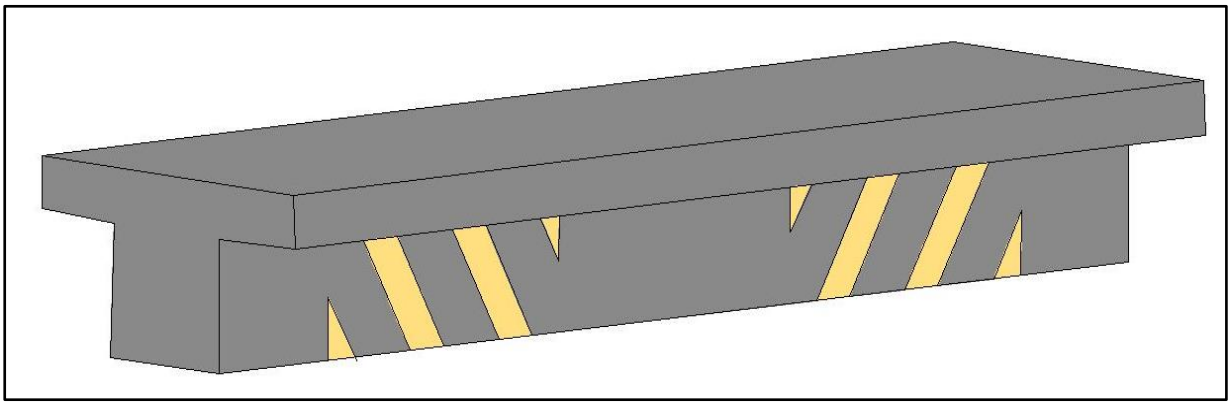

Figure 3.21 Model of beam with 2 layers of BFRP U-strip in 45^0 orientation (SB9)

3.6.1.11 BEAM 11

Strengthened Beam 10 (SB10)

The beam SB10 is strengthened by applying 2 layers of BFRP in 90^0 orientation having U-wrap on the bottommost and web portions in the shear region (i.e. a length of 0 to L/3 and 2L/3 to L from the left support) provided with an anchorage system as shown in Figure 3.22.

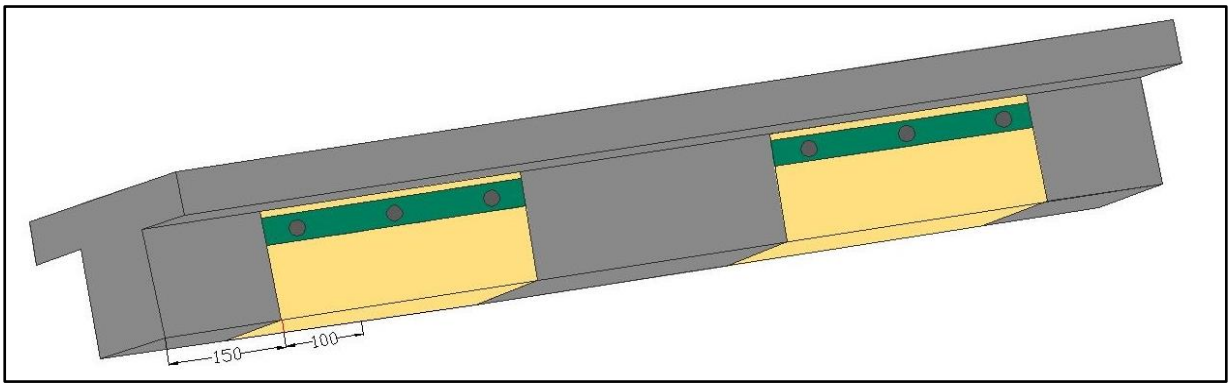

Figure 3.22 Model of beam with 2 layers of BFRP U-wrap in 90^0 orientation with end anchorage (SB10)

3.6.1.12 BEAM 12

Strengthened Beam 11 (SB11)

The beam SB11 is strengthened with 4 layers of BFRP in 90^0 orientation having U-wrap on the bottommost and web portions in the shear region (i.e. a length of 0 to L/3 and 2L/3 to L from the left support) provided with an anchorage system as depicted in Figure 3.23.

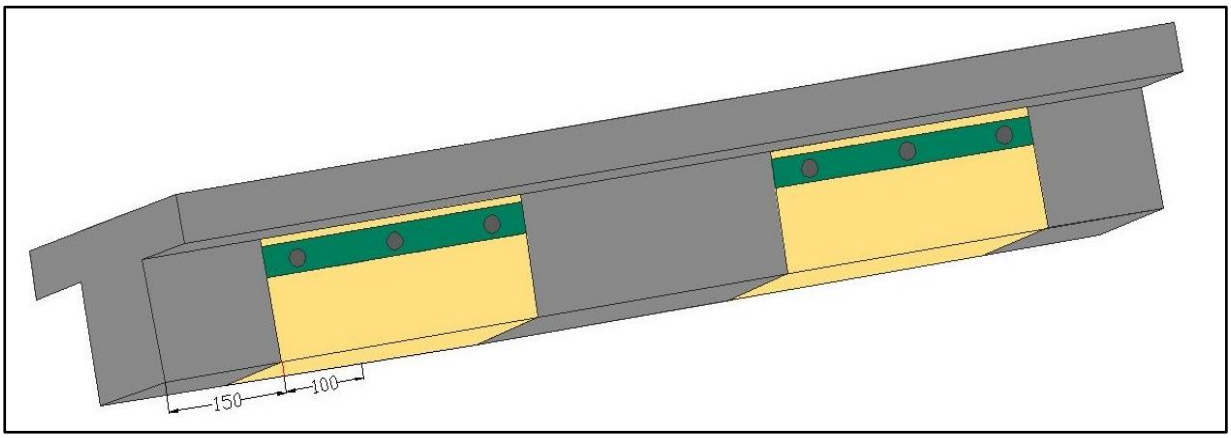

Figure 3.23 Model of beam with 4 layers of BFRP U-wrap in 90^0 orientation with end anchorage (SB11)

3.6.1.13 BEAM 13

Strengthened Beam 12 (SB12)

The beam SB12 is strengthened with BFRP U-strips of 2 layers in 90^0 orientation bonded to the bottommost and web portions in the shear region (i.e. a length of 0 to L/3 and 2L/3 to L from the left support) provided with an anchorage system with 3 strips of equal thickness of 50 mm and spacing between the strips is 50 mm bonded to both the shear spans of the beam as given in Figure 3.24.

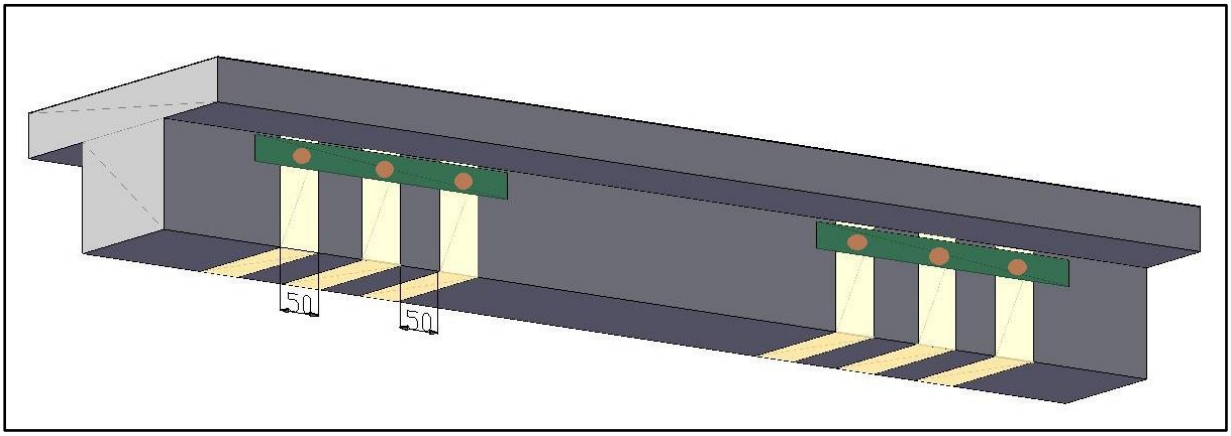

Figure 3.24 Model of beam with 2 layers of BFRP U-strip in 90^0 orientation with end anchorage (SB12)

3.6.2 Series B

Series B consists of 9 numbers of RC beams with T-shaped cross-section with transverse openings of different shapes (circular, rectangular and square).

3.6.2.1 BEAM 14

Control Beam 1 (CB1)

The control beam (CB1) is provided with circular shape web openings in the shear zone and is weak in shear i.e. shear deficient beam given in Figure 3.25.

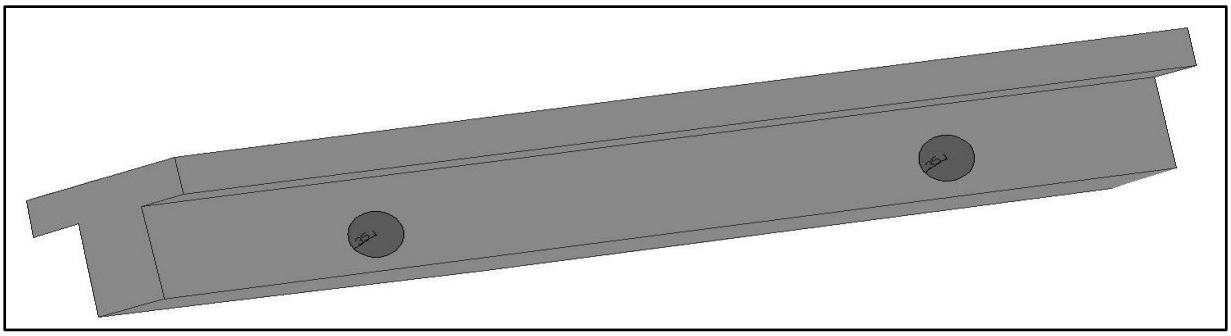

Figure 3.25 Model of control beam with Circular web openings (CB1)

3.6.2.2 BEAM 15

Strengthened Beam 13 (SB13)

The beam SB13 is strengthened with 4 layers of BFRP in 90^0 orientation having U-wrap on the bottommost and web portions in the shear region (i.e. a length of 0 to L/3 and 2L/3 to L from the left support) with circular shape web openings in the shear zone of the RC beam as shown in Figure 3.26.

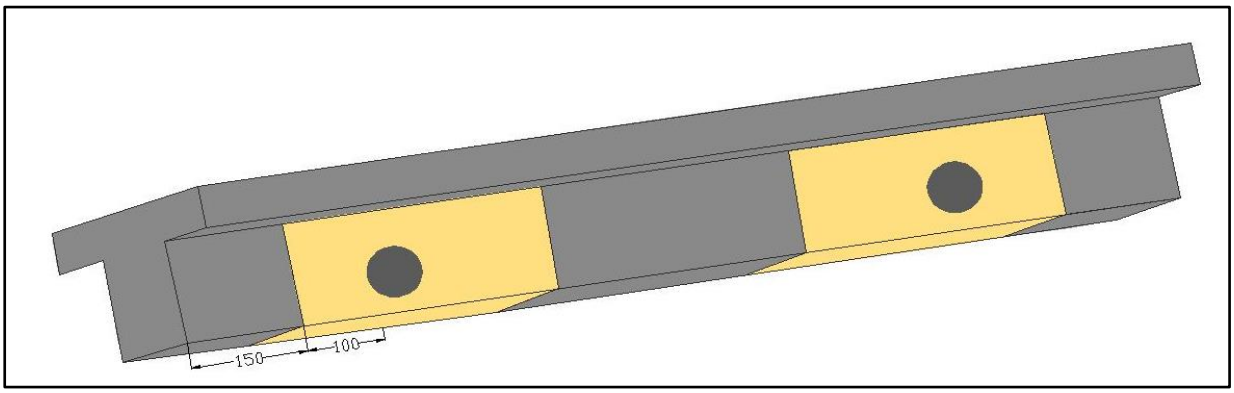

Figure 3.26 Model of beam with 4 layers of BFRP U-wrap in 90^0 orientation with circular web openings (SB13)

3.6.2.3 BEAM 16

Strengthened Beam 14 (SB14)

The beam SB14 is strengthened by applying 4 layers of BFRP in 90^0 orientation having U-wrap on the bottommost and web portions in the shear region (i.e. a length of 0 to L/3 and 2L/3 to L from the left support) with circular shape web openings in the shear zone of the RC beam provided with an anchorage system as shown in Figure 3.27.

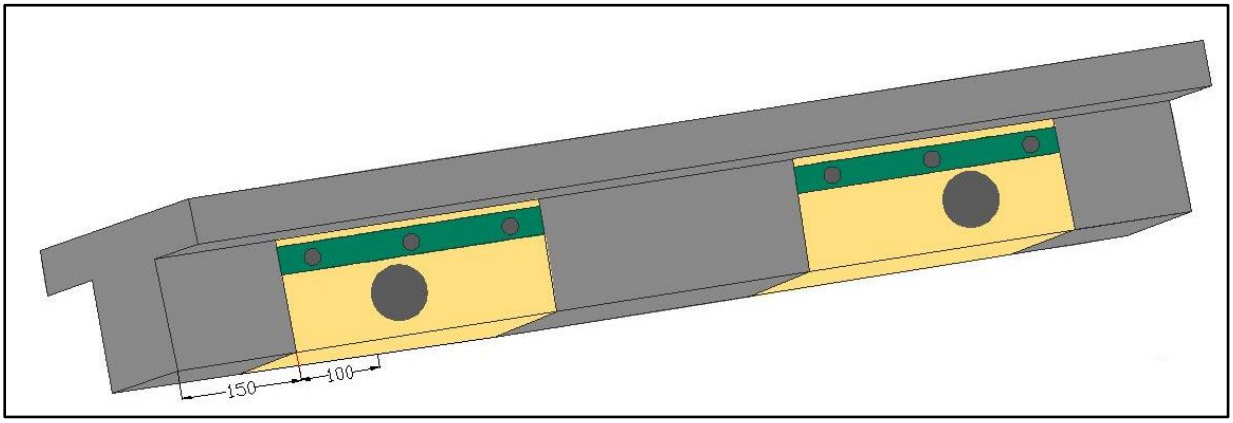

Figure 3.27 Model of beam with 4 layers of BFRP U-wrap in 90^0 orientation with circular web openings and anchorage system (SB14)

3.6.2.4 BEAM 17

Control Beam 2 (CB2)

The control beam (CB2) is provided with rectangular shape web openings in the shear zone and is weak in shear i.e. shear deficient beam given in Figure 3.28.

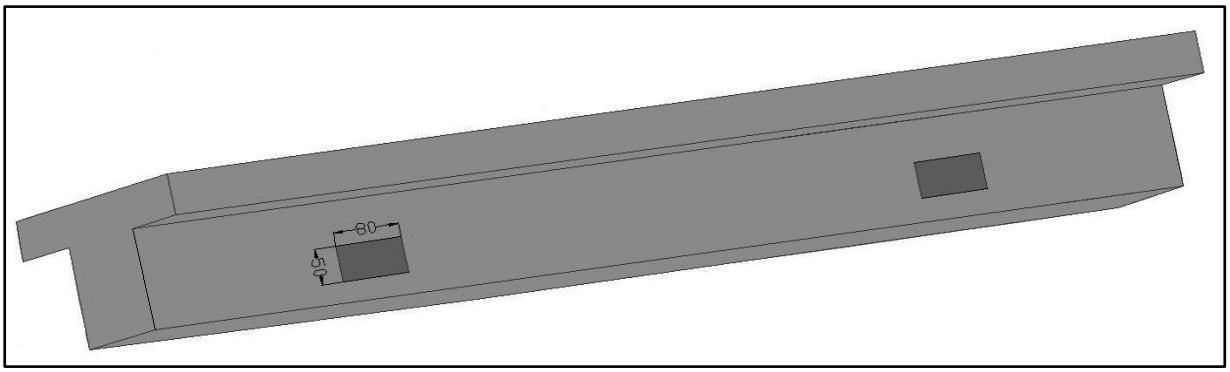

Figure 3.28 Model of control beam with rectangular web openings (CB2)

3.6.2.5 BEAM 18

Strengthened Beam 15 (SB15)

The beam SB15 is strengthened with 4 layers of BFRP in 90^0 orientation having U-wrap on the bottommost and web portions in the shear region (i.e. a length of 0 to L/3 and 2L/3 to L from the left support) with rectangular shape web openings in the shear zone of the RC beam as shown in Figure 3.29.

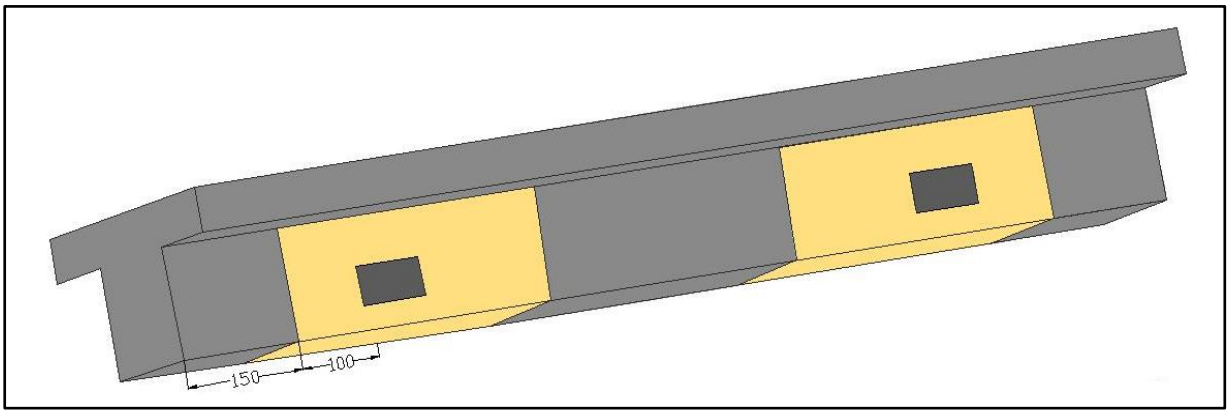

Figure 3.29 Model of beam with 4 layers of BFRP U-wrap in 90^0 orientation with rectangular web openings (SB15)

3.6.2.6 BEAM 19

Strengthened Beam 16 (SB16)

The beam SB16 is strengthened by applying 4 layers of BFRP in 90^0 orientation having U-wrap on the bottommost and web portions in the shear region (i.e. a length of 0 to L/3 and 2L/3 to L from the left support) with rectangular shape web openings in the shear zone of the RC beam provided with an anchorage system as depicted in Figure 3.30.

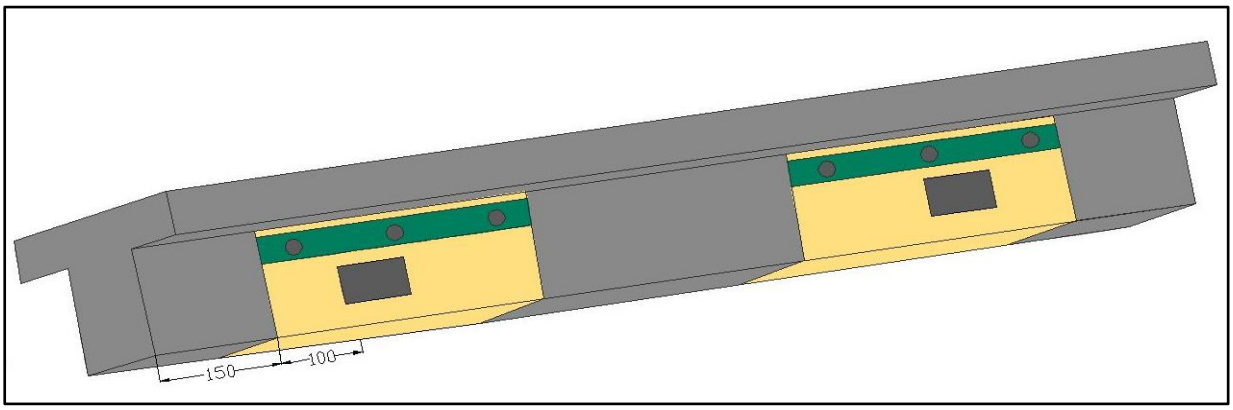

Figure 3.30 Model of beam with 4 layers of BFRP U-wrap in 90^0 orientation with rectangular web openings and anchorage system (SB16)

3.6.2.7 BEAM 20

Control Beam 3 (CB3)

The control beam (CB3) is provided with square shape web openings in the shear zone and is weak in shear i.e. shear deficient beam given in Figure 3.31.

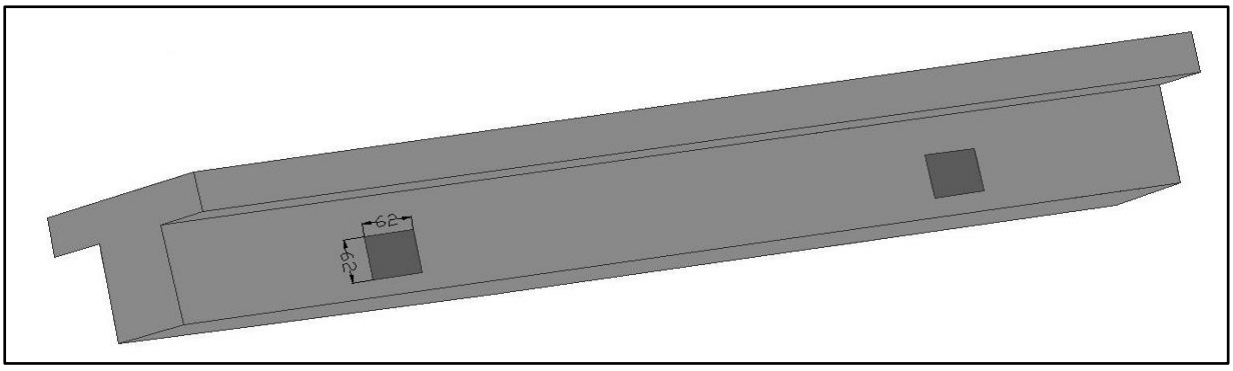

Figure 3.31 Model of control beam with square web openings (CB3)

3.6.2.8 BEAM 21

Strengthened Beam 17 (SB17)

The beam SB17 is strengthened with 4 layers of BFRP in 90^0 orientation having U-wrap on the bottommost and web portions in the shear region (i.e. a length of 0 to L/3 and 2L/3 to L from the left support) with square shape web openings in the shear zone of the RC beam as shown in Figure 3.32.

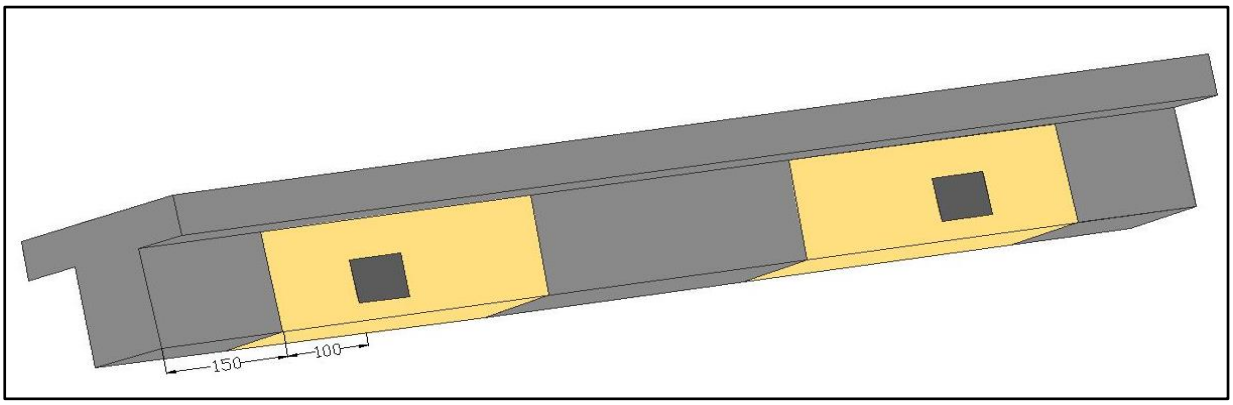

Figure 3.32 Model of beam with 4 layers of BFRP U-wrap in 90^0 orientation with square web openings (SB17)

3.6.2.9 BEAM 22

Strengthened Beam 18 (SB18)

The beam SB18 is strengthened by applying 4 layers of BFRP in 90^0 orientation having U-wrap on the bottommost and web portions in the shear region (i.e. a length of 0 to L/3 and 2L/3 to L from the left support) with square shape web openings in the shear zone of the RC beam provided with an anchorage system as depicted in Figure 3.33.

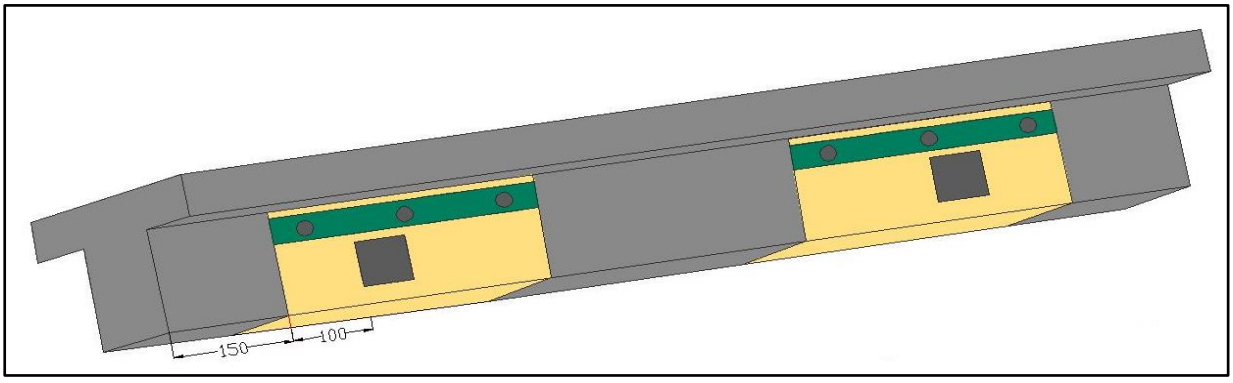

Figure 3.33 Model of beam with 4 layers of BFRP U-wrap in 90^0 orientation with square web openings and anchorage system (SB18)

3.7 Summary

In this experimental program, twenty two numbers of beams are investigated which are separated into two series (A and B). The detail descriptions of all the beams of two series (A and B) are presented in Table 3.6.

Table 3.6 Beam material properties and test parameters

Beam ID	f_c **(MPa)**	**Tension Reinforcement**	**Yield Stress** f_y **(MPa)**	**FRP Thickness (mm)**	**Strengthening Scheme using BFRP sheet**
CB	23.1	2-16mmφ, 1-12mmφ	494, 578	--	Control Beam (without FRP sheets)
SB1	25.27	2-16mmφ, 1-12mmφ	494, 578	0.56	Two layers continuous bonded horizontally to the bottom and sides of shear span of beam (U-wrap)
SB2	24.67	2-16mmφ, 1-12mmφ	494, 578	0.56	Two layers continuous bonded horizontally only to the sides of shear span of beam (Side wrap)
SB3	24.33	2-16mmφ, 1-12mmφ	494, 578	0.56	Two layers strip bonded horizontally to the bottom and sides of shear span of beam (U-strip)

SB4	23.36	2-16mmφ, 1-12mmφ	494, 578	0.56	Two layers strip bonded horizontally only to the sides of shear span of beam (Side strip)
SB5	28	2-16mmφ, 1-12mmφ	494, 578	0.56	Two layers continuous bonded vertically to the bottom and sides of shear span of beam (U-wrap)
SB6	26.81	2-16mmφ, 1-12mmφ	494, 578	0.56	Two layers continuous bonded vertically only to the sides of shear span of beam (Side wrap)
SB7	26.07	2-16mmφ, 1-12mmφ	494, 578	0.56	Two layers strip bonded vertically to the bottom and sides of shear span of beam (U-strip)
SB8	24.45	2-16mmφ, 1-12mmφ	494, 578	0.56	Two layers strip bonded vertically only to the sides of shear span of beam (Side strip)
SB9	28.03	2-16mmφ, 1-12mmφ	494, 578	0.56	Two layers bonded in inclined strip (45^0) to the bottom and sides of shear span of beam (U-strip)

SB10	28.33	2-16mmφ, 1-12mmφ	494, 578	0.56	Two layers continuous bonded vertically to the bottom and sides with composite plate bolt arrangement i.e., anchoring system only in shear span of beam (U-wrap)
SB11	28.89	2-16mmφ, 1-12mmφ	494, 578	1.07	Four layers continuous bonded vertically to the bottom and sides with composite plate bolt arrangement i.e., anchoring system only in shear span of beam (U-wrap)
SB12	28	2-16mmφ, 1-12mmφ	494, 578	0.56	Two layers strip bonded vertically to the bottom and sides with composite plate bolt arrangement i.e., anchoring system only in shear span of beam (U-strip)
CB1	23.55	2-16mmφ, 1-12mmφ	494, 578	--	Control Beam with circular hole (without FRP sheets)

SB13	26.22	2-16mmφ, 1-12mmφ	494, 578	1.07	Four layers continuous bonded vertically to the bottom and sides of shear span excluding the circular hole part of beam (U-wrap)
SB14	28.65	2-16mmφ, 1-12mmφ	494, 578	1.07	Four layers continuous bonded vertically to the bottom and sides of shear span excluding the circular hole part with composite plate bolt arrangement i.e., anchoring system of beam (U-wrap)
CB2	26.14	2-16mmφ, 1-12mmφ	494, 578	--	Control Beam with rectangular hole (without FRP sheets)
SB15	28.14	2-16mmφ, 1-12mmφ	494, 578	1.07	Four layers continuous bonded vertically to the bottom and sides of shear span excluding the rectangular hole part of beam (U-wrap)

SB16	27.26	2-16mmφ, 1-12mmφ	494, 578	1.07	Four layers continuous bonded vertically to the bottom and sides of shear span excluding the rectangular hole part with composite plate bolt arrangement i.e., anchoring system of beam (U-wrap)
CB3	23.26	2-16mmφ, 1-12mmφ	494, 578	--	Control Beam with square hole (without FRP sheets)
SB17	29.04	2-16mmφ, 1-12mmφ	494, 578	1.07	Four layers continuous bonded vertically to the bottom and sides of shear span excluding the square hole part of beam (U-wrap)

SB18	25.18	2-16mmφ, 1-12mmφ	494, 578	1.07	Four layers continuous bonded vertically to the bottom and sides of shear span excluding the square hole part with composite plate bolt arrangement i.e., anchoring system of beam (U-wrap)

CHAPTER 4

4 TEST RESULTS AND DISCUSSIONS

4.1 Introduction

This chapter interprets the results obtained from the experimental investigation which comprises of testing twenty two numbers of RC T-beams divided into two series (A and B). The series A comprises of the shear strengthening of the RC beams with T-shaped cross-section without transverse openings and the series B dealt with the shear strengthening of the RC T-beams with transverse openings of different shapes. The behaviour of the RC T-beams with respect to initial crack load, ultimate load carrying capacity, crack pattern, deflection is studied throughout the test and their failure modes are described.

Except the control beams, all the beams are strengthened with various configurations of unidirectional BFRP sheets/strips. All the beams are made as shear deficient ones.

4.1.1 Series A

The beam SB1 is strengthened by applying 2 layers of unidirectional BFRP sheets in 0^0 orientation having U-wrap on the bottom and web portions in the shear region (i.e. a length of 0 to L/3 and 2L/3 to L from the left support) of the beam. The beam SB2 is strengthened with 2 layers of unidirectional BFRP sheets in 0^0 orientation bonded only on the sides of the beam (i.e. on web portions) in the shear region (i.e. a length of 0 to L/3 and 2L/3 to L from the left support). The beam SB3 is strengthened with unidirectional BFRP U-strips of 2 layers in 0^0 orientation bonded to the bottommost and web portions in the shear region (i.e. a length of 0 to L/3 and 2L/3 to L from the left support). The beam SB4 is strengthened with 2 layers of unidirectional BFRP strips in 0^0 orientation bonded only on the sides of the beam (i.e. on web portions) in the shear region (i.e. a length of 0 to L/3 and 2L/3 to L from the left support). The beam SB5 is strengthened by applying 2 layers of unidirectional BFRP sheets in 90^0 orientation having U-wrap on the bottommost and web portions in the shear region (i.e. a length of 0 to L/3 and 2L/3 to L from the left support). The beam SB6 is strengthened with 2 layers of unidirectional BFRP sheets in 90^0 orientation bonded only on the sides of the beam (i.e. on web portions) in the shear region (i.e. a length of 0 to L/3 and 2L/3 to L from the left

support). The beam SB7 is strengthened with unidirectional BFRP U-strips of 2 layers in 90^0 orientation bonded to the bottommost and web portions in the shear region (i.e. a length of 0 to L/3 and 2L/3 to L from the left support). The beam SB8 is strengthened with 2 layers of unidirectional BFRP strips in 90^0 orientation bonded only on the sides of the beam (i.e. on web portions) in the shear region (i.e. a length of 0 to L/3 and 2L/3 to L from the left support). The beam SB9 is strengthened with unidirectional BFRP U-strips of 2 layers inclined with 45^0 bonded to the bottommost and web portions in the shear region (i.e. a length of 0 to L/3 and 2L/3 to L from the left support). The beam SB10 is strengthened by applying 2 layers of unidirectional BFRP sheets in 90^0 orientation having U-wrap on the bottommost and web portions in the shear region (i.e. a length of 0 to L/3 and 2L/3 to L from the left support) provided with an anchorage system comprising of laminated composite plate with nut and bolt arrangement. The beam SB11 is strengthened with 4 layers of unidirectional BFRP sheets in 90^0 orientation having U-wrap on the bottommost and web portions in the shear region (i.e. a length of 0 to L/3 and 2L/3 to L from the left support) provided with an anchorage system comprising of laminated composite plate with nut and bolt arrangement. The beam SB12 is strengthened with unidirectional BFRP U-strips of 2 layers in 90^0 orientation bonded to the bottommost and web portions in the shear region (i.e. a length of 0 to L/3 and 2L/3 to L from the left support) provided with an anchorage system comprising of laminated composite plate with nut and bolt arrangement.

4.1.2 Series B

The beam SB13 is strengthened with 4 layers of unidirectional BFRP sheets in 90^0 orientation having U-wrap on the bottommost and web portions in the shear region (i.e. a length of 0 to L/3 and 2L/3 to L from the left support) excluding the circular web openings in the shear zone of the RC beam. The beam SB14 is strengthened by applying 4 layers of unidirectional BFRP sheets in 90^0 orientation having U-wrap on the bottommost and web portions in the shear region (i.e. a length of 0 to L/3 and 2L/3 to L from the left support) excluding the circular web openings in the shear zone of the RC beam provided with an anchorage system comprising of laminated composite plate with nut and bolt arrangement. The beam SB15 is strengthened with 4 layers of unidirectional BFRP sheets in 90^0 orientation having U-wrap on the bottommost and web portions in the shear region (i.e. a length of 0 to L/3 and 2L/3 to L from the left support) excluding the rectangular web

openings in the shear zone of the RC beam. The beam SB16 is strengthened by applying 4 layers of unidirectional BFRP sheets in 90^0 orientation having U-wrap on the bottommost and web portions in the shear region (i.e. a length of 0 to L/3 and 2L/3 to L from the left support) excluding the rectangular web openings in the shear zone of the RC beam provided with an anchorage system comprising of laminated composite plate with nut and bolt arrangement. The beam SB17 is strengthened with 4 layers of unidirectional BFRP sheets in 90^0 orientation having U-wrap on the bottommost and web portions in the shear region (i.e. a length of 0 to L/3 and 2L/3 to L from the left support) excluding the square web openings in the shear zone of the RC beam. The beam SB18 is strengthened by applying 4 layers of unidirectional BFRP sheets in 90^0 orientation having U-wrap on the bottommost and web portions in the shear region (i.e. a length of 0 to L/3 and 2L/3 to L from the left support) excluding the square web openings in the shear zone of the RC beam provided with an anchorage system comprising of laminated composite plate with nut and bolt arrangement.

4.2 Crack Behaviour and Failure Modes

The twenty two numbers of RC T-beams are tested under four point static loading system and their cracking behaviour and modes of failure are reported below.

4.2.1 Series A

4.2.1.1 Control Beam (CB)

The control beam (CB) is not strengthened with BFRP composites to study the behaviour of the shear failure without strengthening. It is a shear deficient beam and is tested under the four point static loading system by applying the point loads gradually. The experimental set-up for the control beam under four point static loading frame is shown in Figure 4.1(a). The first hair line crack appeared at a load of 60kN in the shear region of the beam as given in Figure 4.1(b). As the load increased, additional shear cracks are developed and the primary visible crack undergoes widening and propagated as shown in Figure 4.1(c). With the further increase in load, the beam exhibited a wider diagonal shear crack and finally failed in shear at a load of 158kN as illustrated in Figure 4.1(d).

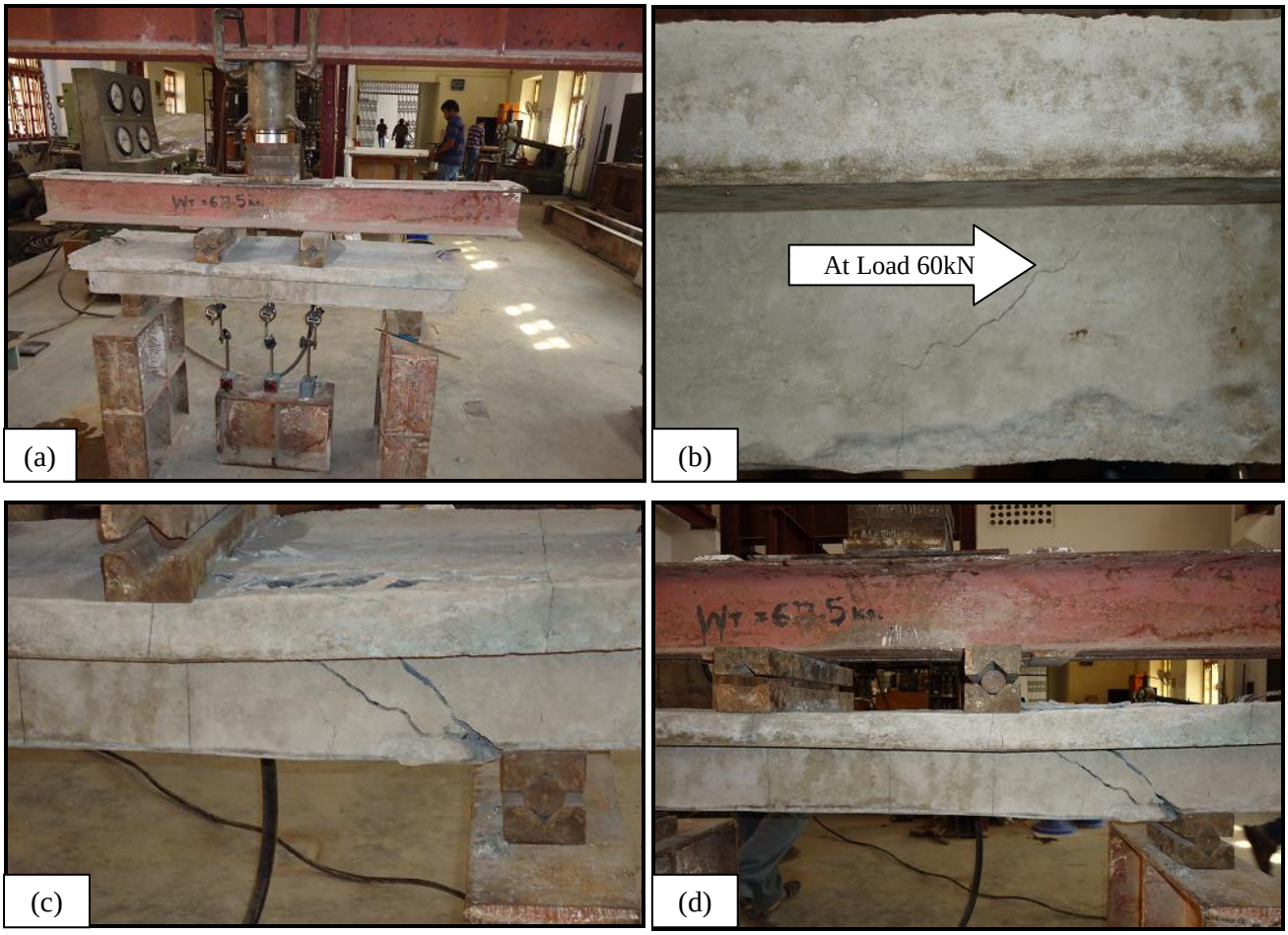

Figure 4.1 (a) Experimental Setup of CB under four-point loading system, (b) Hair line crack started in shear region at a load of 60kN, (c) Crack pattern near Right support, (d) Crack pattern at ultimate failure

4.2.1.2 Strengthened Beam 1 (SB1)

The beam SB1 is strengthened by applying 2 layers of unidirectional BFRP sheets in 0^0 orientation having U-wrap on the bottom and web portions in the shear region (i.e. a length of 0 to L/3 and 2L/3 to L from the left support) of the beam. The experimental setup of the beam SB1 is given in Figure 4.2(a). The initial hair line crack could not be visualized on the concrete surface because the shear regions are completely wrapped with BFRP sheets. The failure of the beam SB1 is initiated due to the splitting of BFRP sheets over the principal shear crack in the same region as appeared in the control beam. Finally the beam failed by the debonding of BFRP sheets followed by a film concrete deposit adhered to them as given in Figure 4.2(b). The failure is followed by a diagonal shear failure with the increasing load and the beam failed at an ultimate load of 178kN as given in Figure 4.2(c). The strengthening of

beam SB1 with BFRP sheets in 0^0 orientation having U-wraps caused 12.66% increase in shear capacity over the control beam.

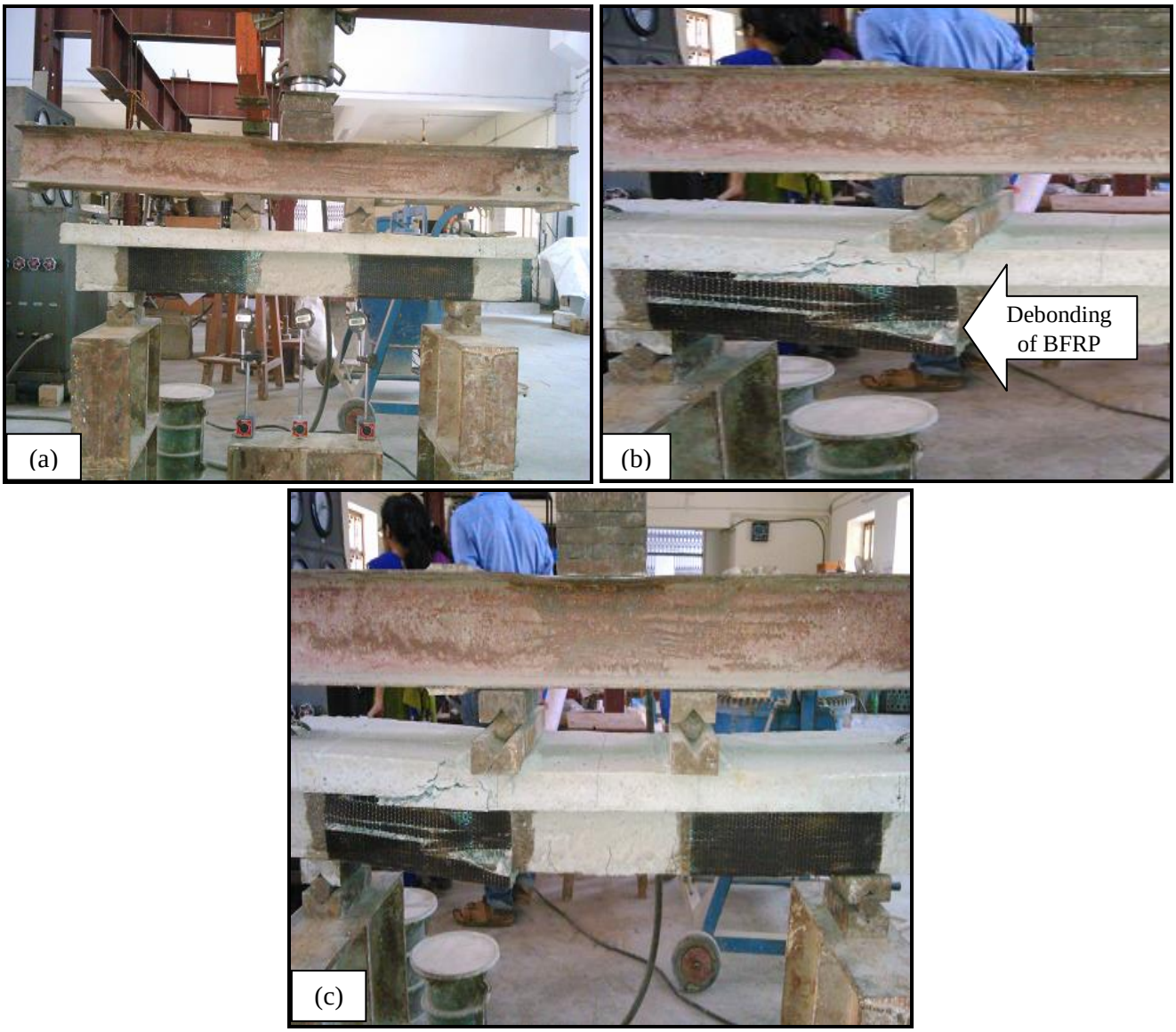

Figure 4.2 (a) Experimental Setup of beam SB1 under four-point loading system, (b) Debonding of BFRP sheet at ultimate load, (c) Ultimate failure of beam SB1 by debonding of BFRP sheet followed by diagonal shear crack

4.2.1.3 Strengthened Beam 2 (SB2)

The beam SB2 is strengthened with 2 layers of unidirectional BFRP sheets in 0^0 orientation bonded only on the sides of the beam (i.e. on web portions) in the shear zone (i.e. a length of 0 to L/3 and 2L/3 to L from the left support). The experimental setup of the beam SB2 is given in Figure 4.3(a). The initial hair line crack could not be traced out on the concrete

surface because the shear zones are fully covered with BFRP sheets. The failure of the beam S2 is started due to the splitting of BFRP sheets in the same region as appeared in the beam SB1. Finally the beam failed by the debonding of BFRP sheets followed by a film concrete deposit adhered to them as given in Figure 4.3(b). The ultimate failure is followed by a diagonal shear failure with the increasing load and the beam failed at an ultimate load of 167kN as given in Figure 4.3(c). The strengthening of beam SB2 caused 5.69% increase in shear capacity over the control beam.

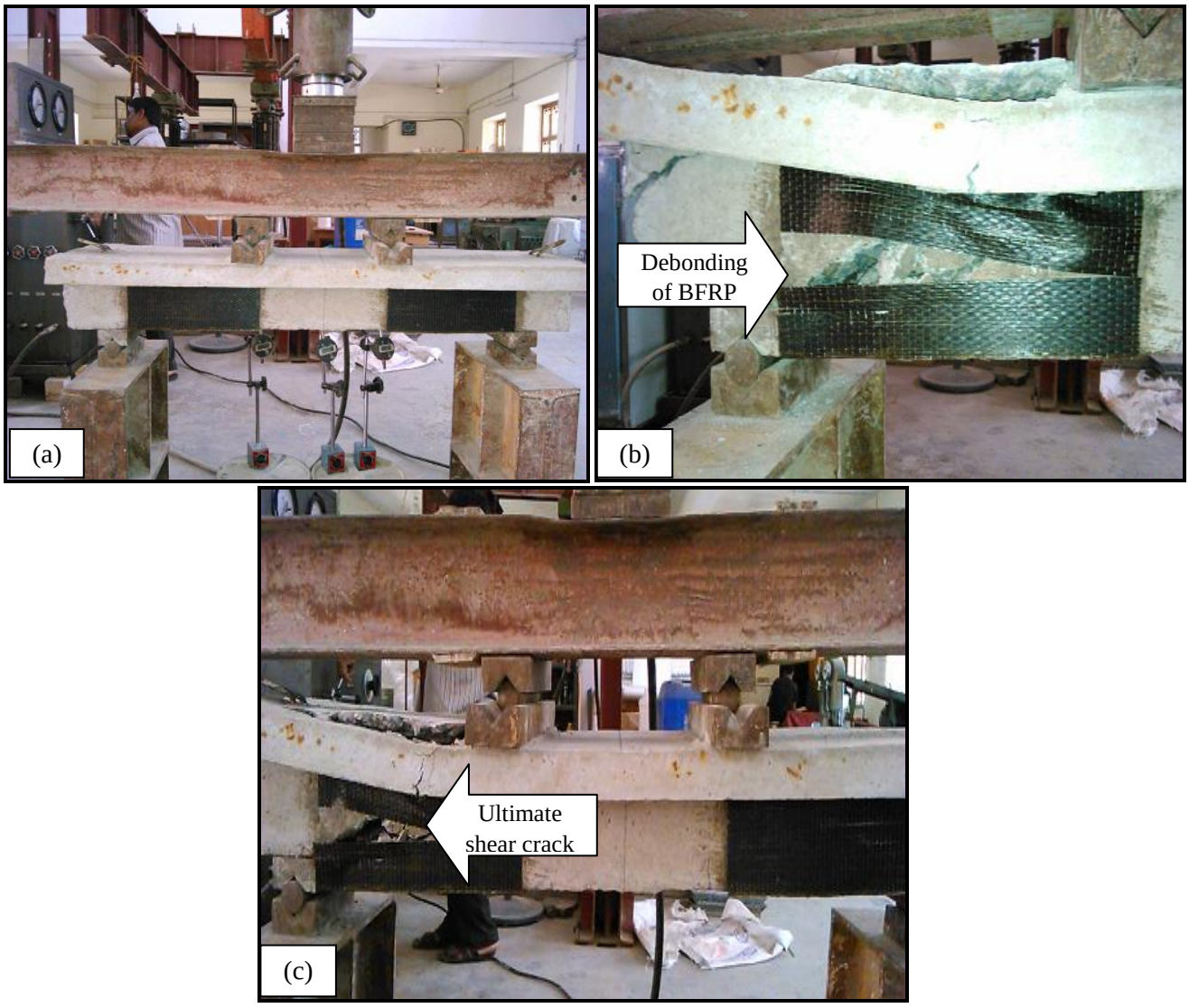

Figure 4.3 (a) Experimental Setup of beam SB2 under four-point loading system, (b) Debonding of BFRP sheet at ultimate load, (c) Ultimate failure of beam SB2 by debonding of BFRP sheet followed by diagonal shear crack

4.2.1.4 Strengthened Beam 3 (SB3)

The beam SB3 is strengthened with BFRP U-strips of 2 layers in 0^0 orientation bonded to the bottommost and web portions in the shear region (i.e. a length of 0 to L/3 and 2L/3 to L from the left support) with 3 strips of equal width of 50 mm and spacing between the strips is 50 mm bonded to both the shear spans of the beam. The experimental setup of the beam SB3 is given in Figure 4.4(a). The first hair line crack is appeared on the concrete surface at a load of 75kN in the shear region of the beam as given in Figure 4.4(b). The failure of the beam SB3 occurred at an ultimate load of 170kN and the ultimate shear failure is due to the debonding of the BFRP strips followed by a wider diagonal shear crack as illustrated in Figure 4.4(c) . The strengthening of beam SB3 with BFRP U-strips caused 7.59% increase in shear capacity over the control beam.

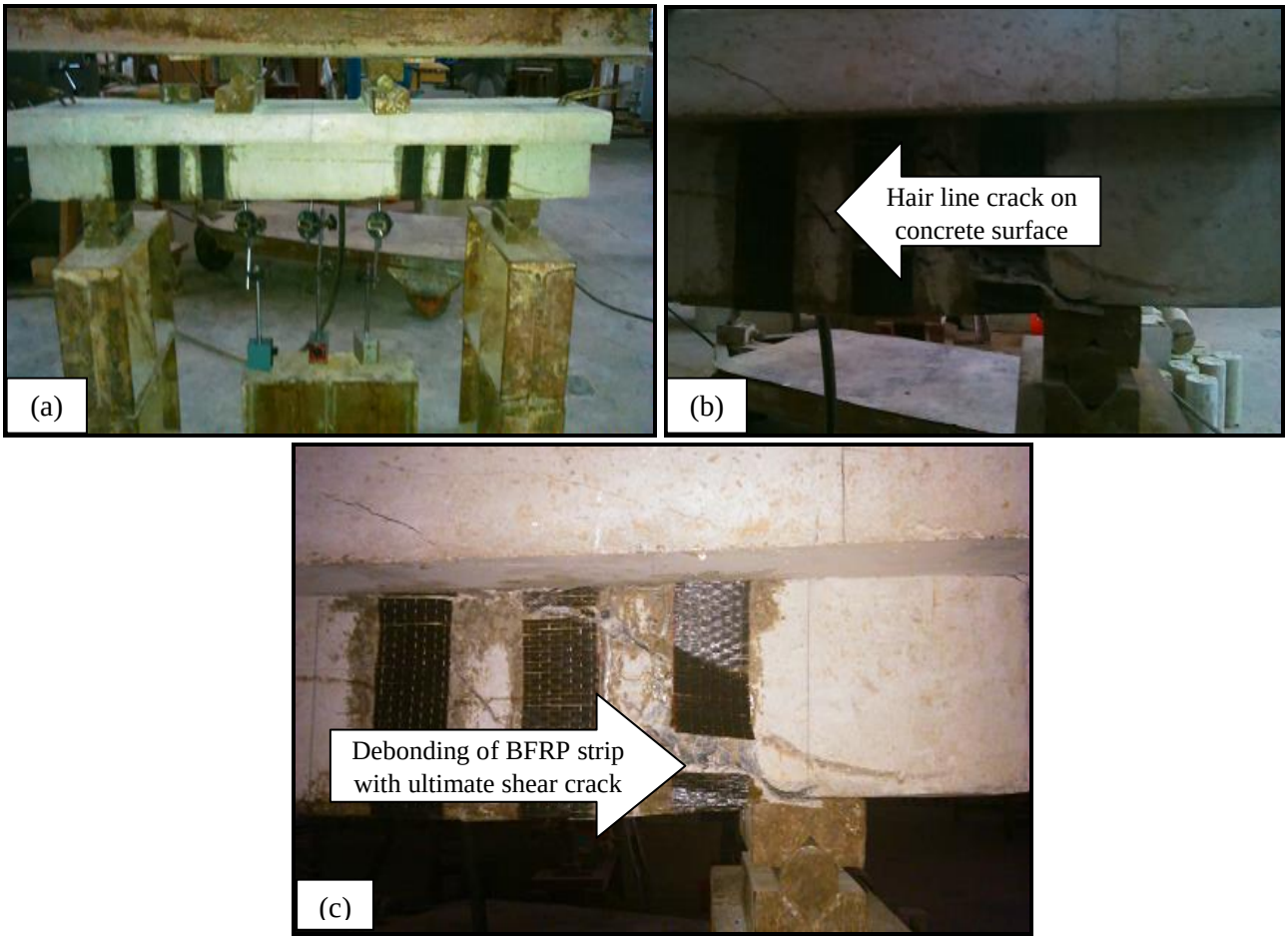

Figure 4.4 (a) Experimental Setup of beam SB3 under four-point loading system, (b) Hair line crack started in shear region at a load of 75kN, (c) Ultimate failure of beam SB3 by debonding of BFRP strip followed by diagonal shear crack

4.2.1.5 Strengthened Beam 4 (SB4)

The beam SB4 is strengthened with 2 layers of BFRP strips in 0^0 orientation bonded only on the sides of the beam (i.e. on web portions) in the shear area (i.e. a length of 0 to L/3 and 2L/3 to L from the left support) with 3 strips of equal width of 50 mm and spacing between the strips is 50 mm bonded to both the shear spans of the beam. The experimental setup of the beam SB4 is given in Figure 4.5(a). The first hair line crack is observed on the concrete surface at a load of 65kN in the shear region of the beam as given in Figure 4.5(b). The ultimate shear failure of the beam SB4 occurred due to the debonding of the BFRP strips followed by a wider diagonal shear crack at an ultimate load of 163kN as illustrated in Figure 4.5(c). The strengthening of beam SB4 with BFRP side strips caused 3.16% increase in shear capacity over the control beam.

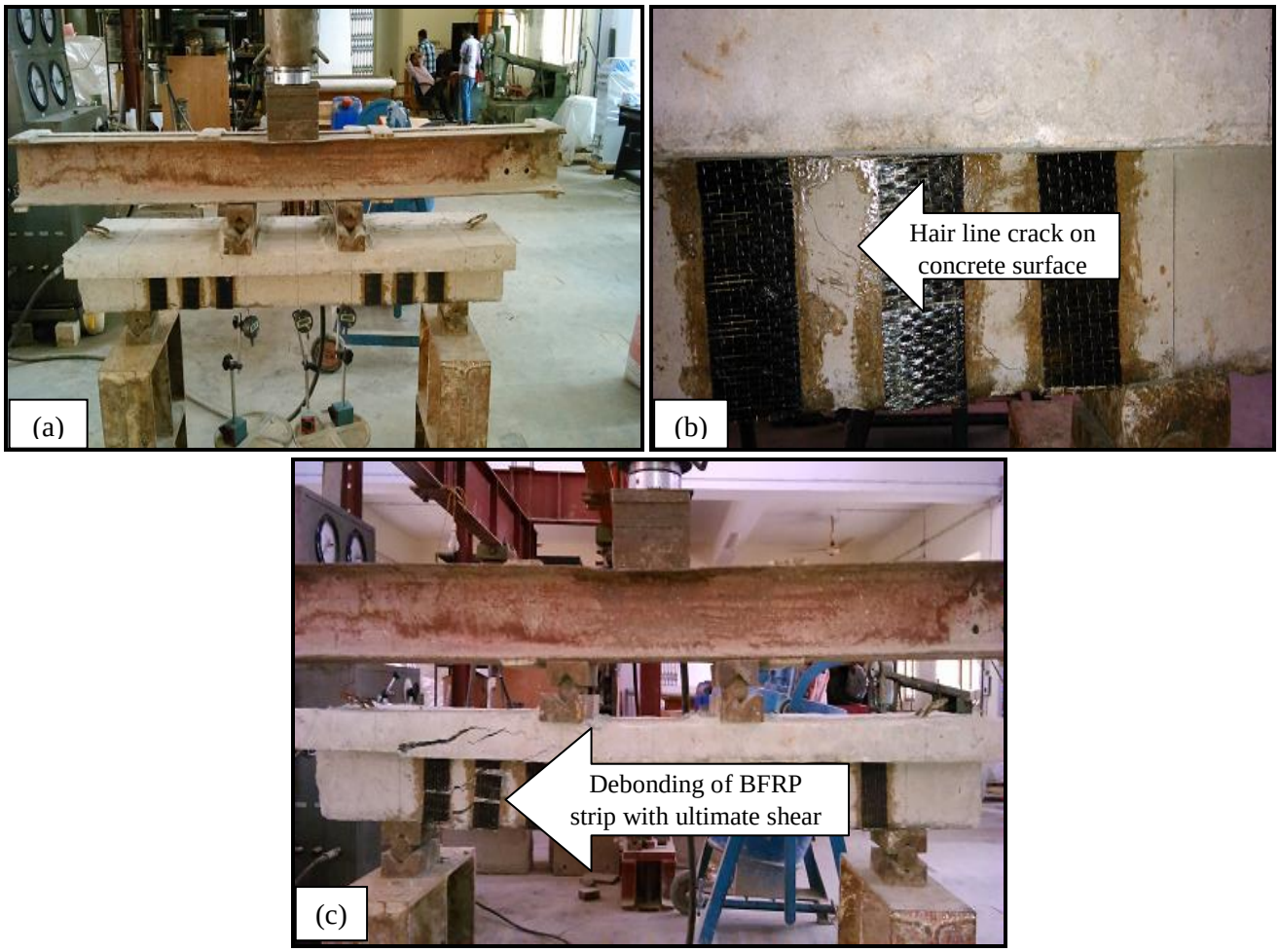

Figure 4.5 (a) Experimental Setup of beam SB4 under four-point loading system, (b) Hair line crack started in shear region at a load of 65kN, (c) Ultimate failure of beam SB4 by debonding of BFRP strip followed by diagonal shear crack

4.2.1.6 Strengthened Beam 5 (SB5)

The beam SB5 is strengthened by applying 2 layers of BFRP in 90^0 orientation having U-wrap on the bottommost and web portions in the shear region (i.e. a length of 0 to L/3 and 2L/3 to L from the left support). The experimental setup of the beam SB5 is given in Figure 4.6(a). The initial hair line crack could not be visualized on the concrete surface because the shear regions are completely wrapped with BFRP sheets. The failure of the beam SB5 is initiated by splitting of BFRP sheets over the principal shear crack in the same region as appeared in control beam as given in Figure 4.6(b) and finally failed by the debonding of BFRP sheets from concrete surface. After the complete debonding of BFRP sheets, the crack patterns became visible. The debonding failure is followed by a diagonal shear failure with the increasing load and the beam finally failed at an ultimate load of 200kN as given in Figure 4.6(c). The strengthening of beam SB5 with BFRP sheets in 90^0 orientation having U-wraps caused 26.58% increase in shear capacity over the control beam.

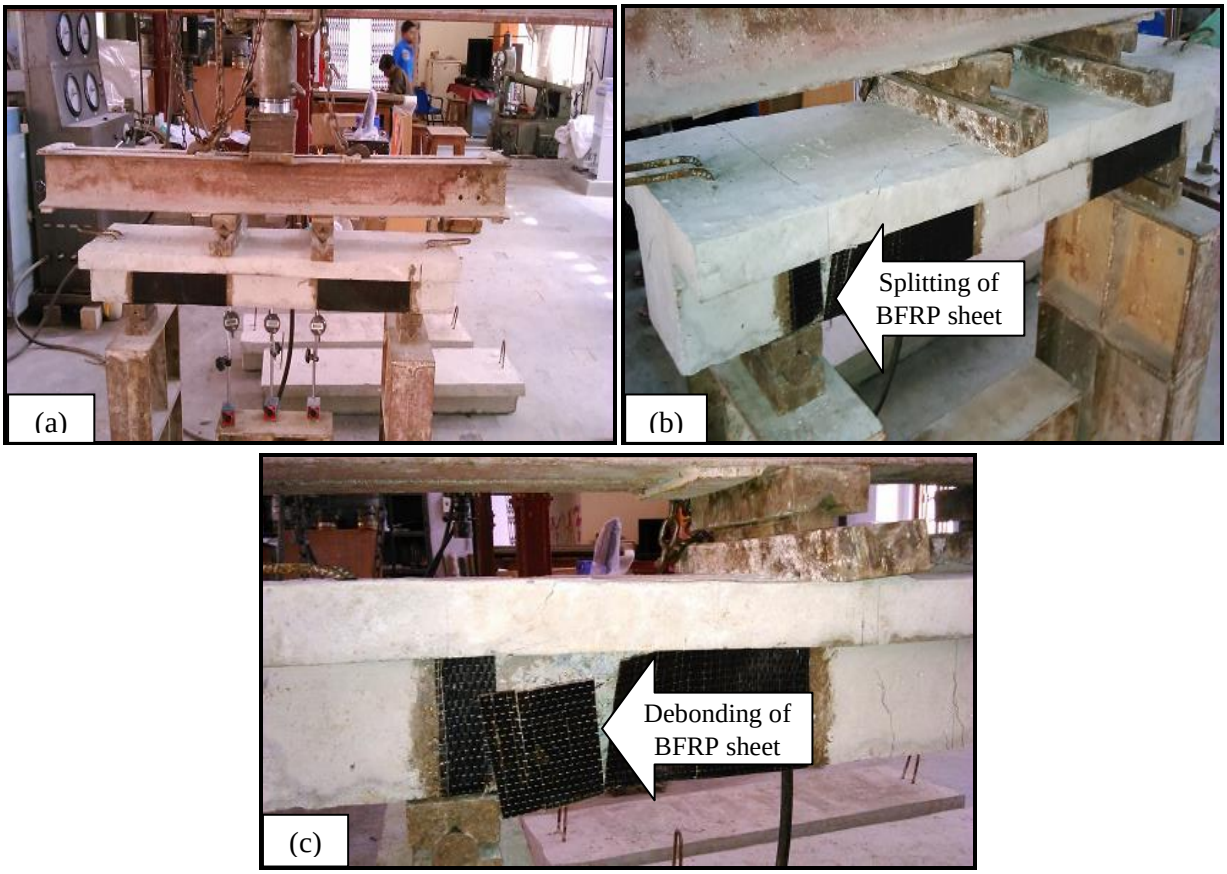

Figure 4.6 (a) Experimental Setup of beam SB5 under four-point loading system, (b) Splitting of BFRP sheet started, (c) Ultimate failure of beam SB5 by debonding of BFRP sheet followed by diagonal shear crack

4.2.1.7 Strengthened Beam 6 (SB6)

The beam SB6 is strengthened with 2 layers of unidirectional BFRP sheets in 90^0 orientation bonded only on the sides of the beam (i.e. on web portions) in the shear zone (i.e. a length of 0 to L/3 and 2L/3 to L from the left support). The experimental setup of the beam SB6 is given in Figure 4.7(a). The initial hair line crack could not be traced out on the concrete surface because the shear zones are fully covered with BFRP sheets. The failure of the beam SB6 is started due to the splitting of BFRP sheets as given in Figure 4.7(b) and finally failed by the debonding of BFRP sheets from concrete surface. After the complete debonding of BFRP sheets, the crack patterns became visible. The debonding failure is followed by a diagonal shear failure with the increasing load and the beam finally failed at an ultimate load of 175kN as given in Figure 4.7(c). The strengthening of beam SB6 caused 10.76% increase in shear capacity over the control beam.

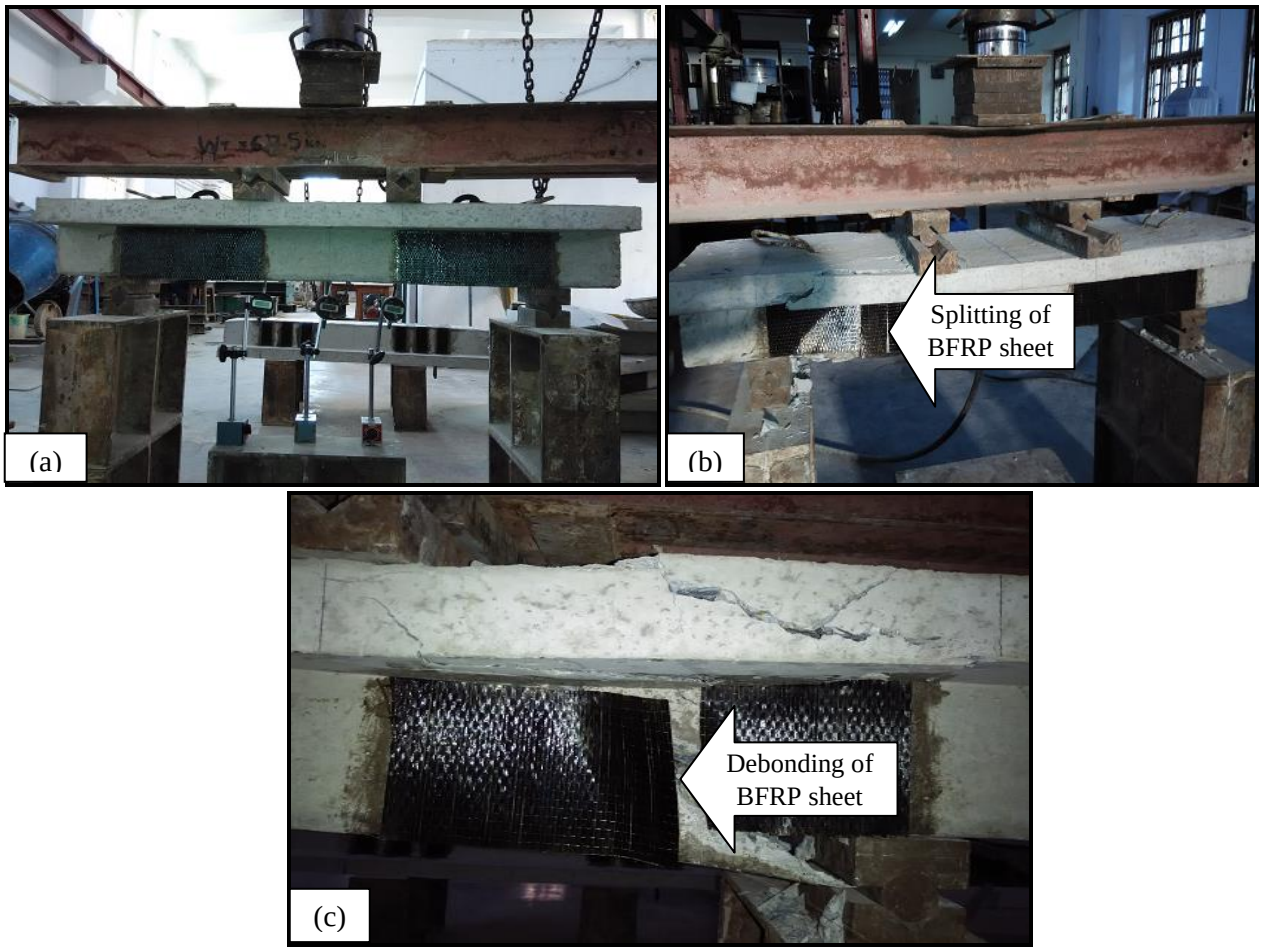

Figure 4.7 (a) Experimental Setup of beam SB6 under four-point loading system, (b) Splitting of BFRP sheet started, (c) Ultimate failure of beam SB6 by debonding of BFRP sheet followed by diagonal shear crack

4.2.1.8 Strengthened Beam 7 (SB7)

The beam SB7 is strengthened with BFRP U-strips of 2 layers in 90^0 orientation bonded to the bottommost and web portions in the shear area (i.e. a length of 0 to L/3 and 2L/3 to L from the left support) with 3 strips of equal width of 50 mm and spacing between the strips is 50 mm bonded to both the shear spans of the beam. The experimental setup of the beam SB7 is given in Figure 4.8(a). The first hair line crack is observed on the concrete surface at a load of 85kN in the shear region of the beam as given in Figure 4.8(b). The failure of the beam SB7 occurred due to the debonding of the BFRP strips at an ultimate load of 185kN followed by a wider diagonal shear crack as illustrated in Figure 4.8(c). The strengthening of beam SB7 with BFRP U-strips caused 17.09% increase in shear capacity over the control beam.

Figure 4.8 (a) Experimental Setup of beam SB7 under four-point loading system, (b) Hair line crack started in shear region at a load of 85kN, (c) Ultimate failure of beam SB7 by debonding of BFRP strip followed by diagonal shear crack

4.2.1.9 Strengthened Beam 8 (SB8)

The beam SB8 is strengthened with 2 layers of BFRP strips in 90^0 orientation bonded only on the sides of the beam (i.e. on web portions) in the shear span (i.e. a length of 0 to L/3 and 2L/3 to L from the left support) with 3 strips of equal width of 50 mm and spacing between the strips is 50 mm bonded to both the shear spans of the beam. The experimental setup of the beam SB8 is given in Figure 4.9(a). The first hair line crack is observed on the concrete surface at a load of 70kN in the shear region of the beam as given in Figure 4.9(b). The ultimate shear failure of the beam SB8 occurred due to the debonding of the BFRP strips followed by a wider diagonal shear crack at an ultimate load of 166kN as given in Figure 4.9(c). The strengthening of beam SB8 with BFRP side strips caused 5.06% increase in shear capacity over the control beam.

Figure 4.9 (a) Experimental Setup of beam SB8 under four-point loading system, (b) Hair line crack started in shear region at a load of 70kN, (c) Ultimate failure of beam SB8 by debonding of BFRP strip followed by diagonal shear crack

4.2.1.10 Strengthened Beam 9 (SB9)

The beam SB9 is strengthened with BFRP U-strips of 2 layers inclined with 45^0 bonded to the bottommost and web portions in the shear region (i.e. a length of 0 to L/3 and 2L/3 to L from the left support) with 3 strips of equal width of 50 mm and spacing between the strips is 50 mm bonded to both the shear spans of the beam. The experimental setup of the beam SB9 is given in Figure 4.10(a). The first hair line crack is visualized on the concrete surface at a load of 110kN in the shear region of the beam as given in Figure 4.10(b). The ultimate shear failure of the beam SB9 occurred due to the debonding of the BFRP strips followed by a wider diagonal shear crack at an ultimate load of 192kN as given in Figure 4.10(c). The strengthening of beam SB9 with BFRP U-strips caused 21.52% increase in shear capacity over the control beam.

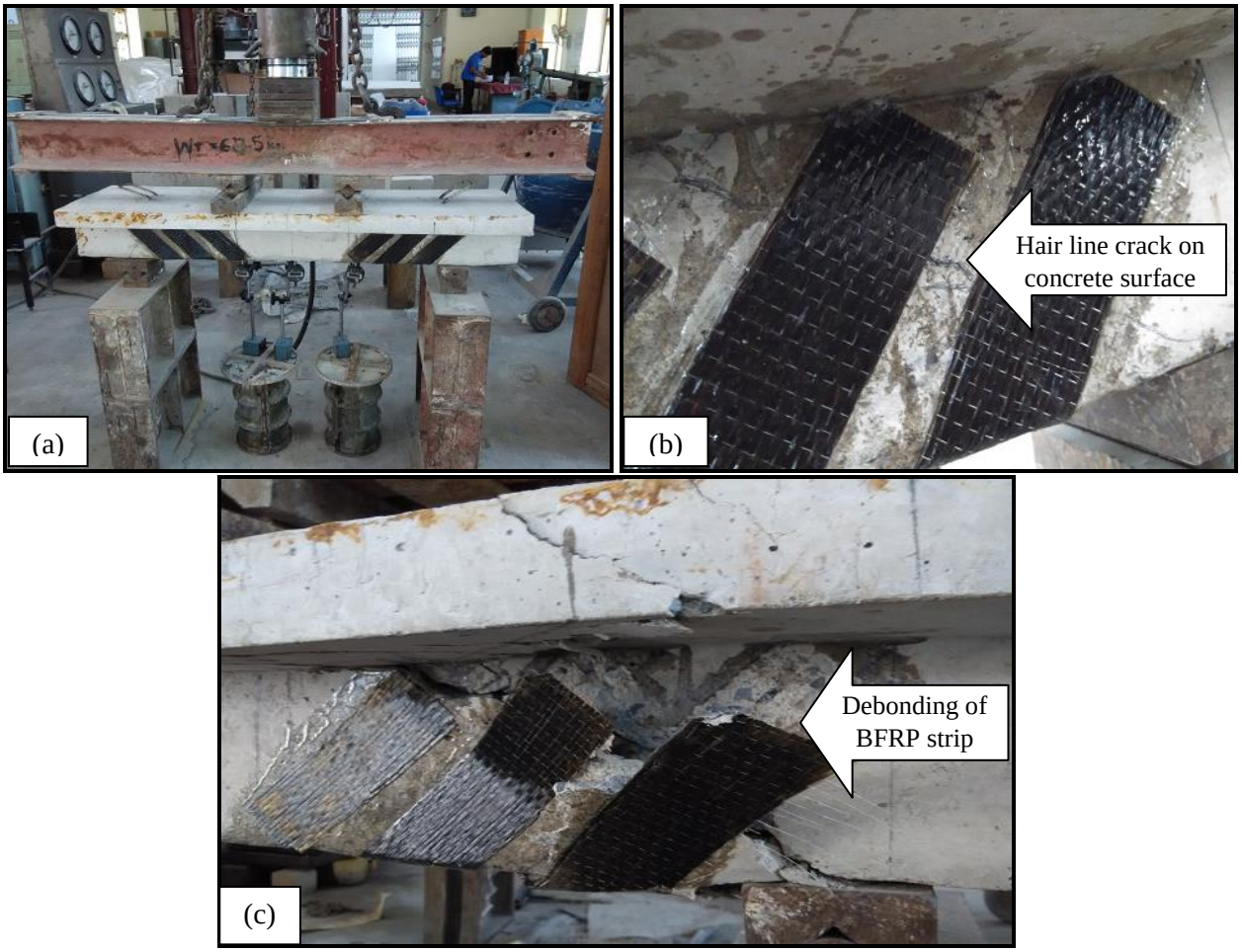

Figure 4.10 (a) Experimental Setup of beam SB9 under four-point loading system, (b) Hair line crack started in shear region at a load of 110kN, (c) Ultimate failure of beam SB9 by debonding of BFRP strip followed by diagonal shear crack

4.2.1.11 Strengthened Beam 10 (SB10)

The beam SB10 is strengthened by applying 2 layers of BFRP in 90^0 orientation having U-wrap on the bottommost and web portions in the shear zone (i.e. a length of 0 to L/3 and 2L/3 to L from the left support). A new anchorage system comprising of laminated composite plate with bolt has been introduced at the free ends of the U-wrap. The experimental setup of the beam SB10 is given in Figure 4.11(a). From the previously tested strengthened beams, it is observed that the failures of the beams are mainly due to the debonding of the BFRP sheets from the concrete surface. This experiment emphasize on the prevention of debonding of BFRP sheets from the concrete surface by using the new anchorage scheme as given in Figure 4.11(b). The initial hair line crack could not be visualized on the concrete surface because the shear zones are completely covered with BFRP sheets. The ultimate failure of the beam SB10 is due to the tearing of he BFRP sheets just below the anchorage plate at an ultimate load of 219kN as illustrated in Figure 4.11(c). The strengthening of beam SB10 with BFRP sheets in 90^0 orientation having U-wraps with end anchorage system caused 38.61% increase in shear capacity over the control beam.

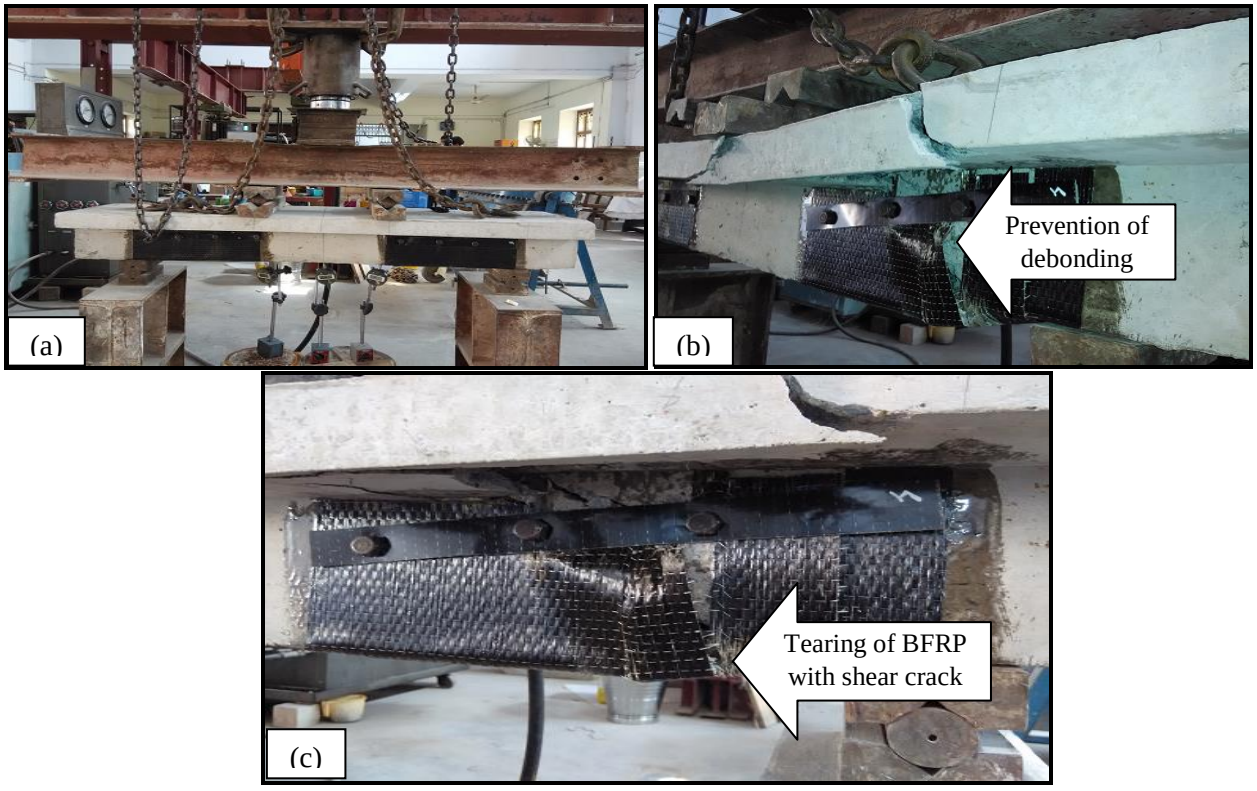

Figure 4.11 (a) Experimental Setup of beam SB10 under four-point loading system, (b) Prevention of debonding of BFRP sheet due to Anchoring System, (c) Ultimate failure of beam SB10 by tearing of BFRP sheet followed by diagonal shear crack

4.2.1.12 Strengthened Beam 11 (SB11)

The beam SB11 is strengthened with 4 layers of BFRP in 90^0 orientation having U-wrap on the bottommost and web portions in the shear span (i.e. a length of 0 to L/3 and 2L/3 to L from the left support) provided with an anchorage system at the free ends of U-wrap. The experimental setup of the beam SB11 is given in Figure 4.12(a). The initial hair line crack could not be traced out on the concrete surface because the shear spans are fully covered with BFRP sheets. Anchorage system is provided to prevent the debonding of the BFRP sheets from the concrete surface as given in Figure 4.12(b). The failure of the beam SB11 occurred due to the tearing of the BFRP sheets just below the anchorage plate followed by a wider diagonal shear crack at an ultimate load of 232kN as illustrated in Figure 4.12(c). An increase in the shear strength is observed as compared with beam SB10. The strengthening of beam SB11 with 4 layers of BFRP sheets in 90^0 orientation having U-wraps with end anchorage system caused 46.83% increase in shear capacity over the control beam.

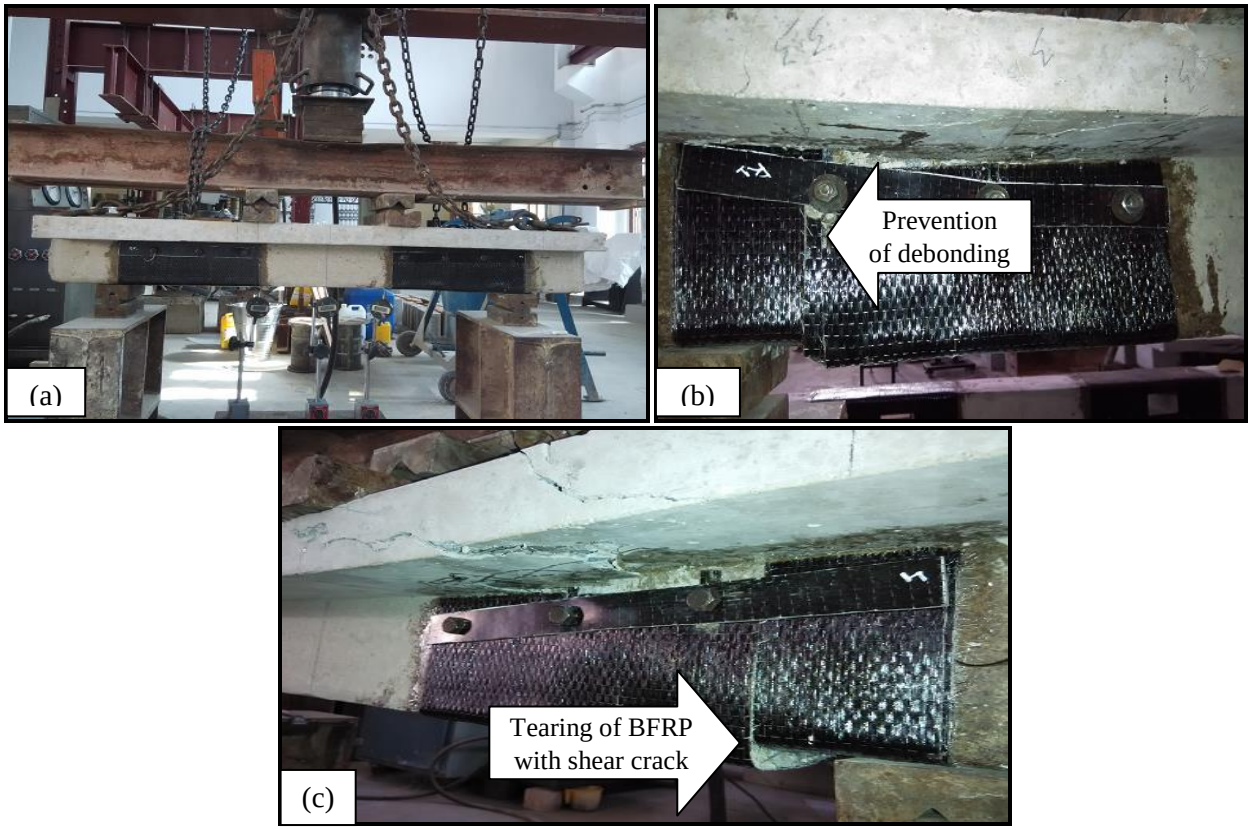

Figure 4.12 (a) Experimental Setup of beam SB11 under four-point loading system, (b) Prevention of debonding of BFRP sheet due to Anchoring System, (c) Ultimate failure of beam SB11 by tearing of BFRP sheet followed by diagonal shear crack

4.2.1.13 Strengthened Beam 12 (SB12)

The beam SB12 is strengthened with BFRP U-strips of 2 layers in 90^0 orientation bonded to the bottommost and web portions in the shear region (i.e. a length of 0 to L/3 and 2L/3 to L from the left support) provided with an anchorage system at the free ends of 3 strips of equal width of 50 mm and spacing between the strips is 50 mm bonded to both the shear spans of the beam. The experimental setup of the beam SB12 is given in Figure 4.13(a). The first hair line crack is observed on the concrete surface at a load of 126kN in the shear zone of the beam. The formation of crack is delayed by the prevention of debonding due to anchorage system as given in Figure 4.13(b). The load carrying capacity of beam SB12 with BFRP U-strips with end anchorage is nearly equal to that of beam SB1 with 2 layers U-wrap continuous sheets in 90^0 orientation. The ultimate failure of the beam SB12 occurred at an ultimate load of 200kN due to the tearing of the BFRP strips followed by a wider diagonal shear crack in the same region as in case of CB as illustrated in Figure 4.13(c). The strengthening of beam SB12 with BFRP U-strips in 90^0 orientation with end anchorage system caused 26.58% increase in shear capacity over the control beam.

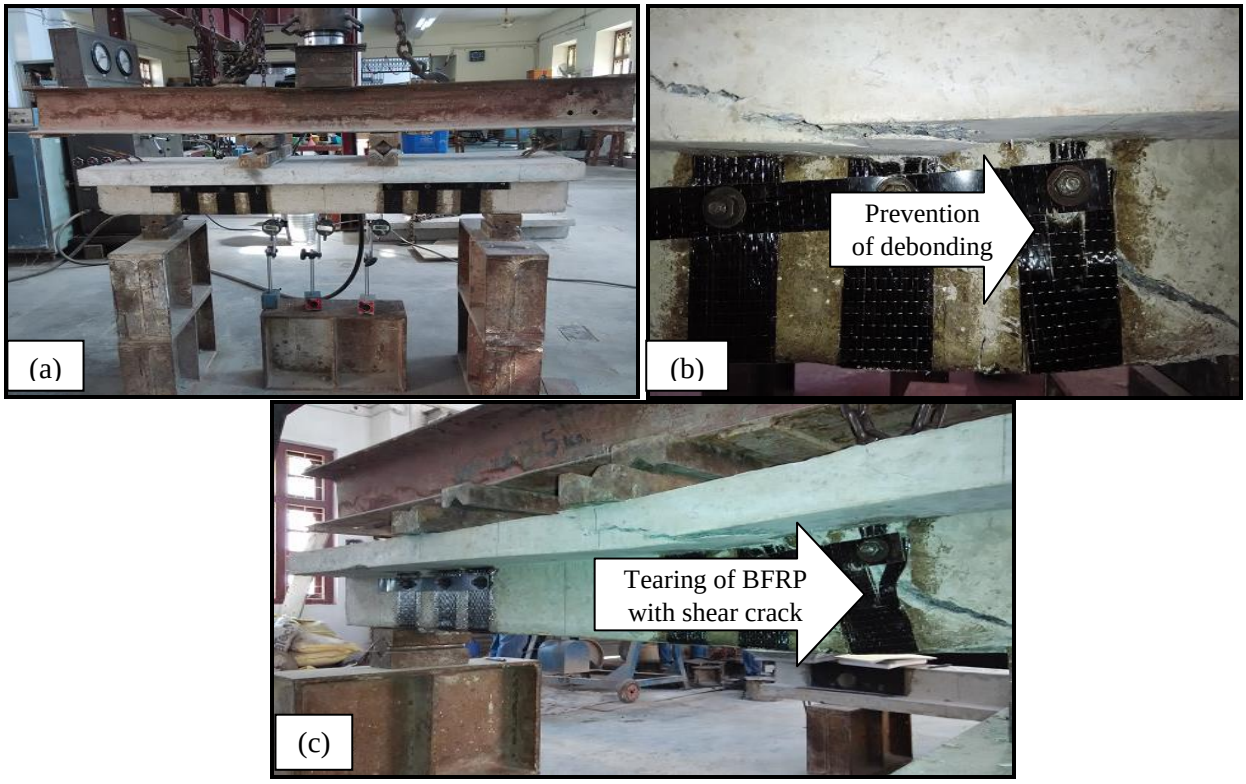

Figure 4.13 (a) Experimental Setup of beam SB12 under four-point loading system, (b) Prevention of debonding of BFRP strip due to Anchoring System, (c) Ultimate failure of beam SB12 by tearing of BFRP strip followed by diagonal shear crack

4.2.2 Series B

4.2.2.1 Control Beam 1 (CB1)

The control beam (CB1) is provided with circular hole in both the shear span of the beam to study the behaviour of the shear failure without strengthening. It is a shear deficient beam and is tested under the four point static loading system by applying the point loads gradually. The experimental set-up for the control beam under four point static loading frame is shown in Figure 4.14(a). The first hair line crack is observed at a load of 50kN in the shear region of the beam as given in Figure 4.14(b). As the load increased, additional shear cracks are developed and the primary visible crack undergoes widening and propagated. With the further increase in load, the beam exhibited a wider diagonal shear crack passing through the circular hole and finally failed in shear at a load of 100kN as illustrated in Figure 4.14(c). For the beam CB1 ultimate failure occurred due to the first visible shear crack which became critical at the ultimate load.

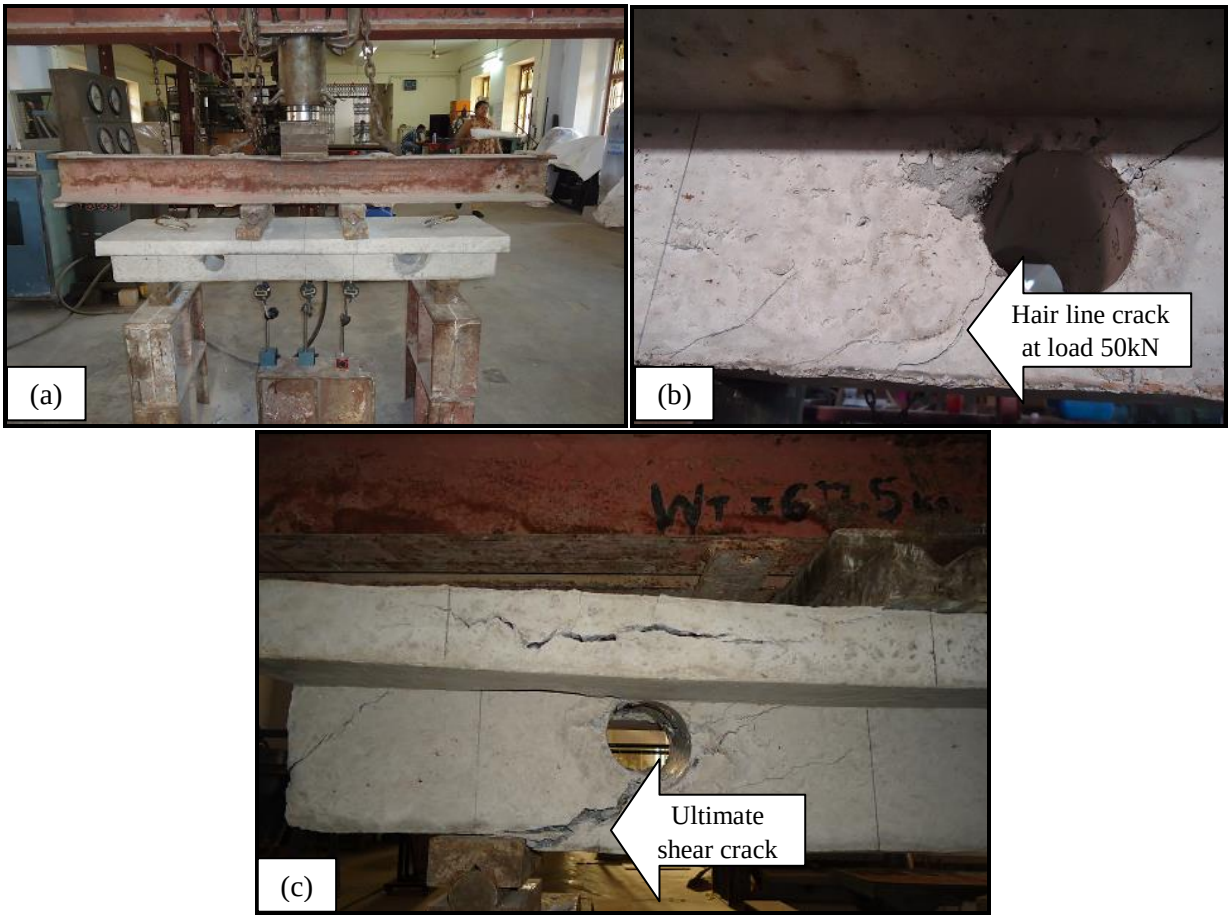

Figure 4.14 (a) Experimental Setup of CB1 under four-point loading system, (b) Hair line crack started in shear region at a load of 50kN, (c) Crack pattern at ultimate failure

4.2.2.2 Strengthened Beam 13 (SB13)

The beam SB13 is strengthened with 4 layers of BFRP sheets in 90^0 orientation having U-wrap on the bottommost and web portions in the shear zone (i.e. a length of 0 to L/3 and 2L/3 to L from the left support) with circular shape web openings in the shear zone of the RC beam. The experimental setup of the beam SB13 is given in Figure 4.15(a). The initial hair line crack could not be observed on the concrete surface because the shear zones are completely wrapped with BFRP sheets. The failure of the beam SB13 is initiated due to the debonding of BFRP sheets (followed by a film of concrete deposit adhered to them) over the principal shear crack in the same region as appeared in the beam CB1. After the complete debonding of BFRP sheets, the crack patterns became visible as given in Figure 4.15(b). The debonding failure is followed by a wider diagonal shear crack passing through the circular hole with the increasing load and the beam finally failed at an ultimate load of 132kN as given in Figure 4.15(c). The modelling of beam SB13 with 4 layers of BFRP sheets in 90^0 orientation having U-wraps caused 32% increase in shear capacity over the beam CB1.

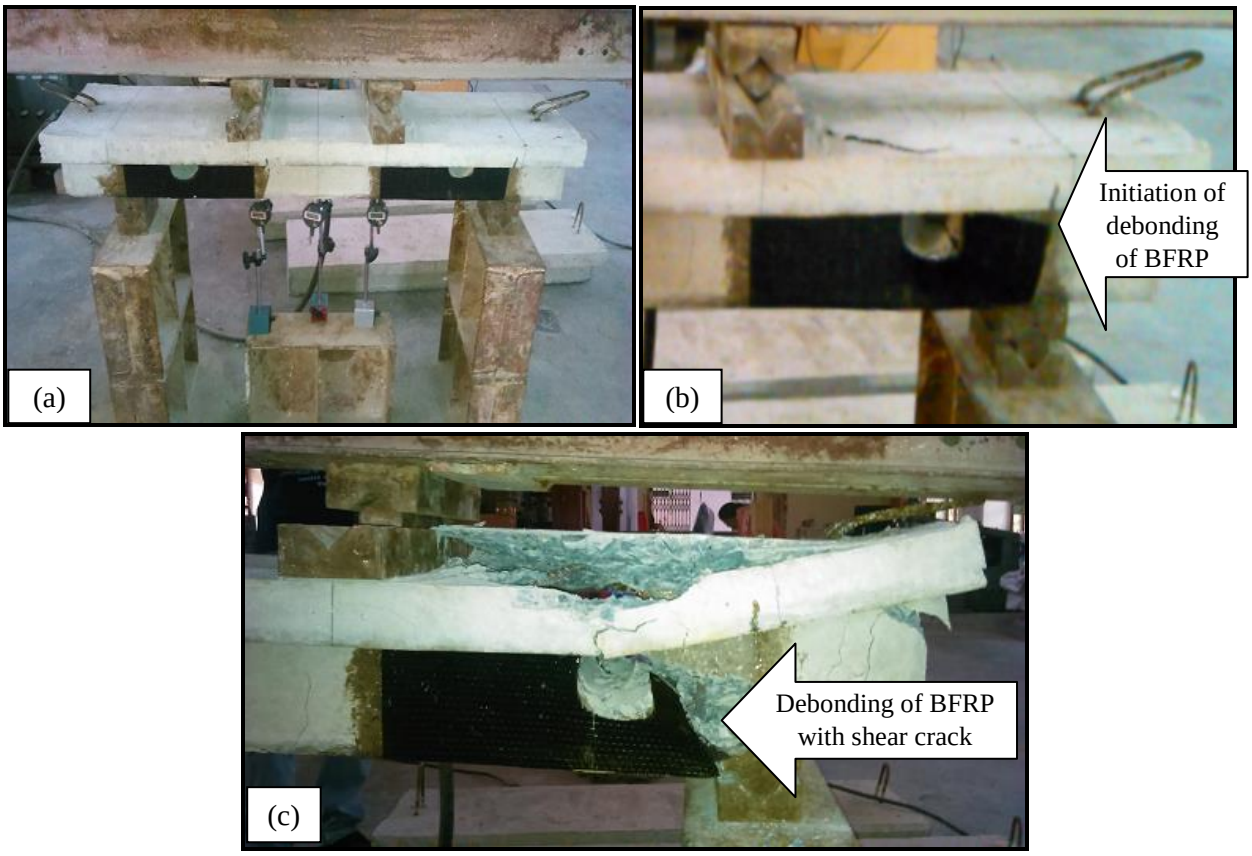

Figure 4.15 (a) Experimental Setup of beam SB13 under four-point loading system, (b) Initiation of debonding of BFRP sheet, (c) Ultimate failure of beam SB13 by debonding of BFRP sheet followed by diagonal shear crack

4.2.2.3 Strengthened Beam 14 (SB14)

The beam SB14 is strengthened by applying 4 layers of BFRP in 90^0 orientation having U-wrap on the bottommost and web portions in the shear region (i.e. distance of 0 to L/3 and 2L/3 to L from the left support) with circular shape web openings in the shear zone of the RC beam provided with an anchorage system as shown in Figure 4.16(a). The anchorage system prevents the debonding of BFRP sheets; hence the shear strength of the beam is enhanced. The initial hair line crack could not be traced out on the concrete surface because the shear regions are fully covered with BFRP sheets. The failure of the beam SB14 is initiated by tearing of BFRP sheets as shown in Figure 4.16(b). As the load enhanced, finally the beam failed in shear at an ultimate load of 162kN by tearing of BFRP sheets as shown in Figure 4.16(c). The strengthening of beam SB14 with 4 layers of BFRP sheets in 90^0 orientation having U-wraps with end anchorage system caused 62% and 22.73% increase in shear capacity over the beam CB1 and SB13, respectively.

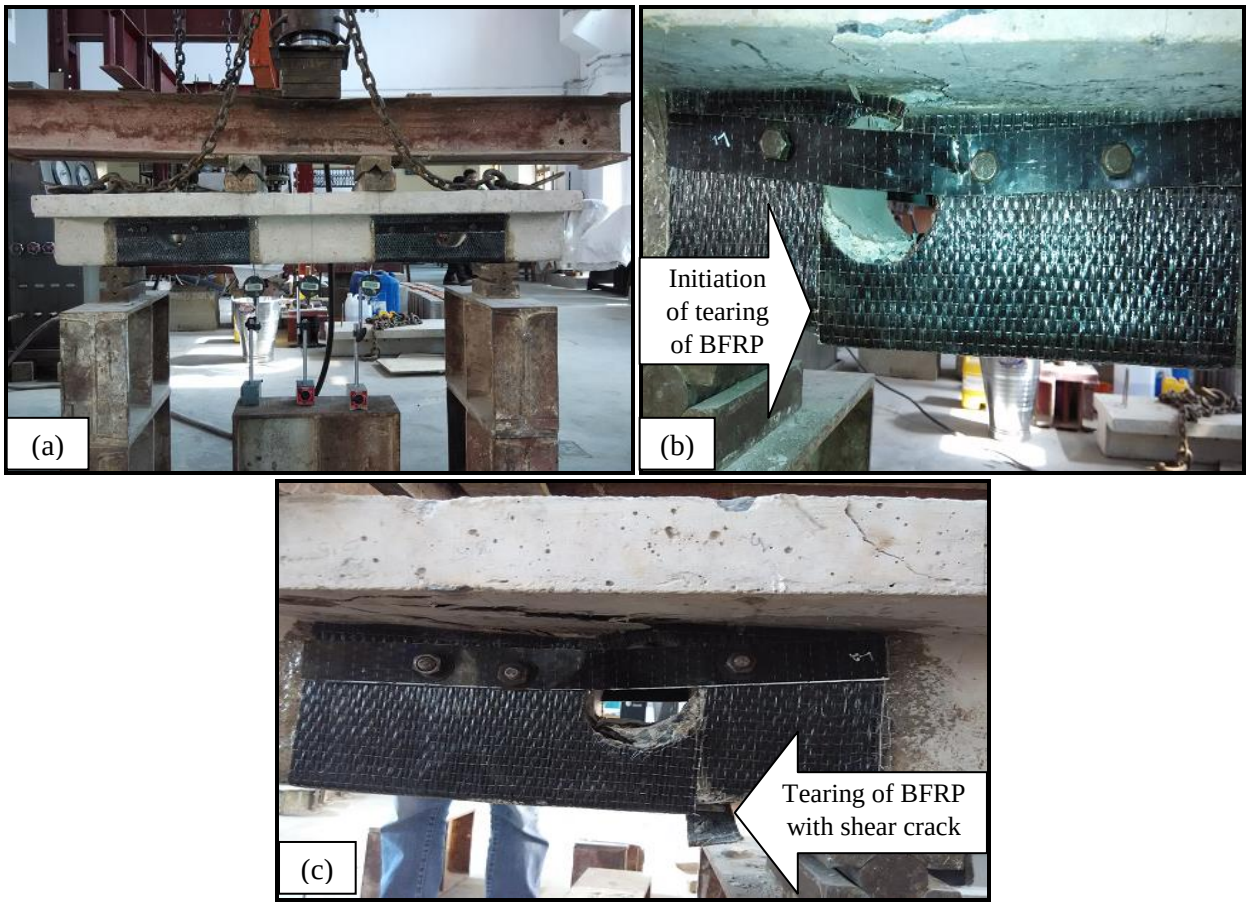

Figure 4.16 (a) Experimental Setup of beam SB14 under four-point loading system, (b) Initiation of tearing of BFRP sheet, (c) Ultimate failure of beam SB14 by tearing of BFRP sheet followed by diagonal shear crack

4.2.2.4 Control Beam 2 (CB2)

The control beam (CB2) is provided with rectangular hole in the shear region of the beam to study the behaviour of the shear failure without strengthening. It is a shear deficient beam and is tested under the four point static loading system by applying the point loads gradually. The experimental set-up for the control beam under four point static loading frame is shown in Figure 4.17(a). The first hair line crack is visualized at a load of 55kN in the shear area of the beam as given in Figure 4.17(b). As the load increased, additional shear cracks are developed and the primary visible crack undergoes widening and propagated. With the further increase in load, the beam exhibited a wider diagonal shear crack passing through the rectangular hole and finally failed in shear at a load of 114kN as illustrated in Figure 4.17(c). For the beam CB2 ultimate failure occurred due to the first visible shear crack which became critical at the ultimate load.

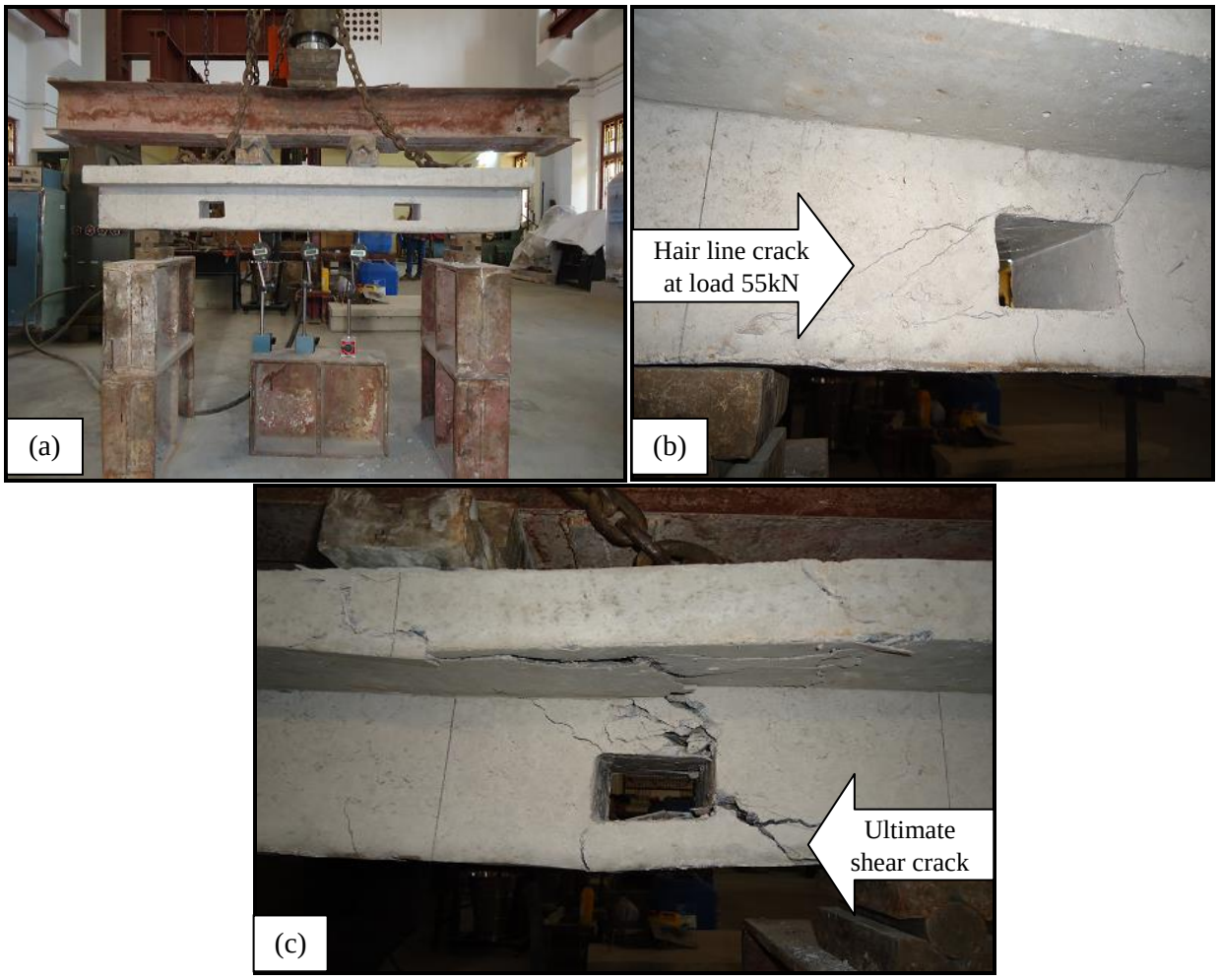

Figure 4.17 (a) Experimental Setup of CB2 under four-point loading system, (b) Hair line crack started in shear region at a load of 55kN, (c) Crack pattern at ultimate failure

4.2.2.5 Strengthened Beam 15 (SB15)

The beam SB15 is strengthened with 4 layers of BFRP sheets in 90^0 orientation having U-wrap on the bottommost and web portions in the shear zone (i.e. a length of 0 to L/3 and 2L/3 to L from the left support) with rectangular shape web openings in the shear span of the RC beam. The experimental setup of the beam SB15 is given in Figure 4.18(a). The initial hair line crack could not be observed because the shear regions are completely covered with BFRP sheets. The failure of the beam SB15 is initiated due to the splitting of BFRP sheets as given in Figure 4.18(b) over the principal shear crack in the same region as appeared in the beam CB2. The beam finally failed by the debonding of BFRP sheets at an ultimate load of 135kN as given in Figure 4.18(c). The strengthening of beam SB15 with 4 layers of BFRP sheets in 90^0 orientation having U-wraps caused 18.42% increase in shear capacity over the beam CB2.

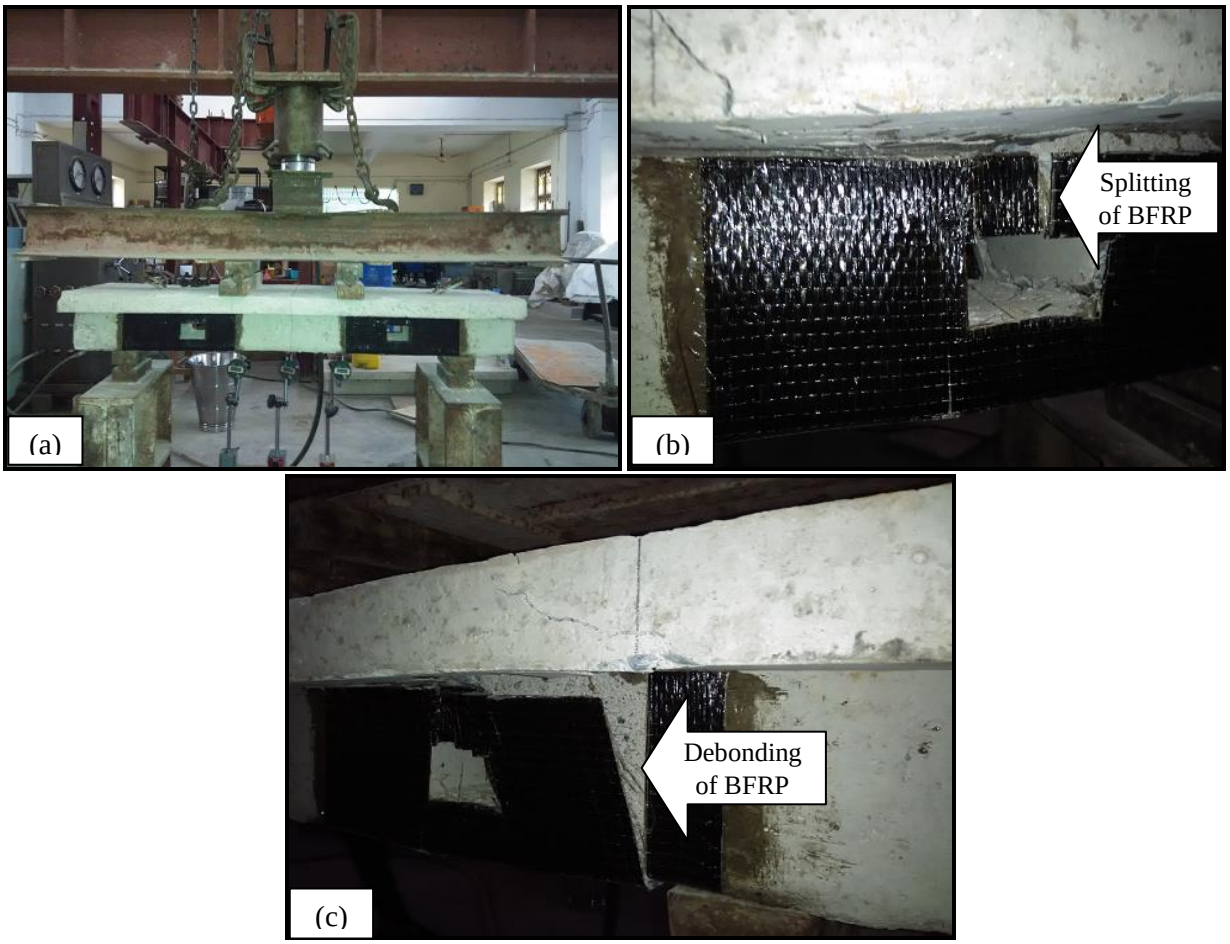

Figure 4.18 (a) Experimental Setup of beam SB15 under four-point loading system, (b) Initiation of splitting of BFRP sheet, (c) Ultimate failure of beam SB15 by debonding of BFRP sheet followed by diagonal shear crack

4.2.2.6 Strengthened Beam 16 (SB16)

The beam SB16 is strengthened by applying 4 layers of BFRP in 90^0 orientation having U-wrap on the bottommost and web portions in the shear region (i.e. distance of 0 to L/3 and 2L/3 to L from the left support) with rectangular shape web openings in the shear area of the RC beam provided with an anchorage system as shown in Figure 4.19(a). The anchorage system is used to prevent the debonding of BFRP sheets from the concrete surface; hence the full strength of the beam has been utilized. The initial hair line crack could not be traced out on the concrete surface because the shear zones are fully wrapped with BFRP sheets. The failure of the beam SB16 is initiated by tearing of BFRP sheets as shown in Figure 4.19(b). As the load enhanced, finally the beam failed in shear at an ultimate load of 154kN by tearing of BFRP sheets as shown in Figure 4.19(c). The strengthening of beam SB16 with 4 layers of BFRP sheets in 90^0 orientation having U-wraps with end anchorage system caused 35.09% and 14.07% increase in shear capacity over the beam CB2 and SB15, respectively.

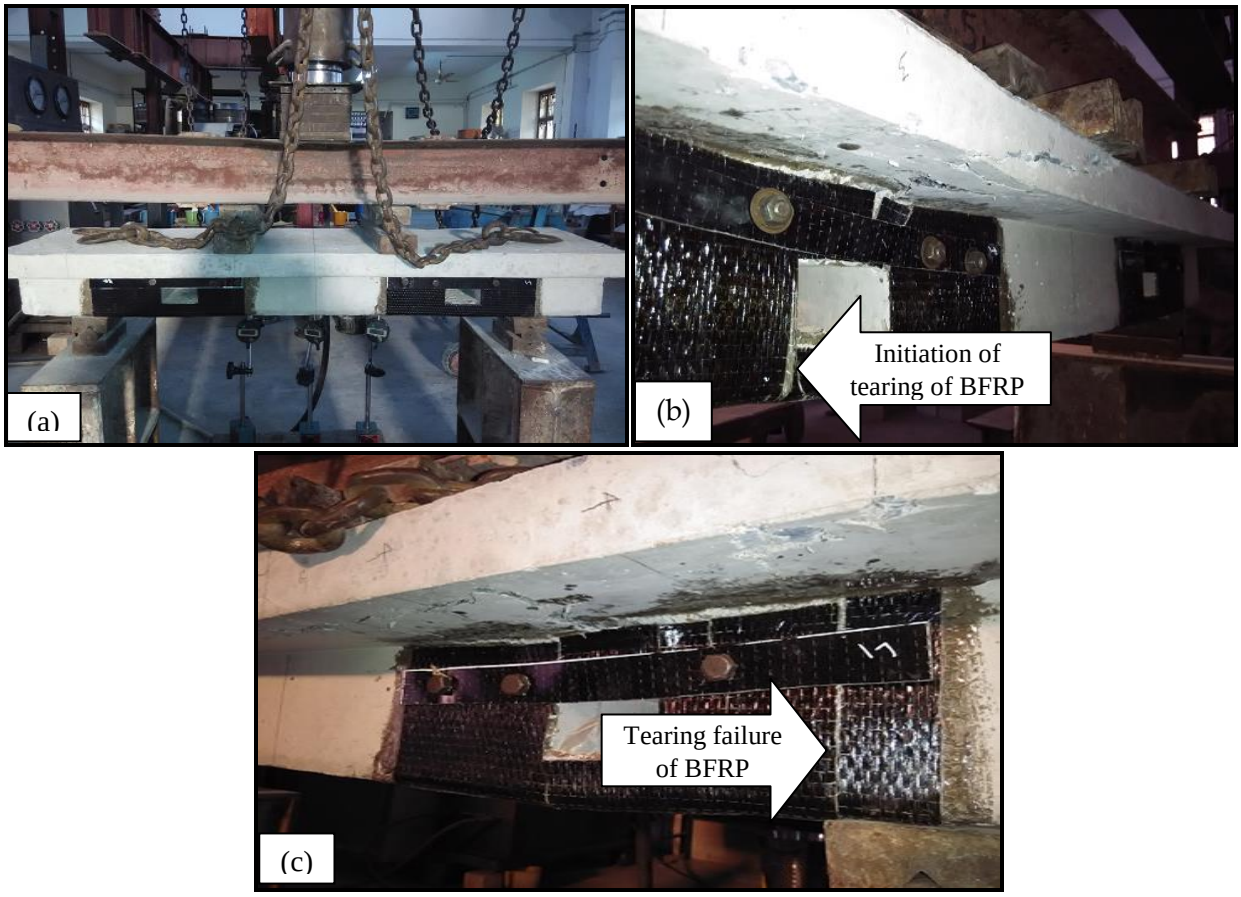

Figure 4.19 (a) Experimental Setup of beam SB16 under four-point loading system, (b) Initiation of tearing of BFRP sheet, (c) Ultimate failure of beam SB16 by tearing of BFRP sheet

4.2.2.7 Control Beam 3 (CB3)

The control beam (CB3) is provided with square shape hole in the shear zone of the beam to study the behaviour of the shear failure without strengthening. It is a shear deficient beam and is tested under the four point static loading system by applying the point loads gradually. The experimental set-up for the beam CB3 under four point static loading frame is shown in Figure 4.20(a). The first hair line crack is visualized at a load of 58kN in the shear region of the beam as given in Figure 4.20(b). As the load enhanced, additional shear cracks are developed and the primary visible crack undergoes widening and propagated. With the further increase in load, the beam exhibited a wider diagonal shear crack passing through the square hole and finally failed in shear at a load of 120kN as illustrated in Figure 4.20(c). For the beam CB3 ultimate failure occurred due to the first visible shear crack which became critical at the ultimate load.

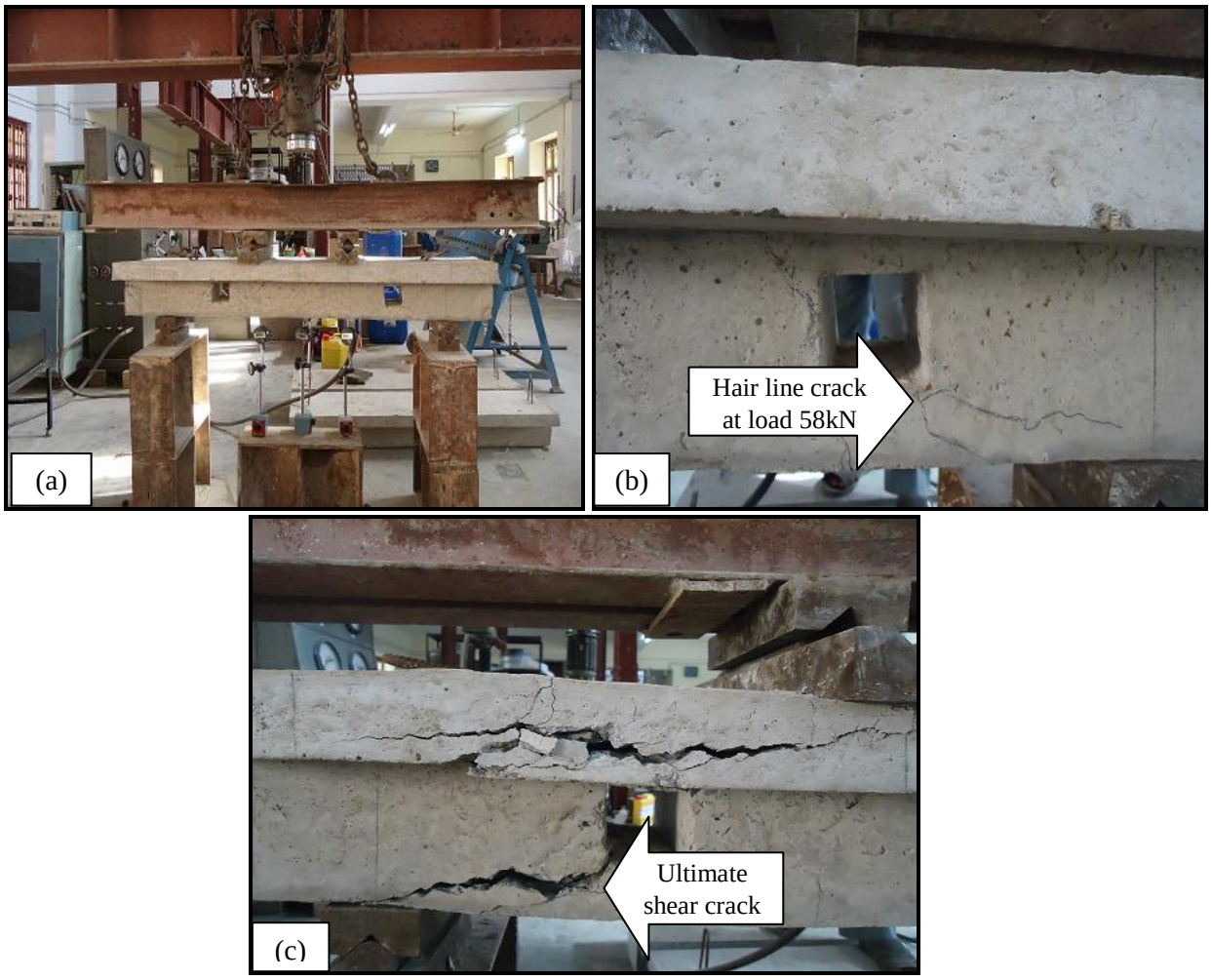

Figure 4.20 (a) Experimental Setup of CB3 under four-point loading system, (b) Hair line crack started in shear region at a load of 58kN, (c) Crack pattern at ultimate failure

4.2.2.8 Strengthened Beam 17 (SB17)

The beam SB17 is strengthened with 4 layers of BFRP sheets in 90^0 orientation having U-wrap on the bottommost and web portions in the shear region (i.e. a length of 0 to L/3 and 2L/3 to L from the left support) with square shape web openings in the shear zone of the RC beam. The experimental setup of the beam SB17 is given in Figure 4.21(a). The initial hair line crack could not be observed on the concrete surface because the shear zones are fully wrapped with BFRP sheets. The failure of the beam SB17 is initiated due to the splitting of BFRP sheets as given in Figure 4.21(b) over the principal shear crack in the same region as appeared in the beam CB3. The beam finally failed by the debonding of BFRP sheets followed by a wider diagonal shear crack passing through the square hole at an ultimate load of 144kN as given in Figure 4.21(c). The strengthening of beam SB17 with 4 layers of BFRP sheets in 90^0 orientation having U-wraps caused 20% increase in shear capacity over the beam CB3.

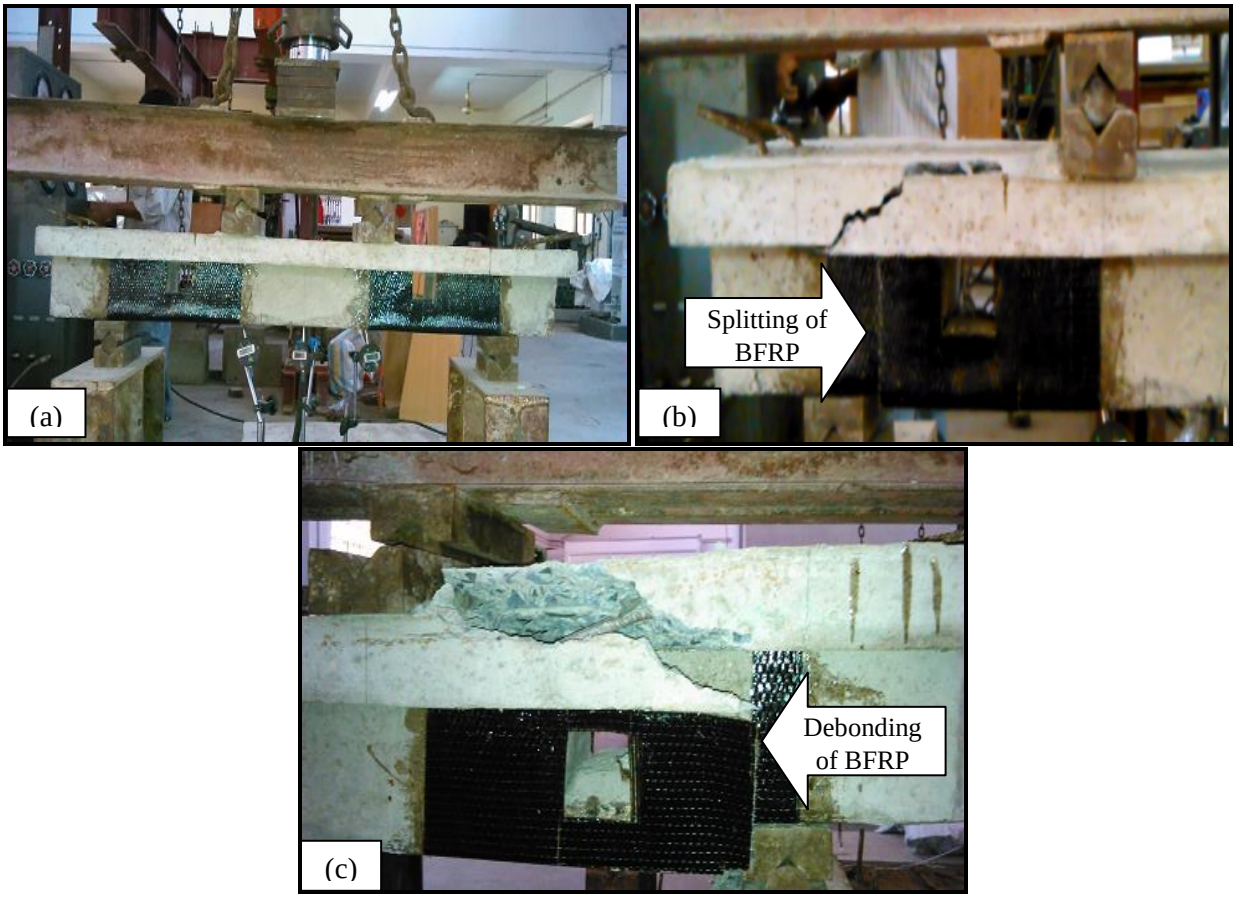

Figure 4.21 (a) Experimental Setup of beam SB17 under four-point loading system, (b) Initiation of splitting of BFRP sheet, (c) Ultimate failure of beam SB17 by debonding of BFRP sheet followed by diagonal shear crack

4.2.2.9 Strengthened Beam 18 (SB18)

The beam SB18 is strengthened by applying 4 layers of BFRP in 90^0 orientation having U-wrap on the bottommost and web portions in the shear area (i.e. distance of 0 to L/3 and 2L/3 to L from the left support) with square shape web openings in the shear zone of the RC beam provided with an anchorage system as shown in Figure 4.22(a). The anchorage system prevents the debonding of BFRP sheets; hence the shear strength of the beam is enhanced. The initial hair line crack could not be visualized because the shear regions are completely covered with BFRP sheets. The failure of the beam SB18 is initiated by tearing of BFRP sheets as shown in Figure 4.22(b). As the load enhanced, finally the beam failed in shear at an ultimate load of 164kN by tearing of BFRP sheets as shown in Figure 4.22(c). The strengthening of beam SB18 with 4 layers of BFRP sheets in 90^0 orientation having U-wraps with end anchorage system caused 36.67% and 13.89% increase in shear capacity over the beam CB3 and SB17, respectively.

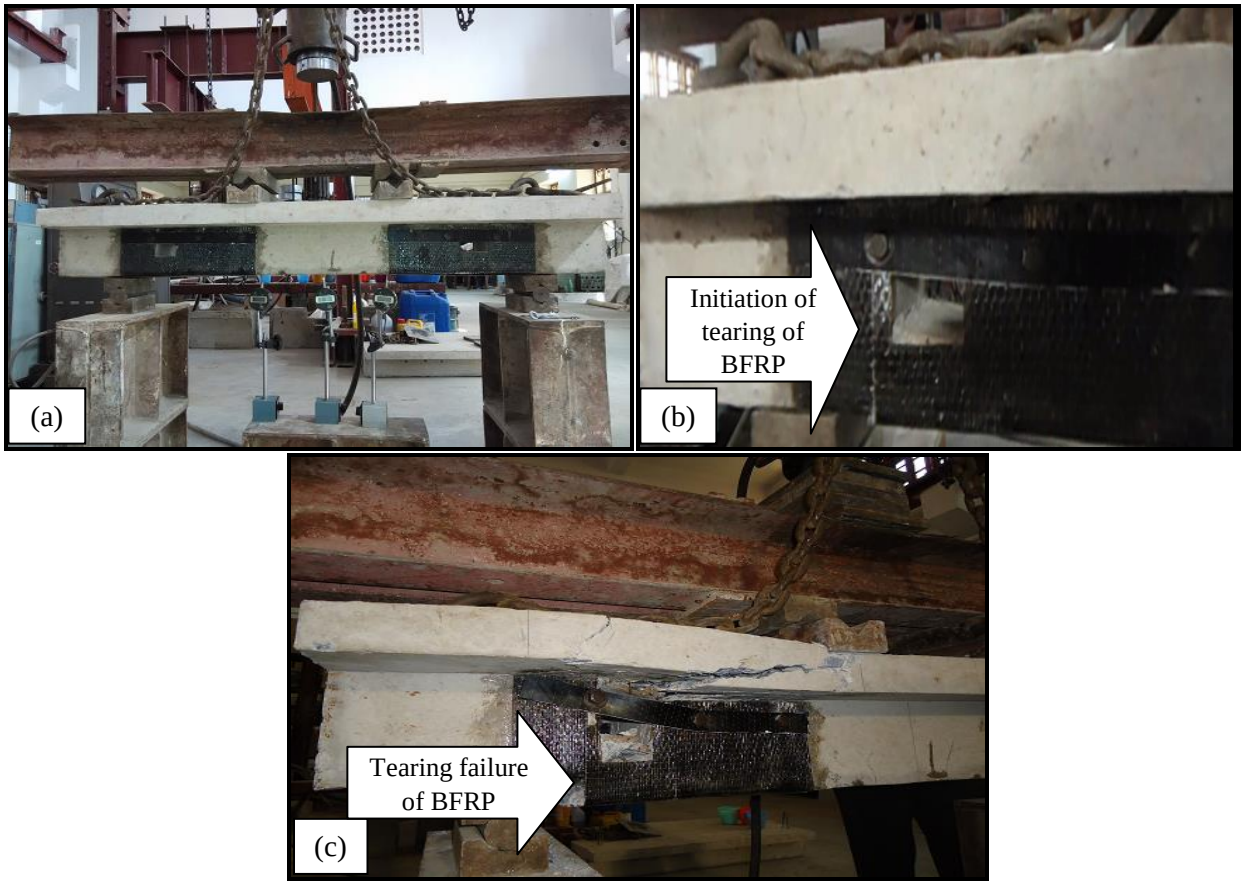

Figure 4.22 (a) Experimental Setup of beam SB18 under four-point loading system, (b) Initiation of tearing of BFRP sheet, (c) Ultimate failure of beam SB18 by tearing of BFRP sheet followed by diagonal shear crack

4.3 Load-deflection history

In order to evaluate the effectiveness of the proposed strengthening schemes, the mid-span deflections and deflection under point loads of the shear deficient beams are measured at different load steps for the control beam and beams strengthened with BFRP sheets/strips. The load-deflection histories are presented in Figures 4.23 to 4.44. It is observed that the mid-span deflections are greater than the deflections under the point loads. The load-deflection profile remains straight initially which represents the linear behavior up to certain load step and then becomes non-linear with further increase of load.

4.3.1 Series A

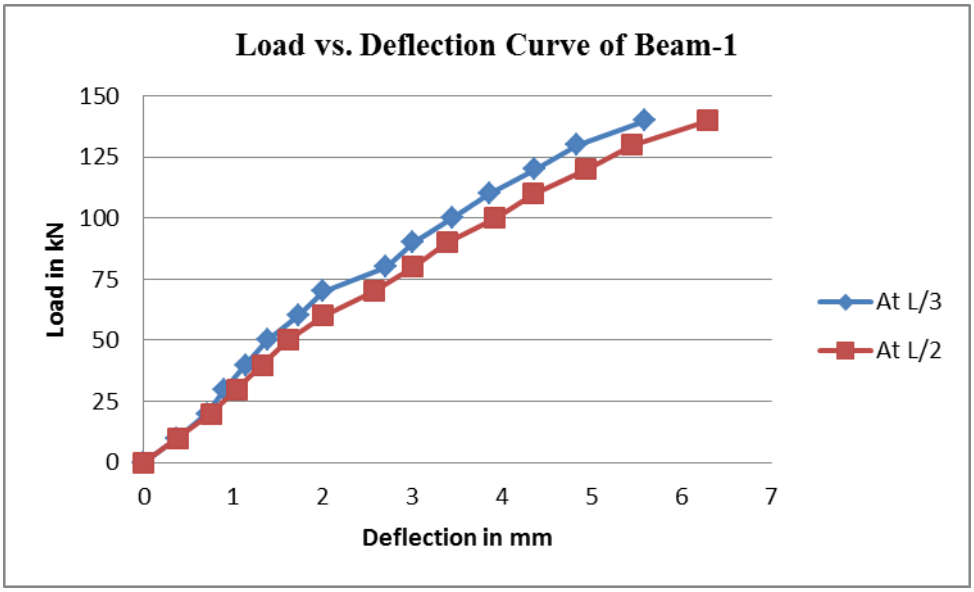

Figure 4.23 Load vs. Deflection Curve for CB

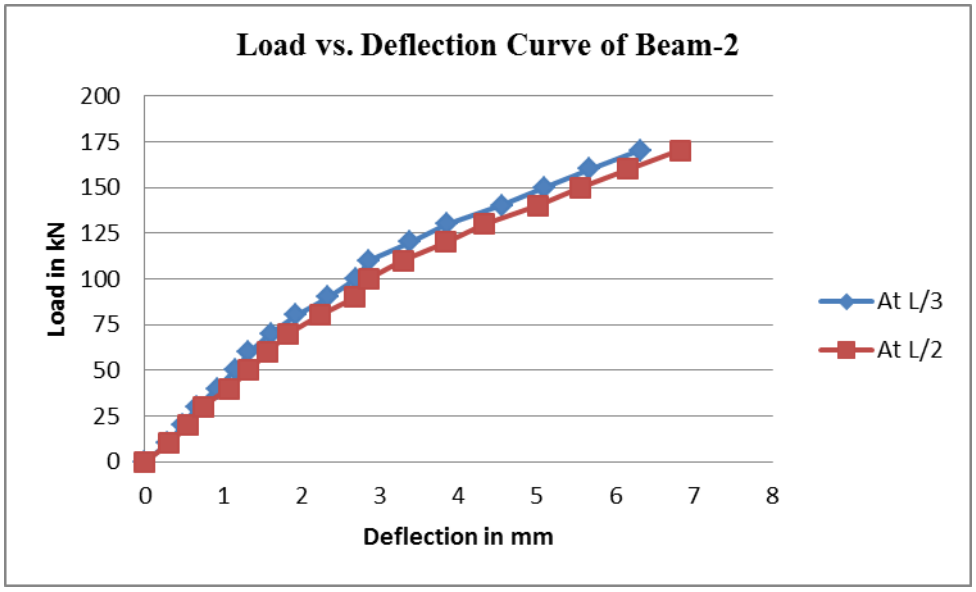

Figure 4.24 Load vs. Deflection Curve for SB1

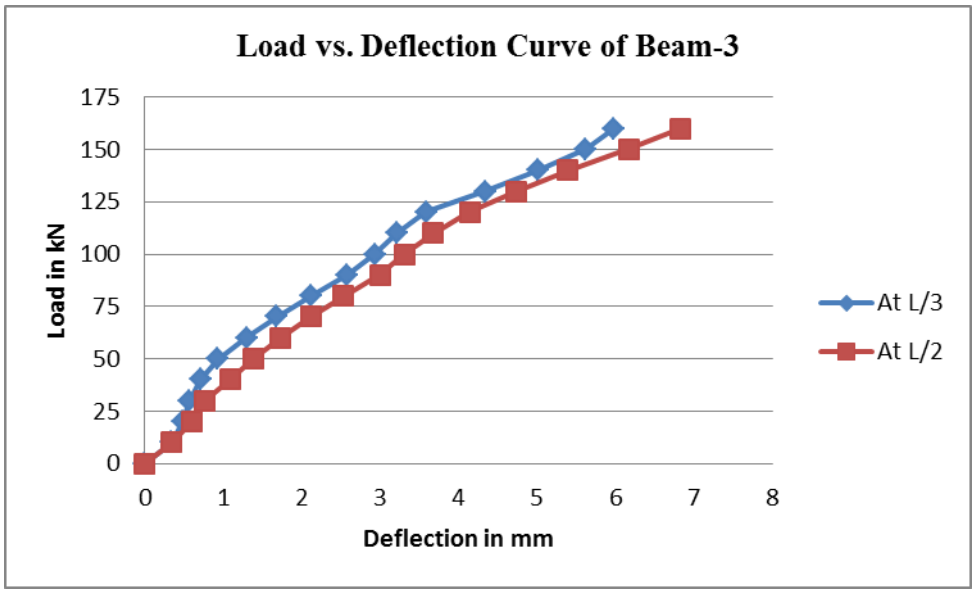

Figure 4.25 Load vs. Deflection Curve for SB2

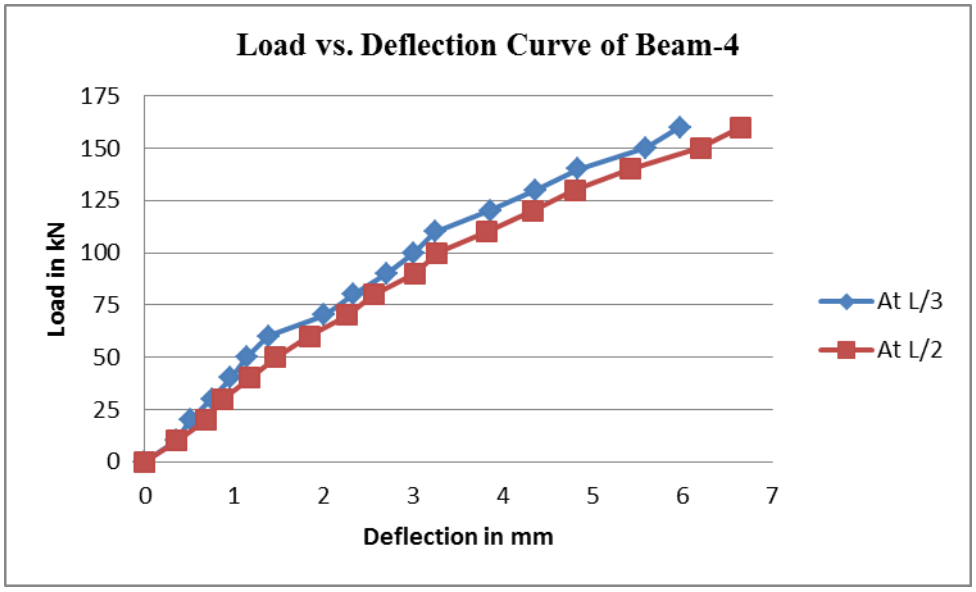

Figure 4.26 Load vs. Deflection Curve for SB3

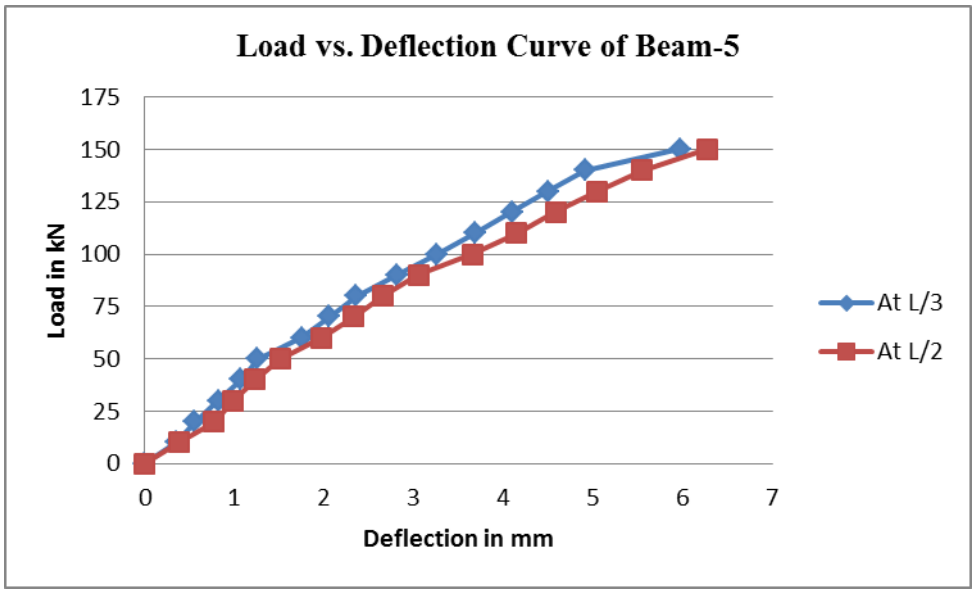

Figure 4.27 Load vs. Deflection Curve for SB4

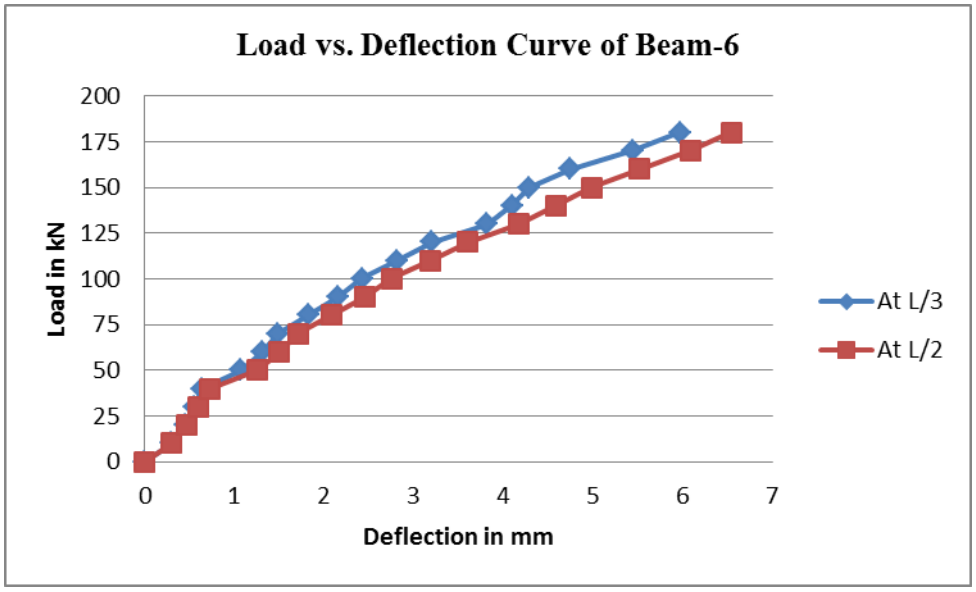

Figure 4.28 Load vs. Deflection Curve for SB5

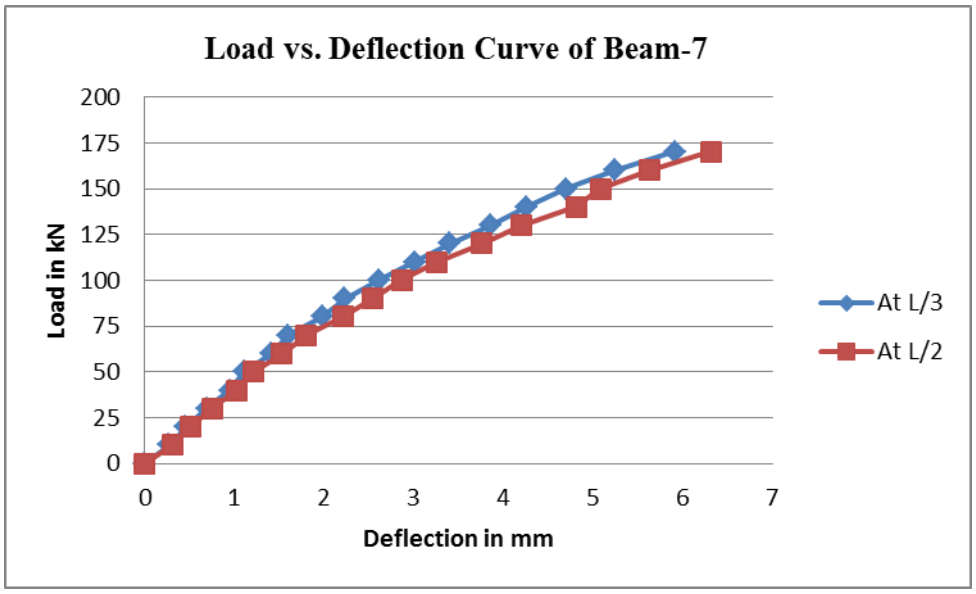

Figure 4.29 Load vs. Deflection Curve for SB6

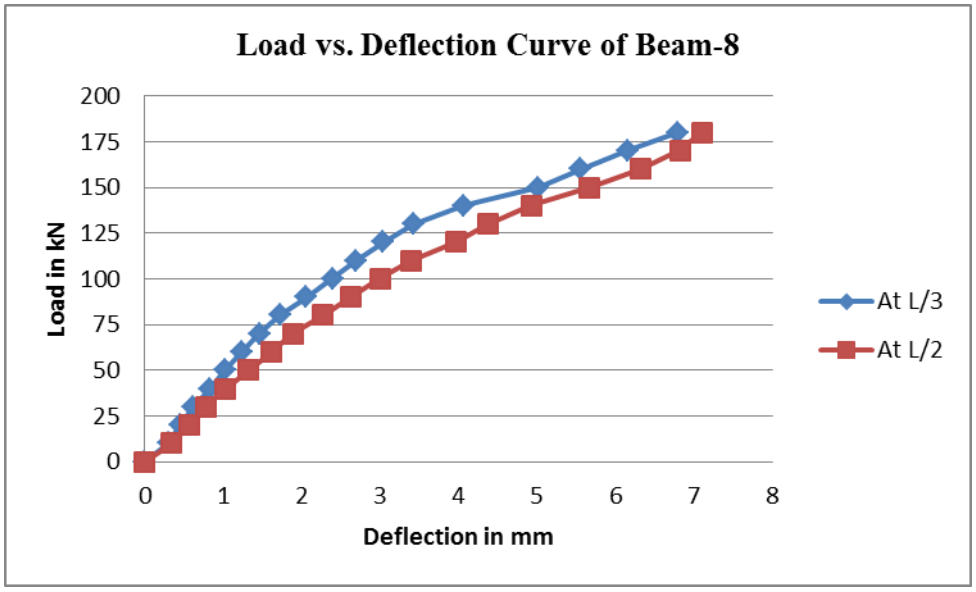

Figure 4.30 Load vs. Deflection Curve for SB7

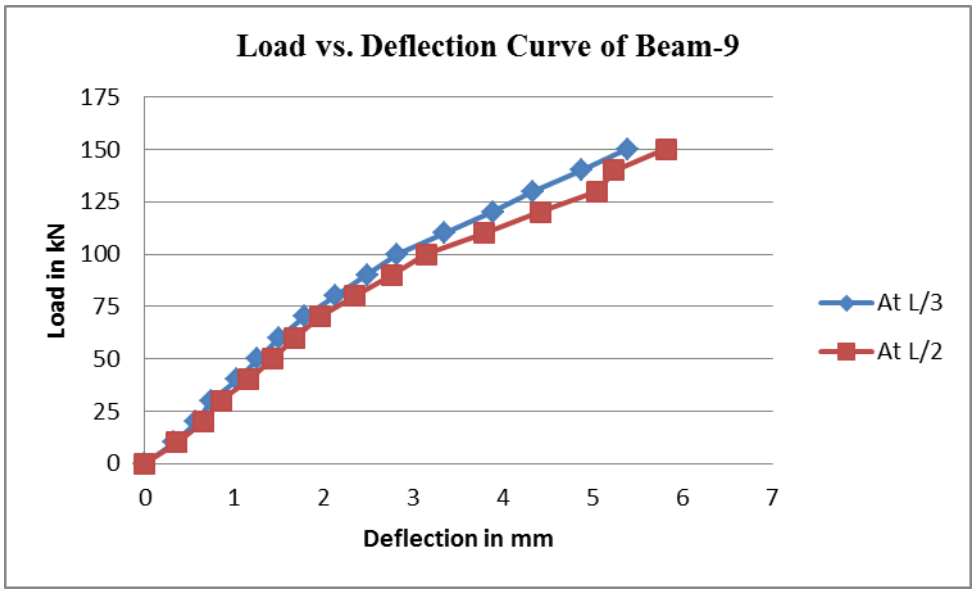

Figure 4.31 Load vs. Deflection Curve for SB8

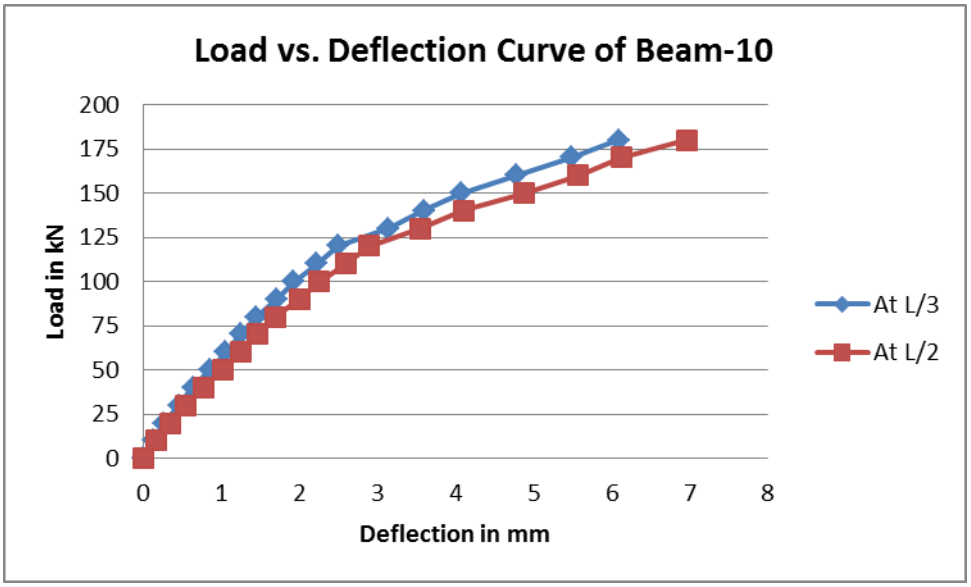

Figure 4.32 Load vs. Deflection Curve for SB9

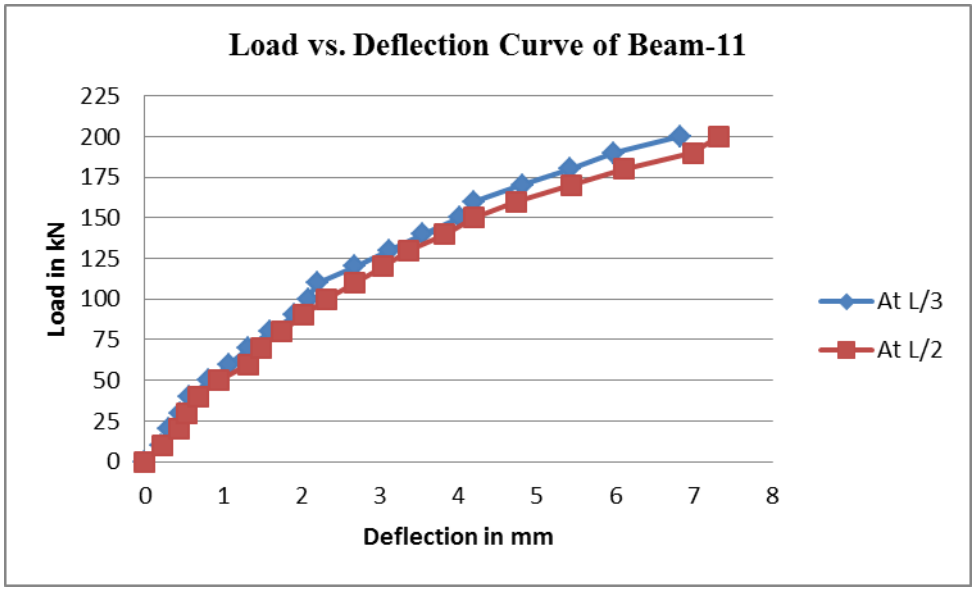

Figure 4.33 Load vs. Deflection Curve for SB10

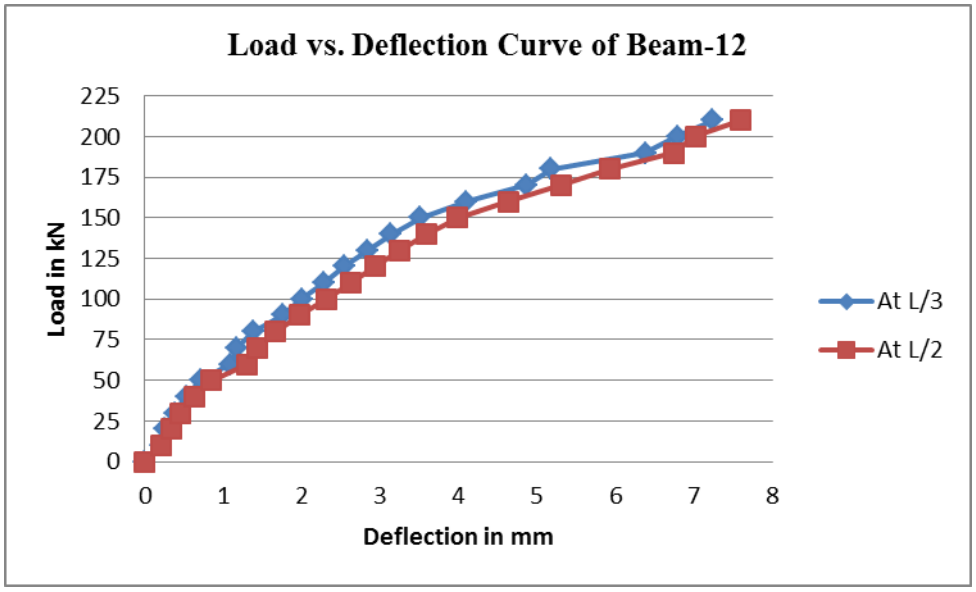

Figure 4.34 Load vs. Deflection Curve for SB11

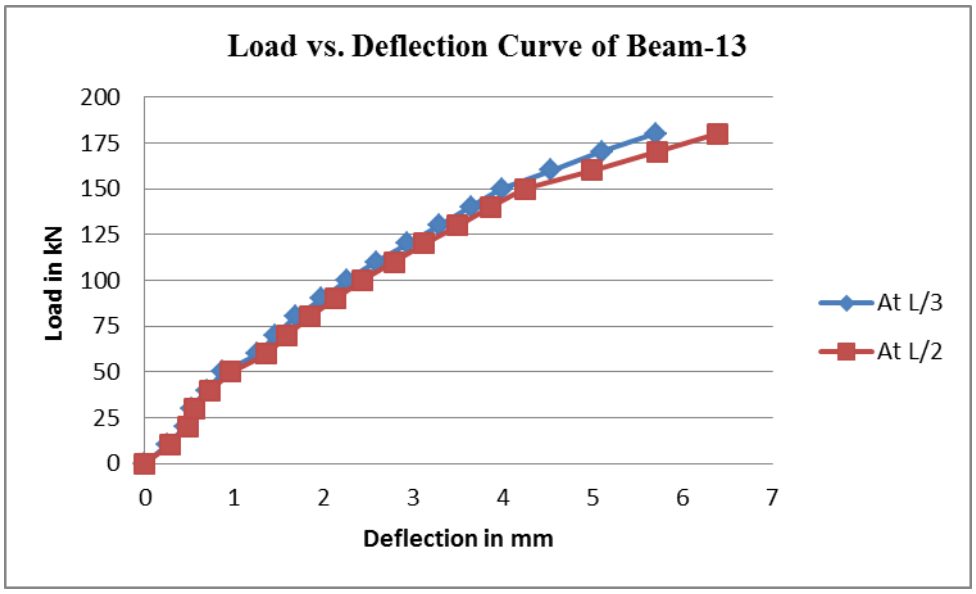

Figure 4.35 Load vs. Deflection Curve for SB12

4.3.2 Series B

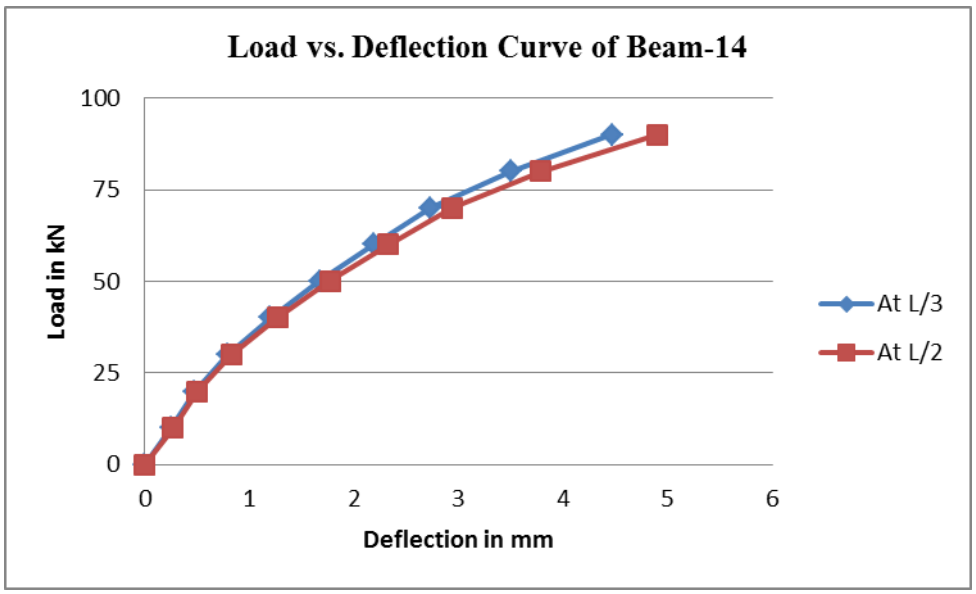

Figure 4.36 Load vs. Deflection Curve for CB1

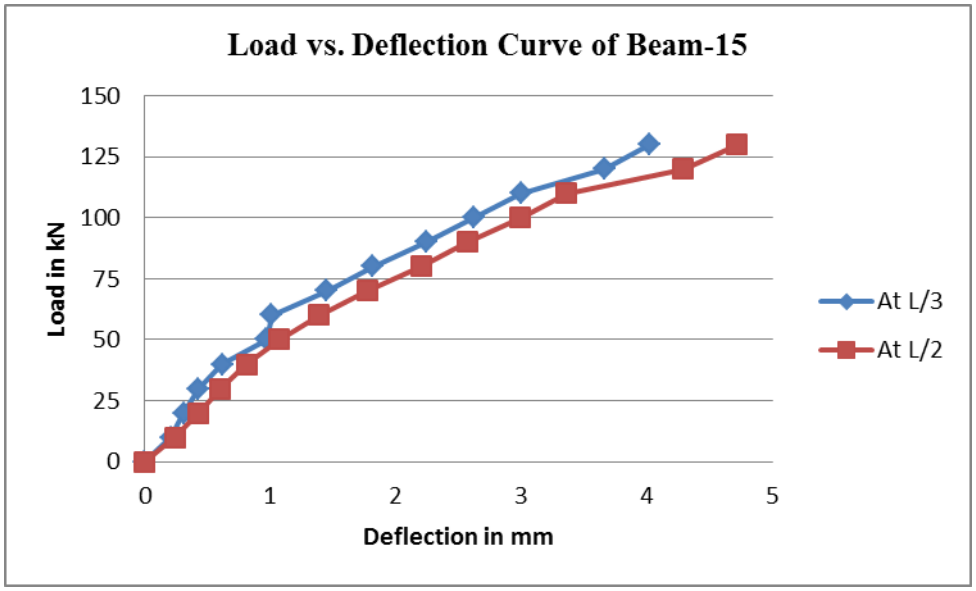

Figure 4.37 Load vs. Deflection Curve for SB13

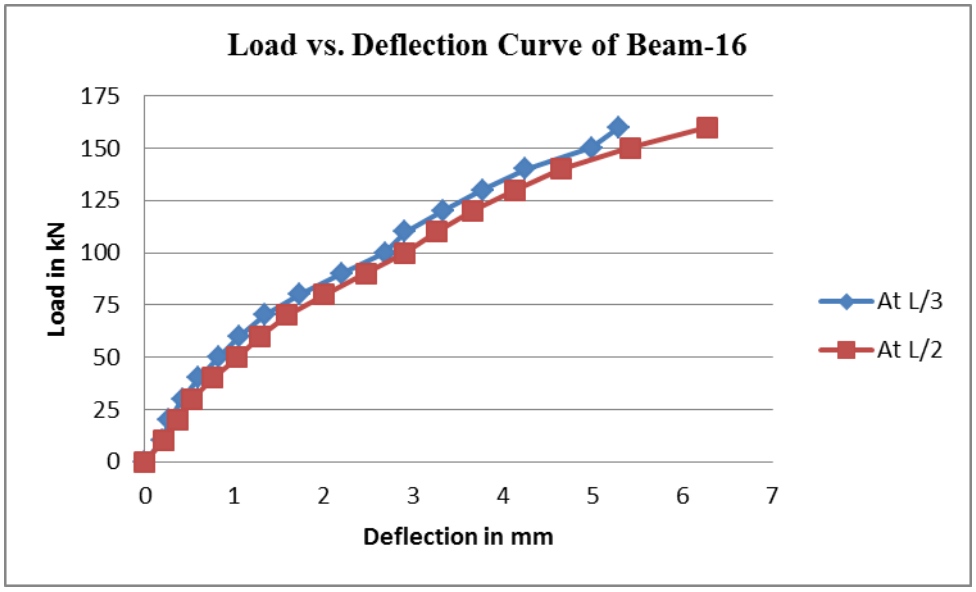

Figure 4.38 Load vs. Deflection Curve for SB14

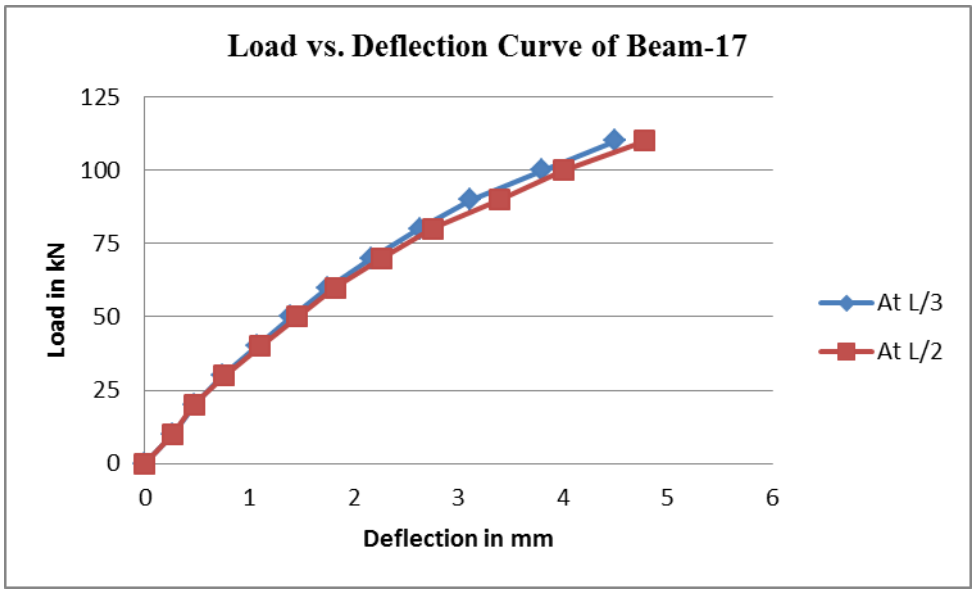

Figure 4.39 Load vs. Deflection Curve for CB2

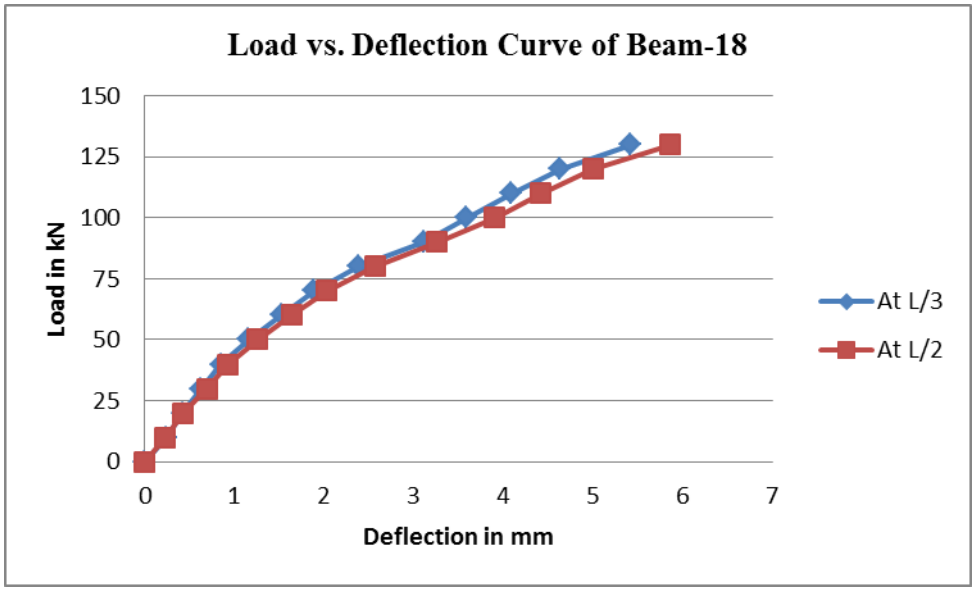

Figure 4.40 Load vs. Deflection Curve for SB15

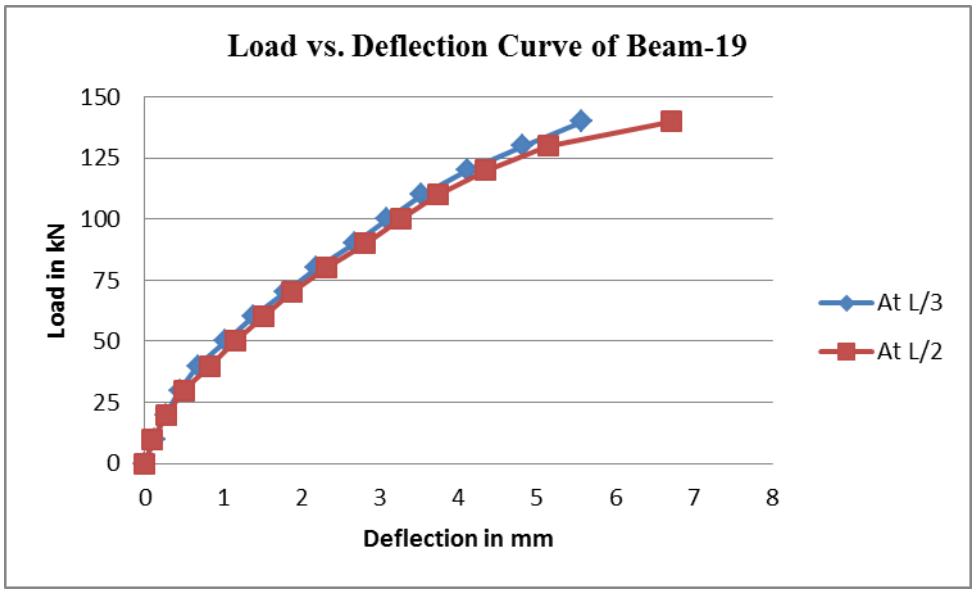

Figure 4.41 Load vs. Deflection Curve for SB16

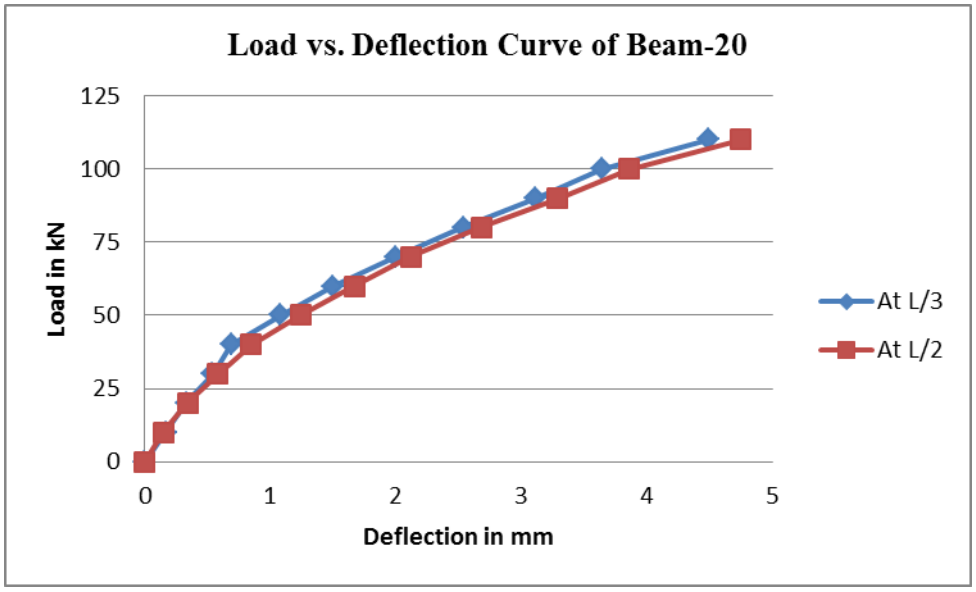

Figure 4.42 Load vs. Deflection Curve for CB3

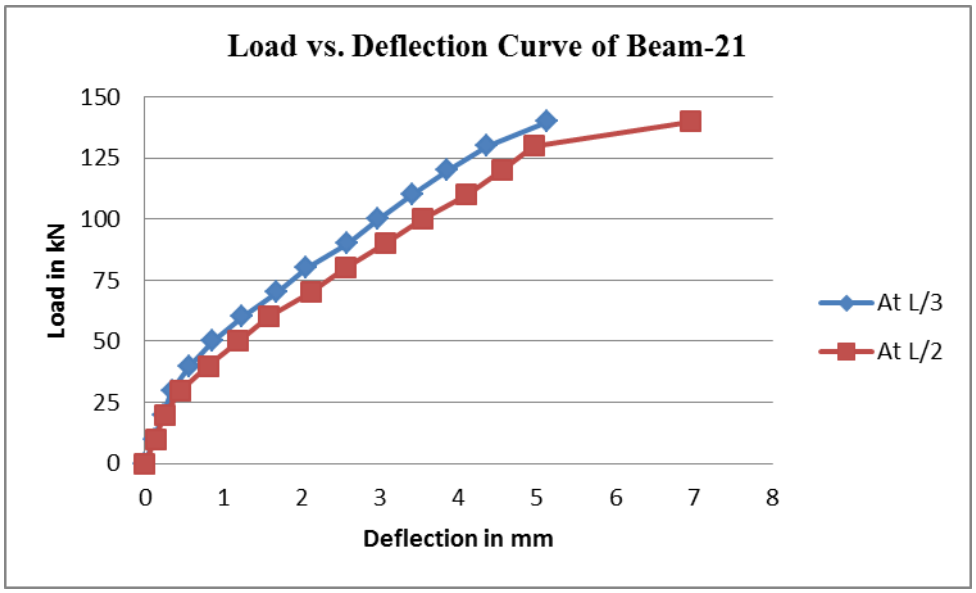

Figure 4.43 Load vs. Deflection Curve for SB17

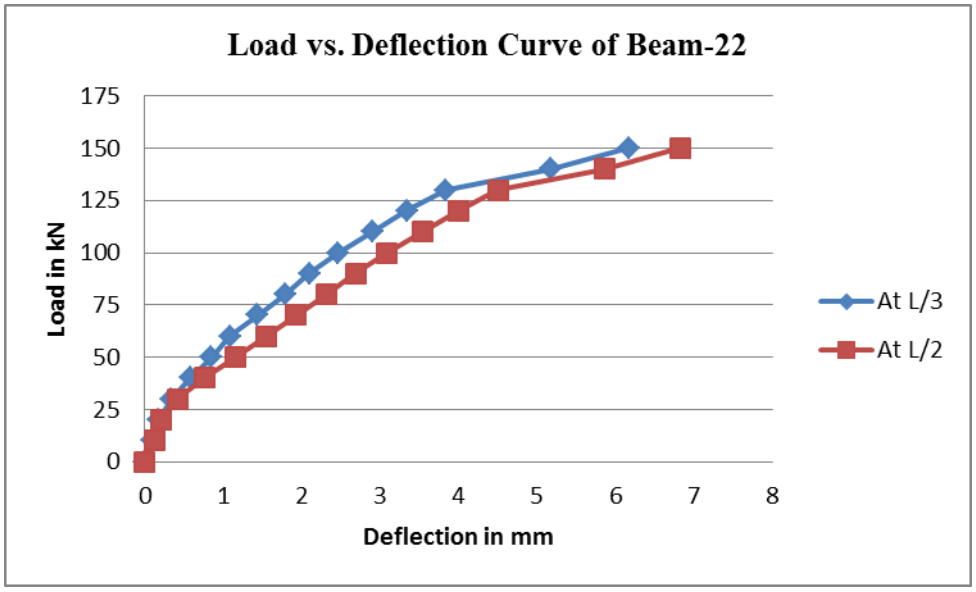

Figure 4.44 Load vs. Deflection Curve for SB18

The deflection profile for the control beam CB and beams SB1 (strengthened with continuous U-wrap with 0^0 fiber direction) and SB2 (strengthened with continuous side wrap with 0^0 fiber direction) and SB3 (strengthened with strip U-wrap with 0^0 fiber direction) and SB4 (strengthened with strip side wrap with 0^0 fiber direction) are shown in Figure 4.45. It is observed that the strengthen beams experienced less mid-span deflection as compared to the control beam under the same loading condition. The percentage reduction in mid-span deflection of SB1, SB2, SB3 and SB4 compared to CB are 20.19, 14.31, 13.99 and 11.76 respectively.

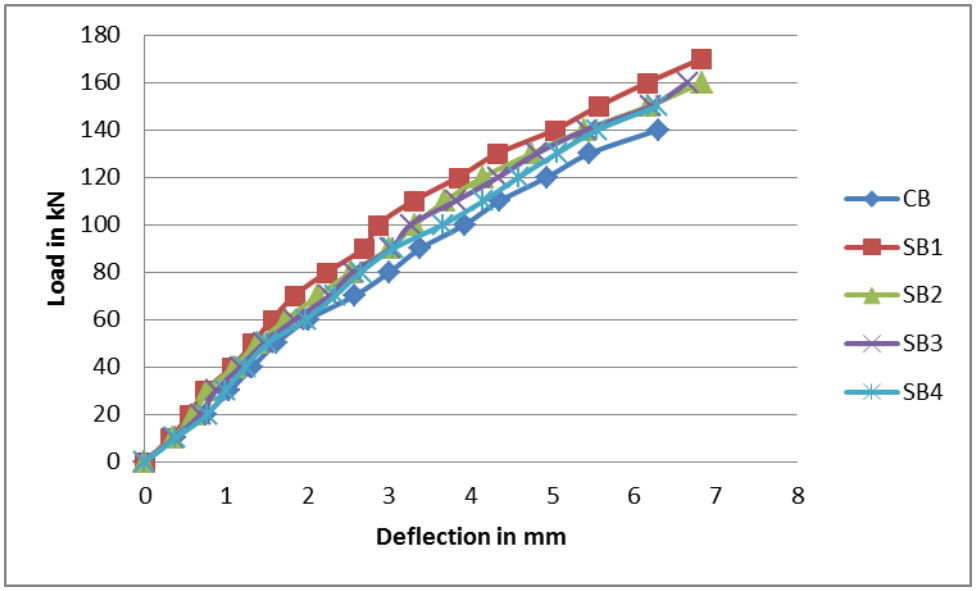

Figure 4.45 Load vs. Deflection Curve for CB vs. SB1 & SB2 & SB3 & SB4

The deflection profile for the control beam CB and beams SB5 (strengthened with continuous U-wrap with 90^0 fiber direction) and SB6 (strengthened with continuous side wrap with 90^0 fiber direction) and SB7 (strengthened with strip U-wrap with 90^0 fiber direction) and SB8 (strengthened with strip side wrap with 90^0 fiber direction) are given in Figure 4.46. It is revealed that the percentage decrease in the central deflection of SB5, SB6, SB7 and SB8 compared to CB are 27.03, 23.53, 21.62 and 16.85 respectively under the same loading condition.

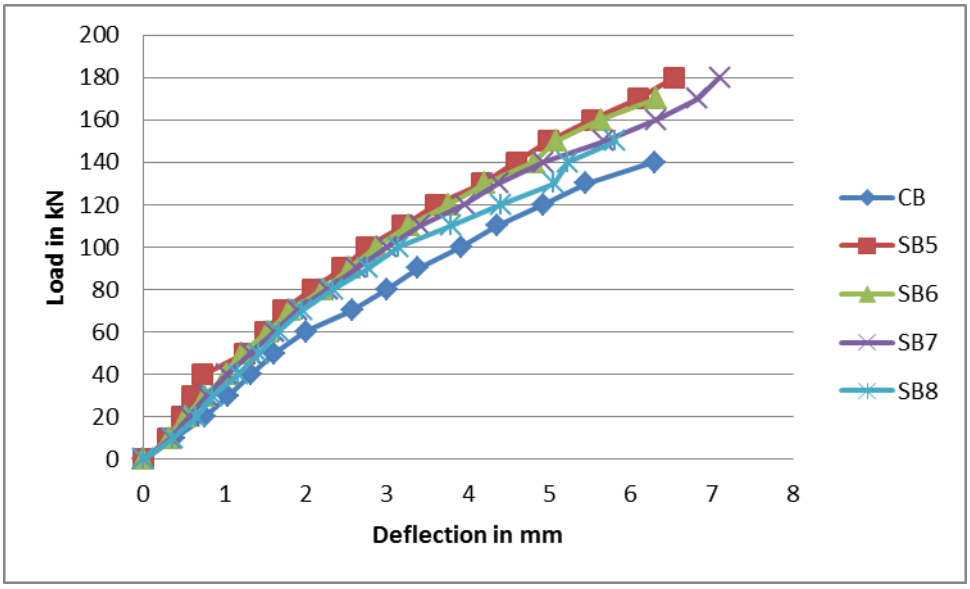

Figure 4.46 Load vs. Deflection Curve for CB vs. SB5 & SB6 & SB7 & SB8

The deflection profile for the control beam CB and beams SB3 (strengthened with strip U-wrap with 0^0 fiber direction) and SB7 (strengthened with strip U-wrap with 90^0 fiber direction) and SB9 (strengthened with strip U-wrap with 45^0 fiber direction) are shown in Figure 4.47. It is observed that all the strengthened beams experienced less deflection than the control beam under the same loading condition. The beam strengthened with inclined strips (SB9) performs better in shear than that with the horizontal (SB3) and vertical strips (SB7). The percentage reduction in mid-span deflection of SB9, SB7 and SB3 compared to CB are reported to be 34.82, 21.62 and 13.99 respectively.

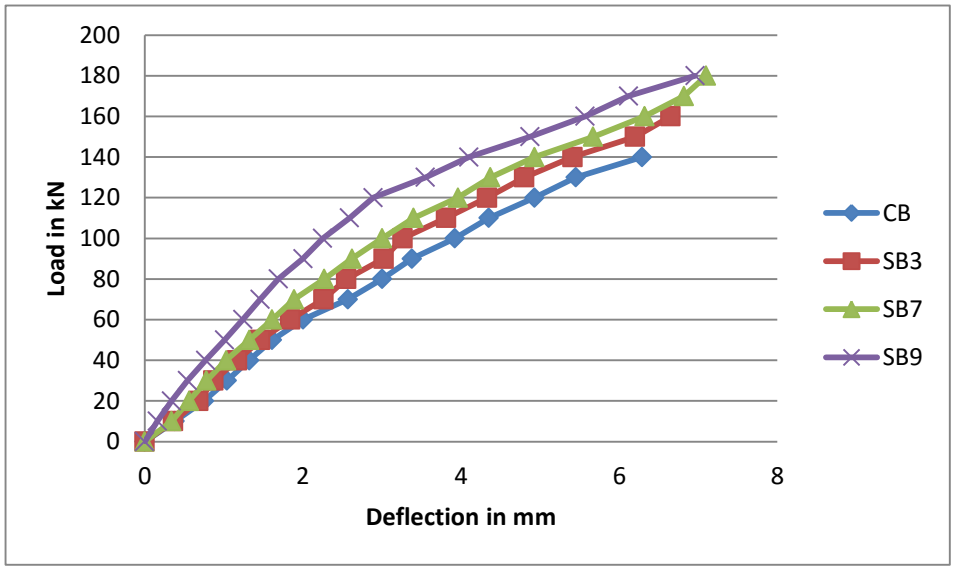

Figure 4.47 Load vs. Deflection Curve for CB vs. SB3 & SB7 & SB9

The deflection profile for the control beam CB and beams SB1 (strengthened with continuous U-wrap with 0^0 fiber direction) and SB5 (strengthened with continuous U-wrap with 90^0 fiber direction) and SB10 (strengthened with two layers continuous U-wrap with 90^0 fiber direction with end anchorage) are presented in Figure 4.48. It is observed that the beam SB10 performs better as compared to beams CB, SB1 and SB5 due to the introduction of end anchorage system which prevents the debonding failure. The percentage reduction in mid-span deflection of SB1, SB5 and SB10 compared to CB are 20.19, 27.03 and 39.27 respectively.

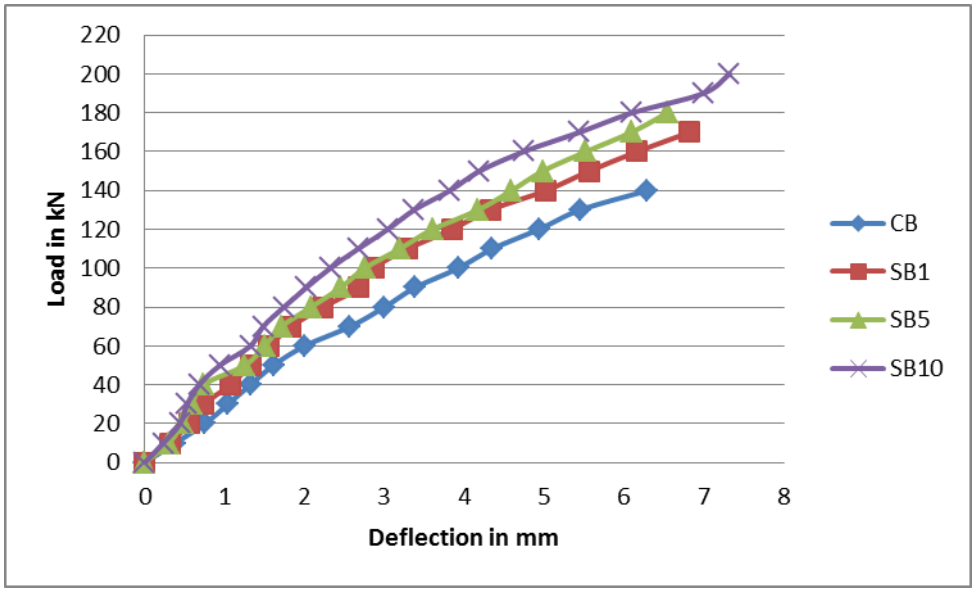

Figure 4.48 Load vs. Deflection Curve for CB vs. SB1 & SB5 & SB10

The deflection profile for the control beam CB and beams SB3 (strengthened with strip U-wrap with 0^0 fiber direction) and SB7 (strengthened with strip U-wrap with 90^0 fiber direction) and SB12 (strengthened with two layers strip U-wrap with 90^0 fiber direction with end anchorage) are shown in Figure 4.49. It is revealed that there is a significant increase in the shear capacity of the beam SB12 with the introduction of end anchorage system which prevents the debonding failure. The percentage decrease in the central deflection of SB3, SB7 and SB12 compared to CB are 13.99, 21.62 and 38.63 respectively under the same loading condition.

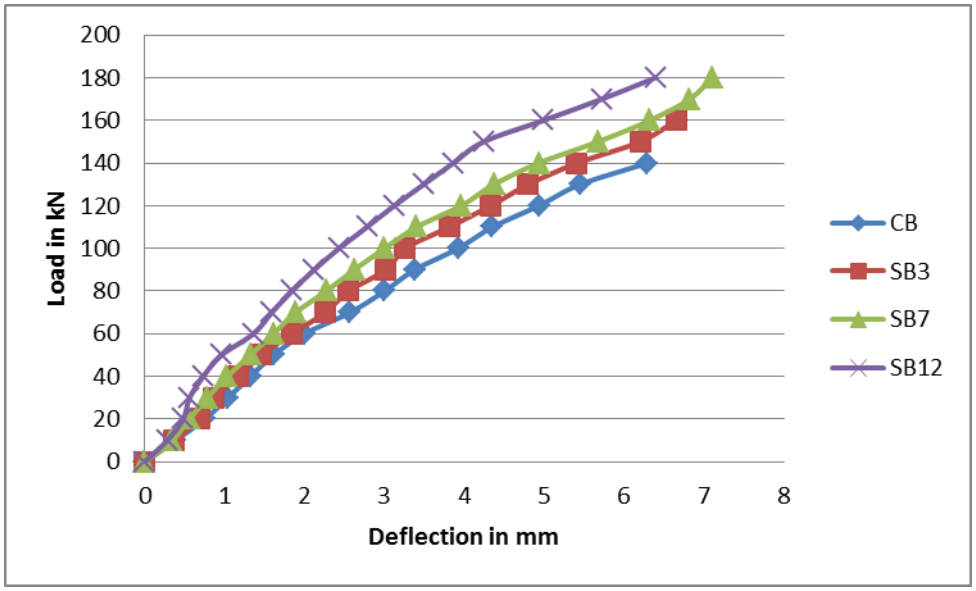

Figure 4.49 Load vs. Deflection Curve for CB vs. SB3 & SB7 & SB12

The deflection profile for the control beam CB and beams SB10 (strengthened with two layers continuous U-wrap with 90^0 fiber direction with end anchorage) and SB11 (strengthened with four layers continuous U-wrap with 90^0 fiber direction with end anchorage) are presented in Figure 4.50. It is observed that there is a significant increase in the shear performance of the beam by increasing the number of layers of BFRP. The percentage reduction in mid-span deflection of SB10 and SB11 compared to CB are 39.27 and 42.92 respectively.

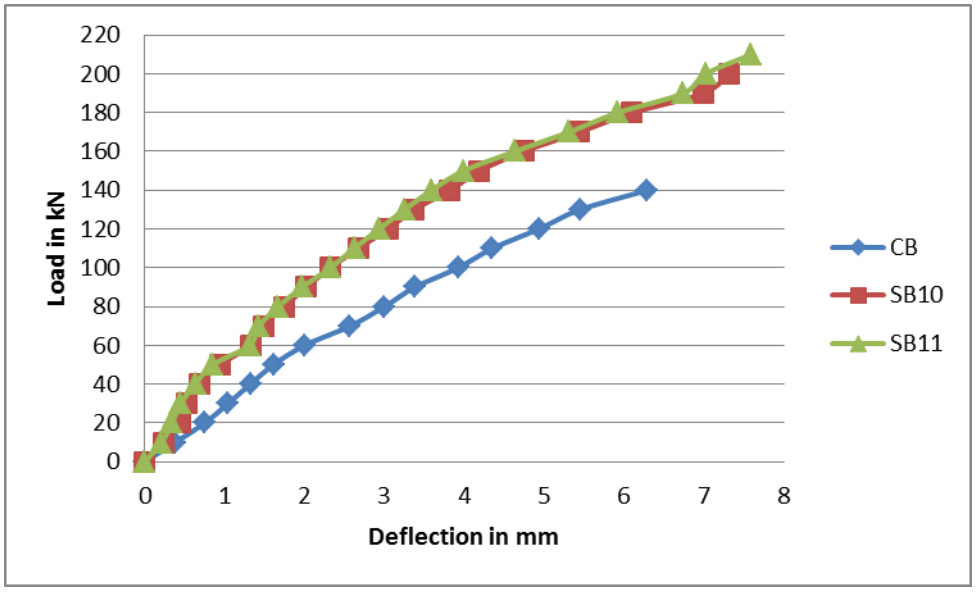

Figure 4.50 Load vs. Deflection Curve for CB vs. SB10 & SB11

The deflection profile for the control beam CB and beams SB10 (strengthened with two layers continuous U-wrap with 90^0 fiber direction with end anchorage) and SB11 (strengthened with four layers continuous U-wrap with 90^0 fiber direction with end anchorage) and SB12 (strengthened with two layers strip U-wrap with 90^0 fiber direction with end anchorage) are given in Figure 4.51. It is revealed that the percentage decrease in the central deflection of SB10, SB11 and SB12 compared to CB are 39.27, 42.92 and 38.63 respectively under the same loading condition.

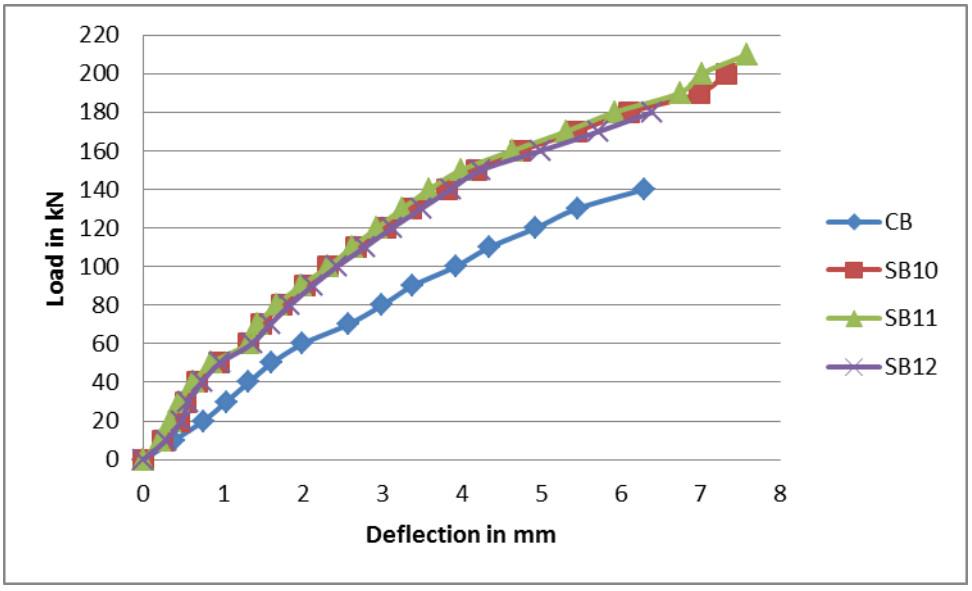

Figure 4.51 Load vs. Deflection Curve for CB vs. SB10 & SB11 & SB12

The deflection profile for the control beam CB1 and beams SB13 (strengthened with four layers continuous U-wrap with 90^0 fiber direction with circular shape web opening) and SB14 (strengthened with four layers continuous U-wrap with 90^0 fiber direction with circular shape web opening with end anchorage) are presented in Figure 4.52. It is observed that the beam SB14 performs better as compared to beams CB1 and SB13 due to the introduction of end anchorage system which prevents the premature failure. The percentage reduction in mid-span deflection of SB13 and SB14 compared to CB1 are 47.55 and 49.59 respectively under the same loading condition.

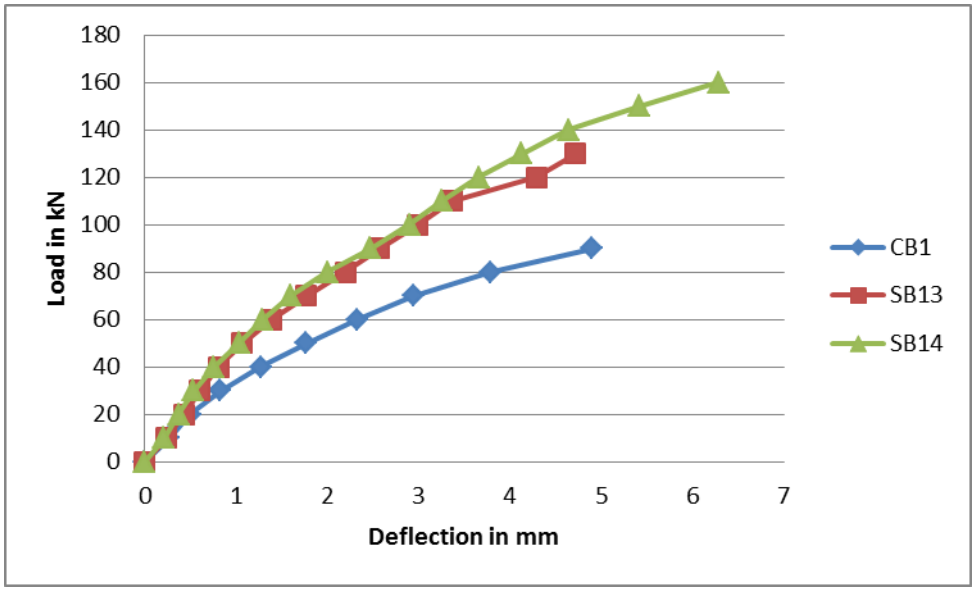

Figure 4.52 Load vs. Deflection Curve for CB1 vs. SB13 & SB14

The deflection profile for the control beam CB2 and beams SB15 (strengthened with four layers continuous U-wrap with 90^0 fiber direction with rectangular shape web opening) and SB16 (strengthened with four layers continuous U-wrap with 90^0 fiber direction with rectangular shape web opening with end anchorage) are shown in Figure 4.53. It is revealed that there is a significant increase in the shear capacity of the beam SB16 with the introduction of end anchorage system which prevents the debonding failure. The percentage decrease in the central deflection of SB15 and SB16 compared to CB2 are 7.53 and 21.97 respectively under the same loading condition.

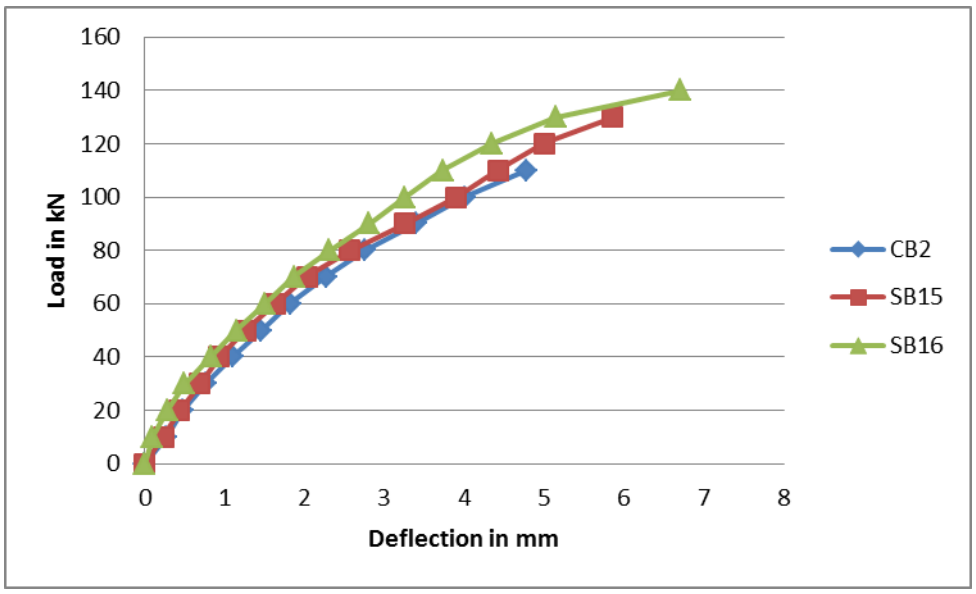

Figure 4.53 Load vs. Deflection Curve for CB2 vs. SB15 & SB16

The deflection profile for the control beam CB3 and beams SB17 (strengthened with four layers continuous U-wrap with 90^0 fiber direction with square shape web opening) and SB18 (strengthened with four layers continuous U-wrap with 90^0 fiber direction with square shape web opening with end anchorage) are depicted in Figure 4.54. It is noticed that the beam SB18 performs better as compared to beams CB3 and SB17 due to the introduction of end anchorage system which prevents the debonding failure. The percentage reduction in mid-span deflection of SB17 and SB18 compared to CB3 are 13.68 and 25.47 respectively under the same loading condition.

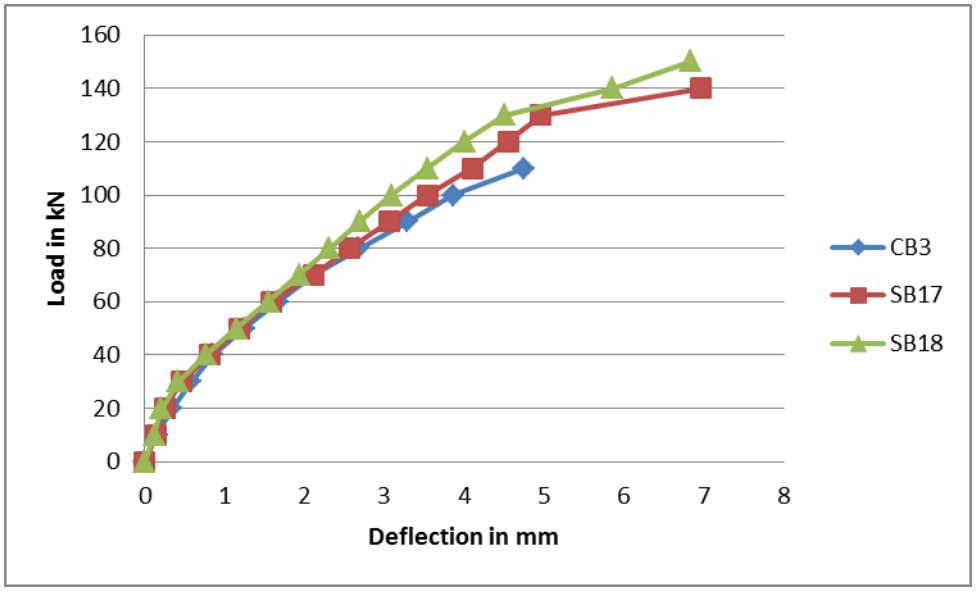

Figure 4.54 Load vs. Deflection Curve for CB3 vs. SB17 & SB18

4.4 Load at initial crack

The crack patterns of the beams are visualized with the progress of the load. The initial cracks are visualized for the beams which are not fully wrapped with BFRP sheets. The load corresponding to initial crack of the beams is recorded and depicted in Figure 4.55. It is observed that the initial cracks in the strengthened RC T-beams are developed at a higher load than the control beam. From Figure 4.55, it is noticed that the load at first crack of SB12 is the highest among all the strengthen beams and is 110% higher than the control beam.

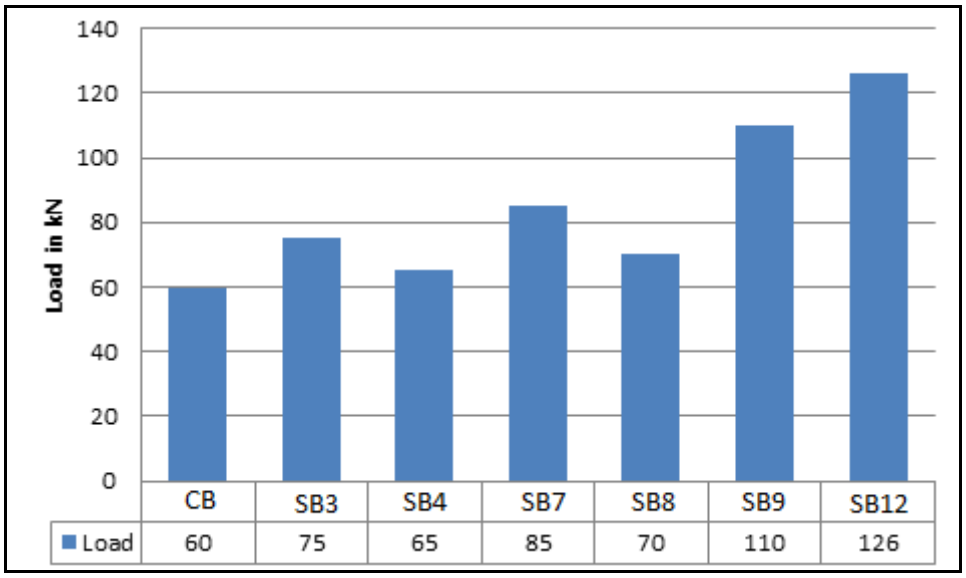

Figure 4.55 Load at initial crack of beams CB, SB3, SB4, SB7, SB8, SB9 and SB12

4.5 Ultimate Load Carrying Capacity

4.5.1 Series A

A comparison in ultimate load carrying capacity is made among the control beam CB, SB1 (strengthened with continuous U-wrap with 0^0 fiber direction) and SB5 (strengthened with continuous U-wrap with 90^0 fiber direction) and presented in Figure 4.56. It is observed that the ultimate load carrying capacity of SB5 is 26.58% higher than the control beam and is 12.36% higher than the beam SB1.

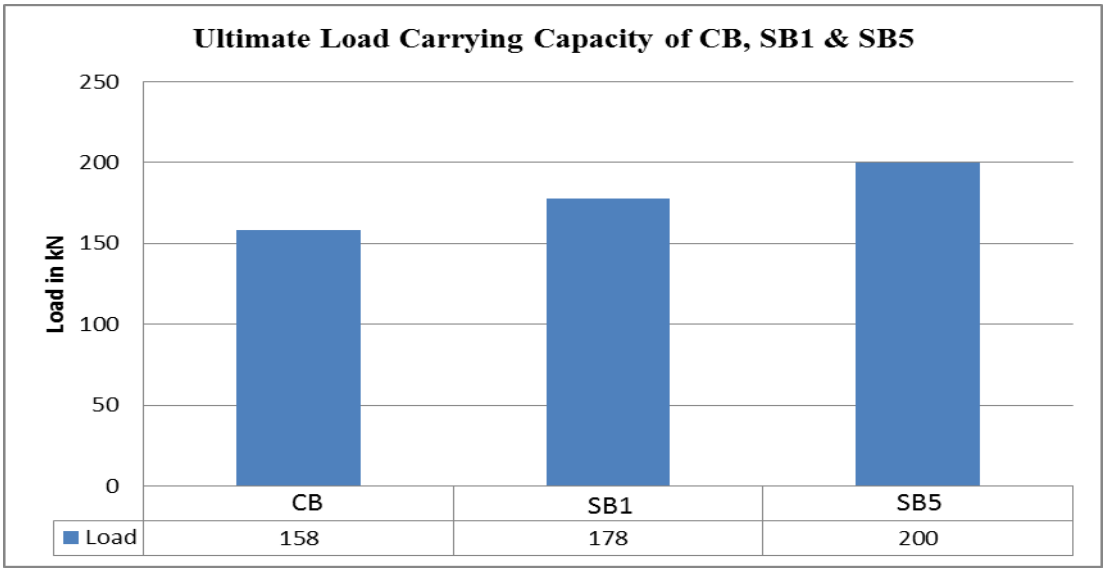

Figure 4.56 Ultimate load carrying capacity of beams CB, SB1 and SB5

The ultimate load carrying capacity of the control beam CB, SB3 (strengthened with strip U-wrap with 0^0 fiber direction) and SB7 (strengthened with strip U-wrap with 90^0 fiber direction) beams are compared and shown in Figure 4.57. It is revealed that the ultimate load carrying capacity of SB7 is 17.08% higher than the control beam and is 8.82% higher than the beam SB3.

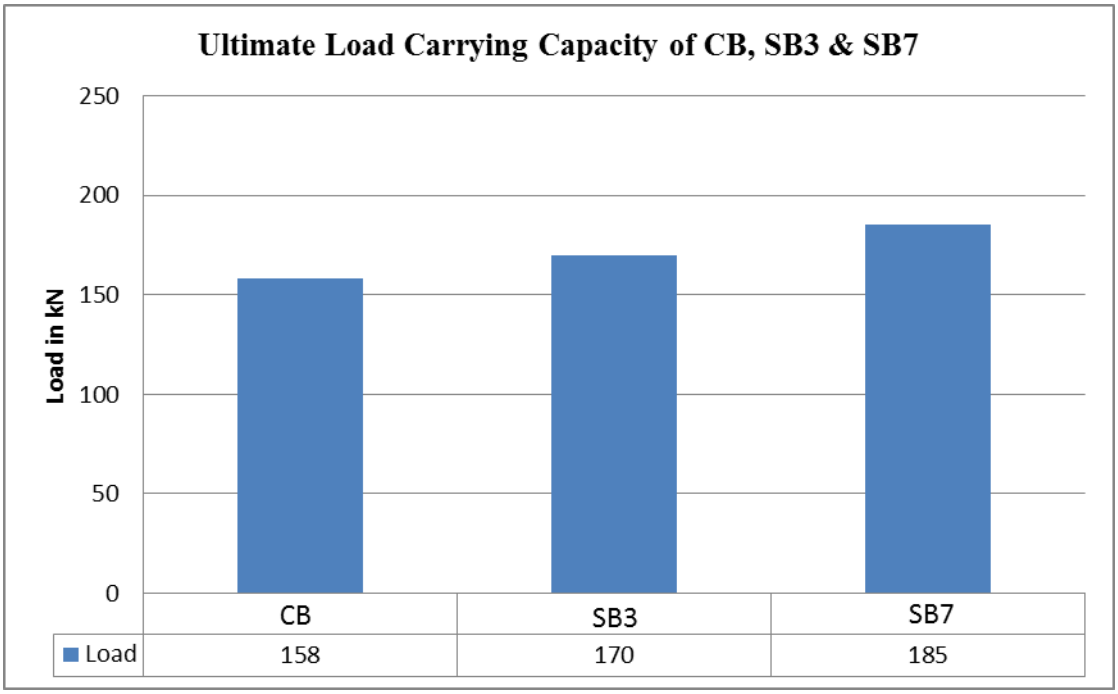

Figure 4.57 Ultimate load carrying capacity of beams CB, SB3 and SB7

Among the control beam CB, beams SB2 (strengthened with continuous side wrap with 0^0 fiber direction) and SB6 (strengthened with continuous side wrap with 90^0 fiber direction), the ultimate load carrying capacity of SB6 is 10.76% and 4.79% higher than the control beam and SB2, respectively and is depicted in Figure 4.58.

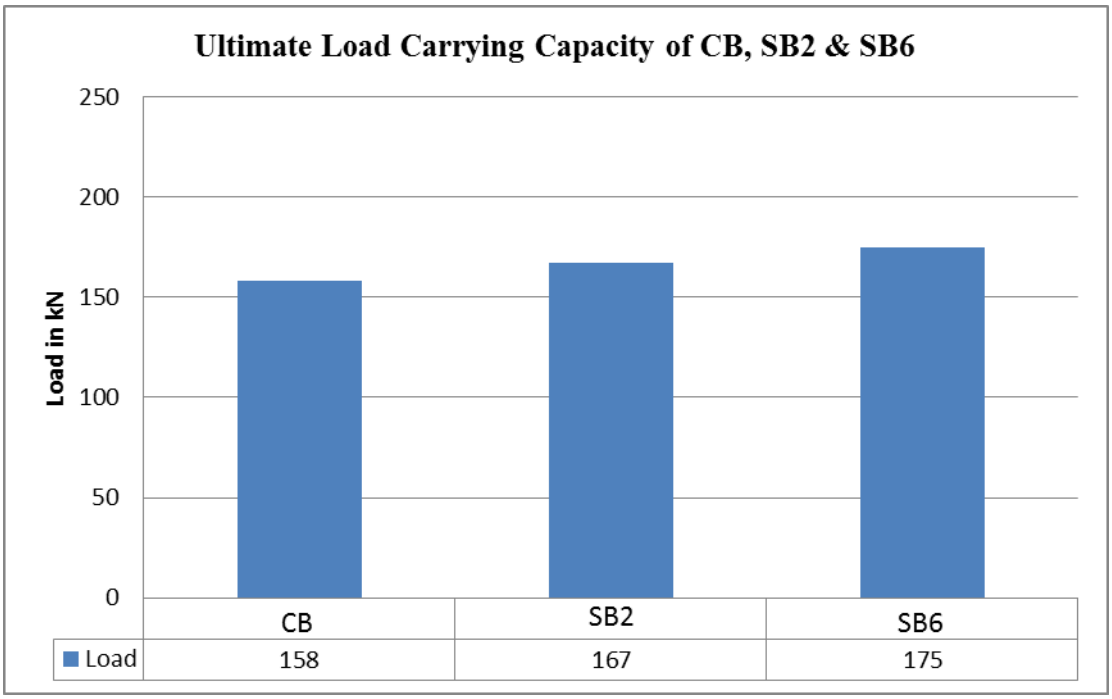

Figure 4.58 Ultimate load carrying capacity of beams CB, SB2 and SB6

A comparison in ultimate load carrying capacity is made among the control beam CB, SB4 (strengthened with strip side wrap with 0^0 fiber direction) and SB8 (strengthened with strip side wrap with 90^0 fiber direction) and is given in Figure 4.59. It is noticed that the ultimate load carrying capacity of SB8 is 5.06% higher than the control beam and is 1.84% higher than the beam SB4.

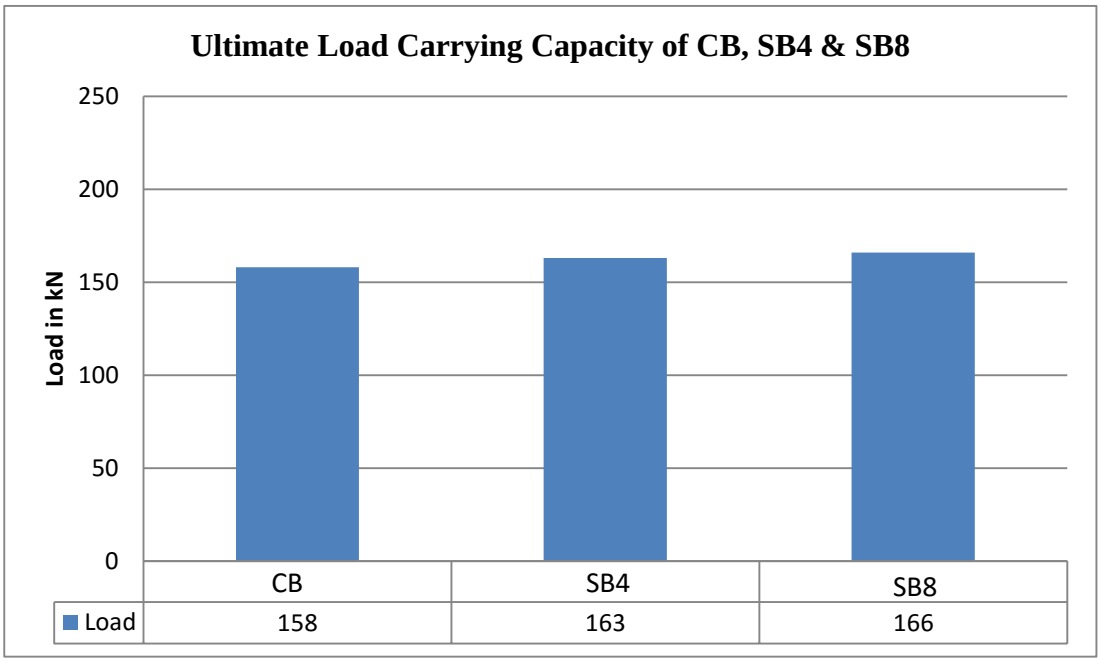

Figure 4.59 Ultimate load carrying capacity of beams CB, SB4 and SB8

The ultimate load carrying capacity of the control beam CB, SB3 (strengthened with strip U-wrap with 0^0 fiber direction), SB7 (strengthened with strip U-wrap with 90^0 fiber direction) and SB9 (strengthened with strip U-wrap with 45^0 fiber direction) beams are compared and is presented in Figure 4.60. It is observed that the ultimate load carrying capacity of SB9 is 21.52% higher than the control beam and is 3.78% and 12.94% higher than the beams SB7 and SB3 respectively.

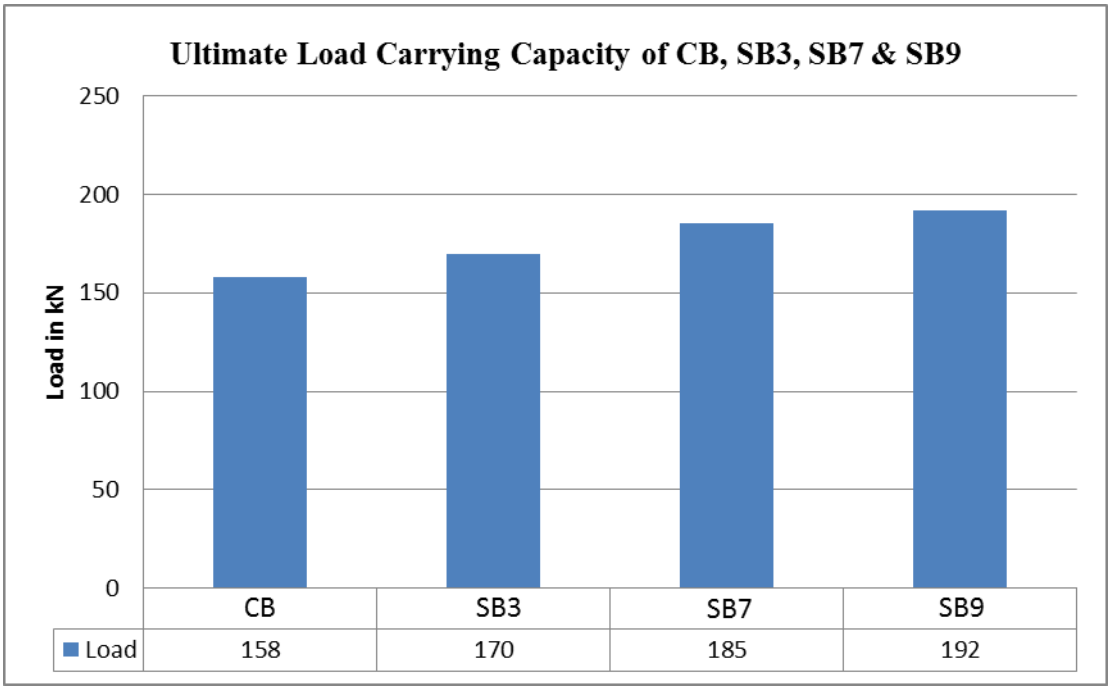

Figure 4.60 Ultimate load carrying capacity of beams CB, SB3, SB7 and SB9

Among the control beam CB, beams SB5 (strengthened with continuous U-wrap with 90^0 fiber direction) and SB6 (strengthened with continuous side wrap with 90^0 fiber direction), the ultimate load carrying capacity of SB5 is 26.58% and 14.28% higher than the control beam and SB6, respectively and is shown in Figure 4.61.

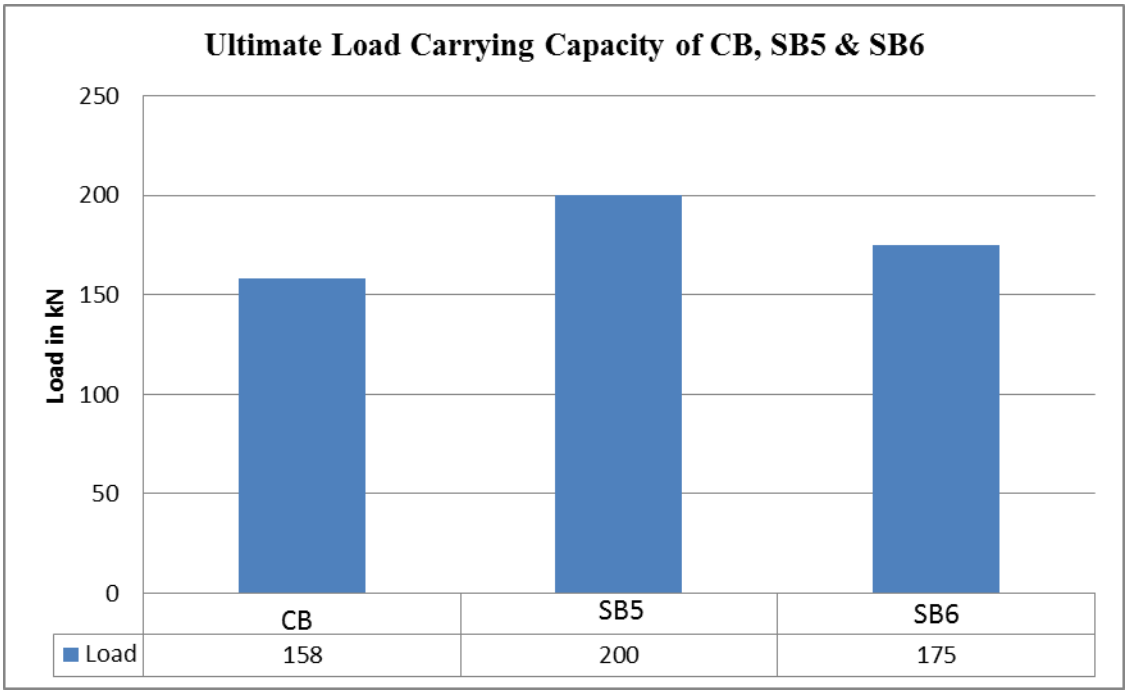

Figure 4.61 Ultimate load carrying capacity of beams CB, SB5 and SB6

A comparison in ultimate load carrying capacity is made among the control beam CB, SB7 (strengthened with strip U-wrap with 90^0 fiber direction) and SB8 (strengthened with strip side wrap with 90^0 fiber direction) and is depicted in Figure 4.62. It is revealed that the ultimate load carrying capacity of SB7 is 17.09% higher than the control beam and is 11.44% higher than the beam SB8.

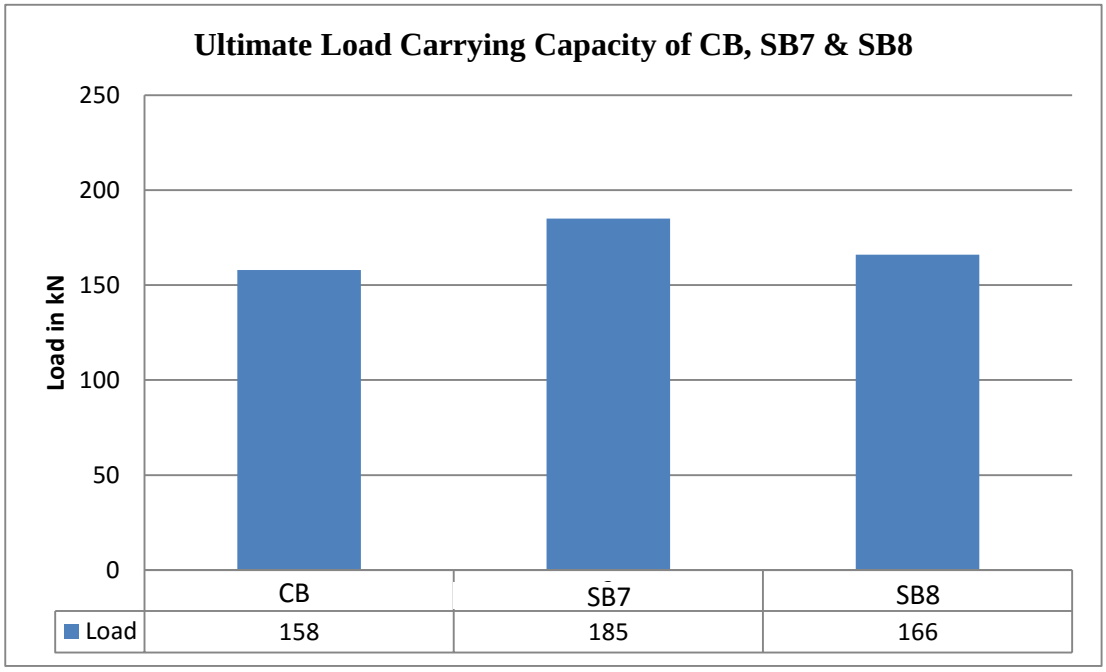

Figure 4.62 Ultimate load carrying capacity of beams CB, SB7 and SB8

The ultimate load carrying capacity of the control beam CB, SB5 (strengthened with continuous U-wrap with 90^0 fiber direction) and SB10 (strengthened with two layers continuous U-wrap with 90^0 fiber direction with end anchorage) beams are compared and is given in Figure 4.63. It is noticed that the ultimate load carrying capacity of SB10 is 38.61% higher than the control beam and is 9.5% higher than the beam SB5.

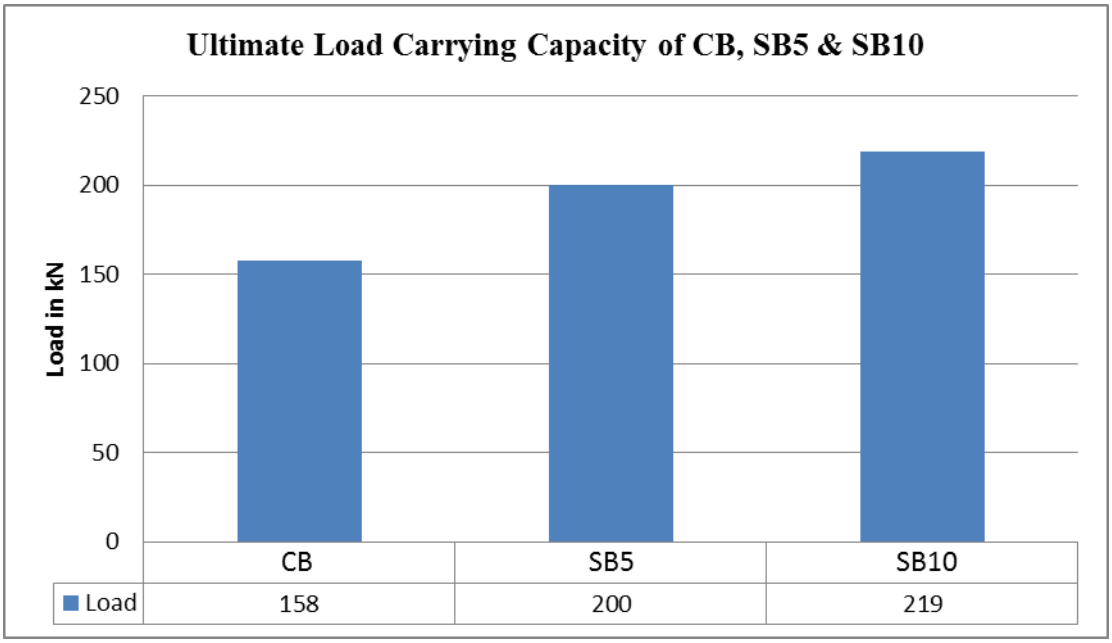

Figure 4.63 Ultimate load carrying capacity of beams CB, SB5 and SB10

Among the control beam CB, beams SB10 (strengthened with two layers continuous U-wrap with 90^0 fiber direction with end anchorage) and SB11 (strengthened with four layers continuous U-wrap with 90^0 fiber direction with end anchorage), the ultimate load carrying capacity of SB11 is 46.83% and 5.94% higher than the control beam and SB10, respectively and is presented in Figure 4.64.

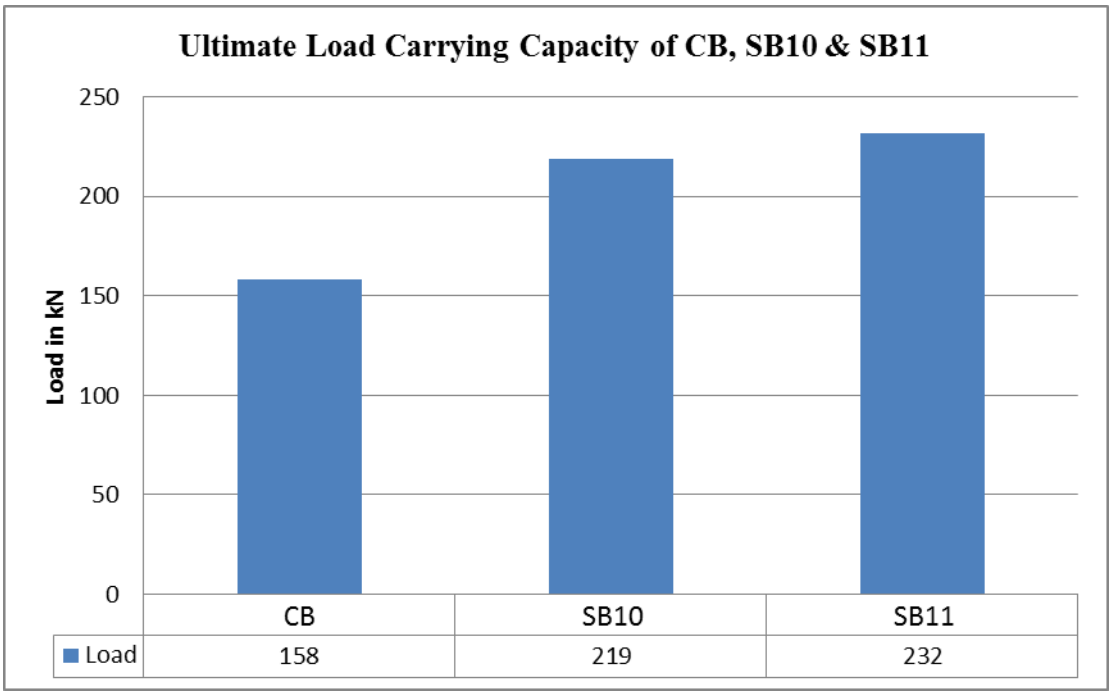

Figure 4.64 Ultimate load carrying capacity of beams CB, SB10 and SB11

A comparison in ultimate load carrying capacity is made among the control beam CB, SB7 (strengthened with strip U-wrap with 90^0 fiber direction) and SB12 (strengthened with two layers strip U-wrap with 90^0 fiber direction with end anchorage) and is shown in Figure 4.65. It is observed that the ultimate load carrying capacity of SB12 is 26.58% higher than the control beam and is 8.11% higher than the beam SB7.

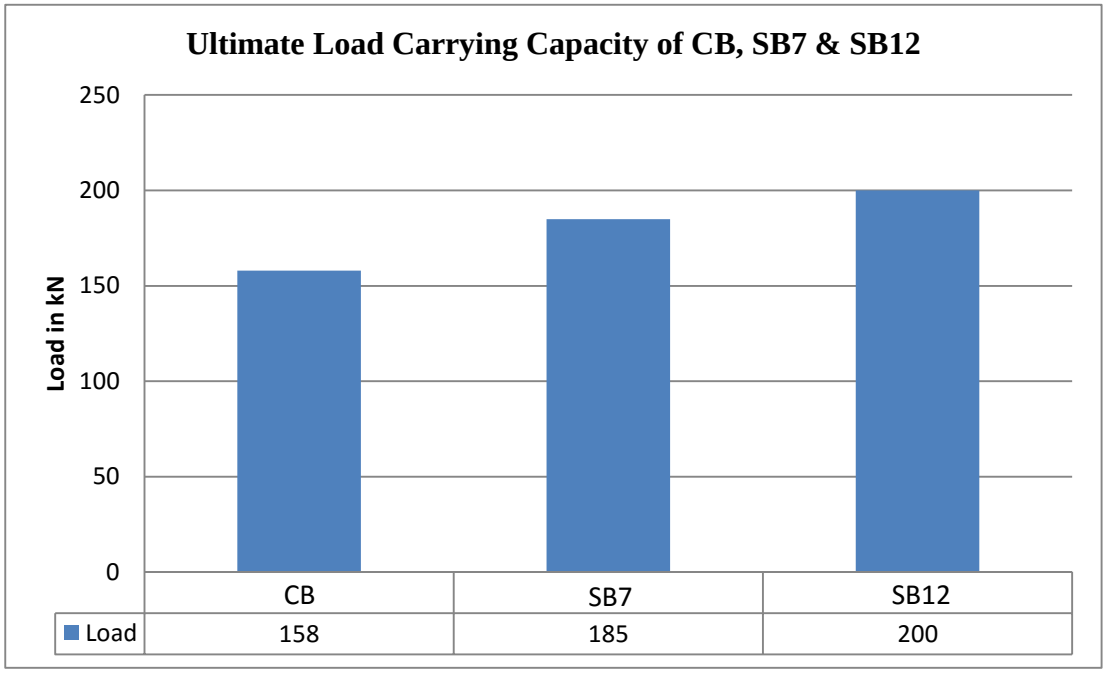

Figure 4.65 Ultimate load carrying capacity of beams CB, SB7 and SB12

The ultimate load carrying capacity of the control beam CB, SB10 (strengthened with two layers continuous U-wrap with 90^0 fiber direction with end anchorage) and SB12 (strengthened with two layers strip U-wrap with 90^0 fiber direction with end anchorage) beams are compared and is depicted in Figure 4.66. It is revealed that the ultimate load carrying capacity of SB10 is 38.61% higher than the control beam and is 9.5% higher than the beam SB12.

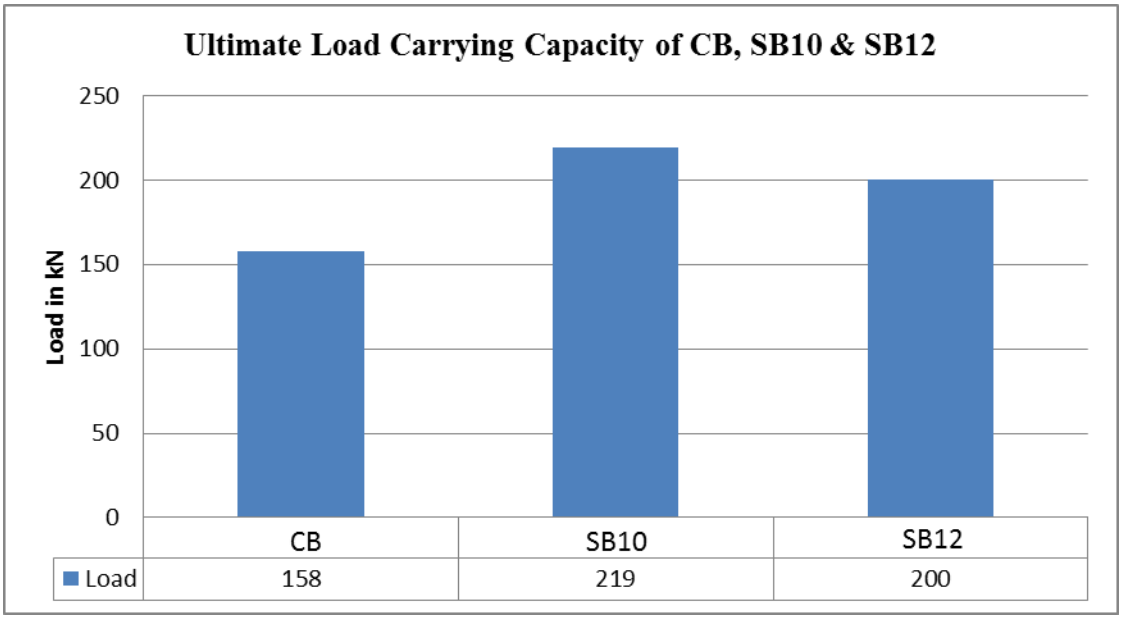

Figure 4.66 Ultimate load carrying capacity of beams CB, SB10 and SB12

4.5.2 Series B

Among the control beam CB1, beams SB13 (strengthened with four layers continuous U-wrap with 90^0 fiber direction with circular shape web opening) and SB14 (strengthened with four layers continuous U-wrap with 90^0 fiber direction with circular shape web opening with end anchorage), the ultimate load carrying capacity of SB14 is 62% and 22.73% higher than the control beam CB1 and SB13, respectively and is given in Figure 4.67.

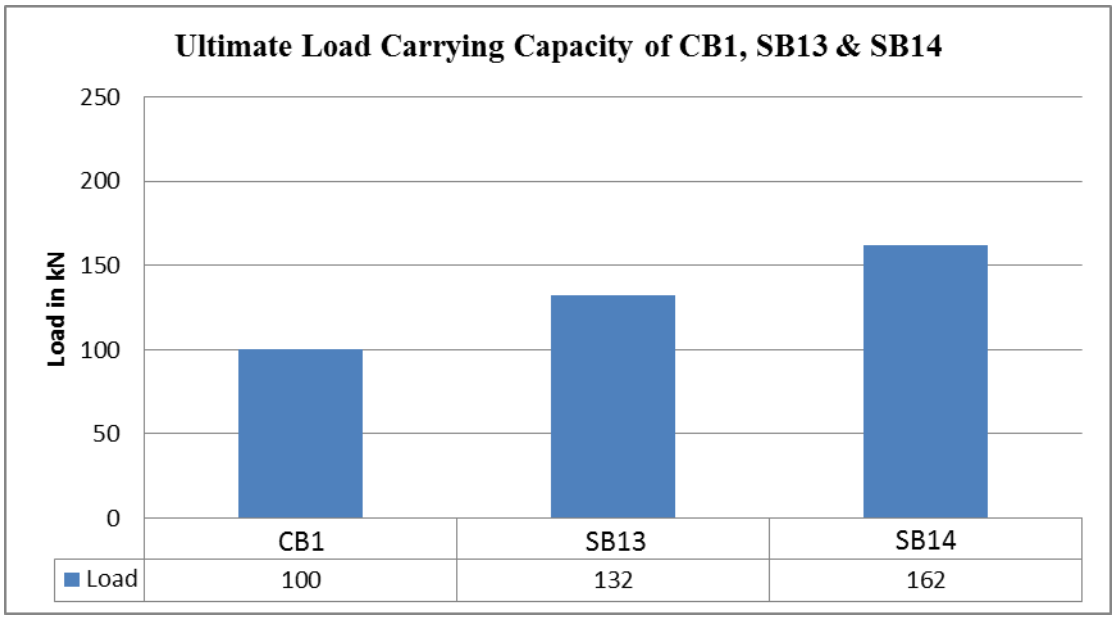

Figure 4.67 Ultimate load carrying capacity of beams CB1, SB13 and SB14

A comparison in ultimate load carrying capacity is made among the control beam CB2, SB15 (strengthened with four layers continuous U-wrap with 90^0 fiber direction with rectangular shape web opening) and SB16 (strengthened with four layers continuous U-wrap with 90^0 fiber direction with rectangular shape web opening with end anchorage) and is presented in Figure 4.68. It is noticed that the ultimate load carrying capacity of SB16 is 35.09% higher than the control beam CB2 and is 14.07% higher than the beam SB15.

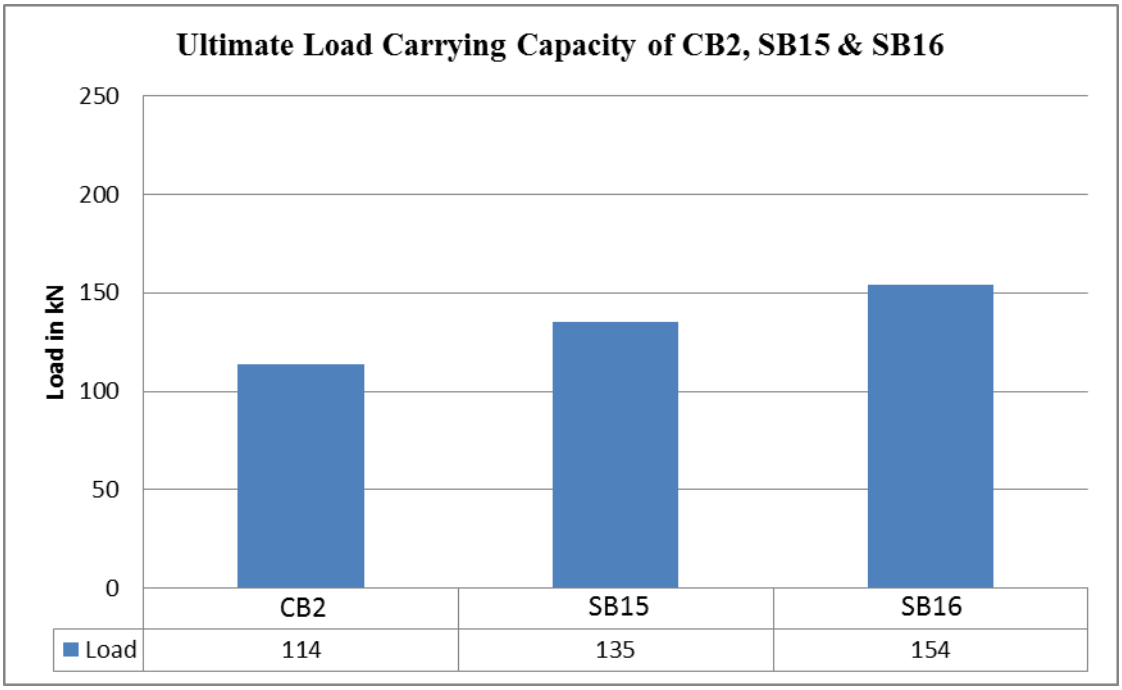

Figure 4.68 Ultimate load carrying capacity of beams CB2, SB15 and SB16

The ultimate load carrying capacity of the control beam CB3, SB17 (strengthened with four layers continuous U-wrap with 90^0 fiber direction with square shape web opening) and SB18 (strengthened with four layers continuous U-wrap with 90^0 fiber direction with square shape web opening with end anchorage) beams are compared and is depicted in Figure 4.69. It is revealed that the ultimate load carrying capacity of SB18 is 36.67% higher than the control beam CB3 and is 13.89% higher than the beam SB17.

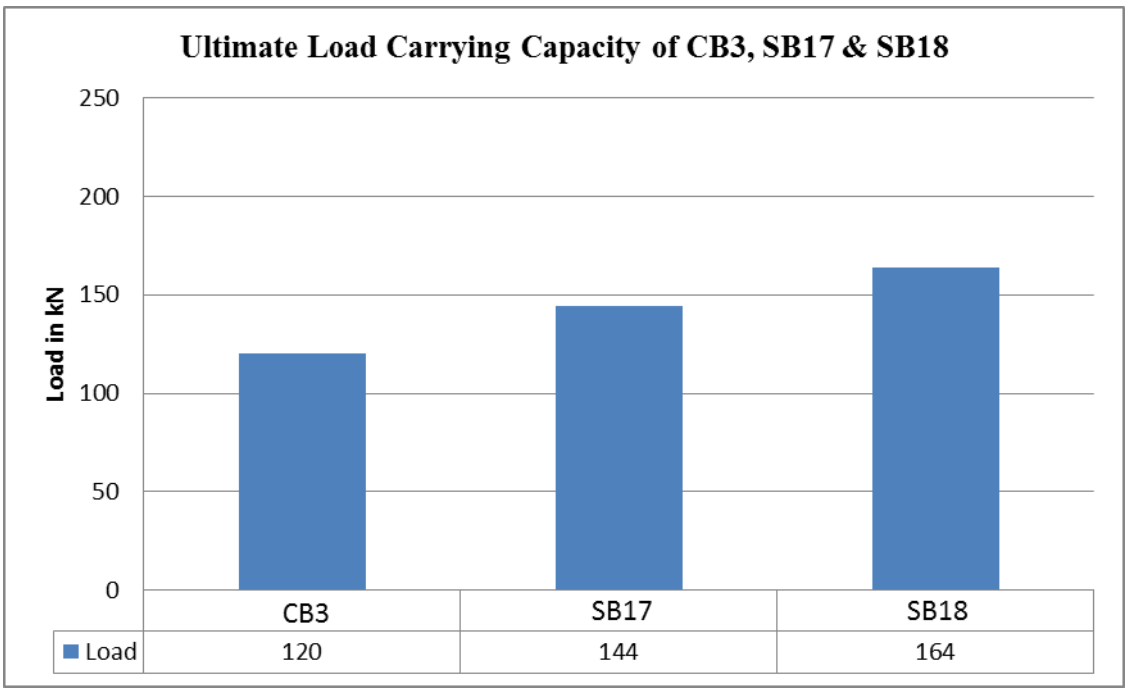

Figure 4.69 Ultimate load carrying capacity of beams CB3, SB17 and SB18

Among the beams SB13 (strengthened with four layers continuous U-wrap with 90^0 fiber direction with circular shape web opening), SB15 (strengthened with four layers continuous U-wrap with 90^0 fiber direction with rectangular shape web opening) and SB17 (strengthened with four layers continuous U-wrap with 90^0 fiber direction with square shape web opening), the ultimate load carrying capacity of SB17 is 9.09% and 6.67% higher than SB13 and SB15, respectively and is shown in Figure 4.70.

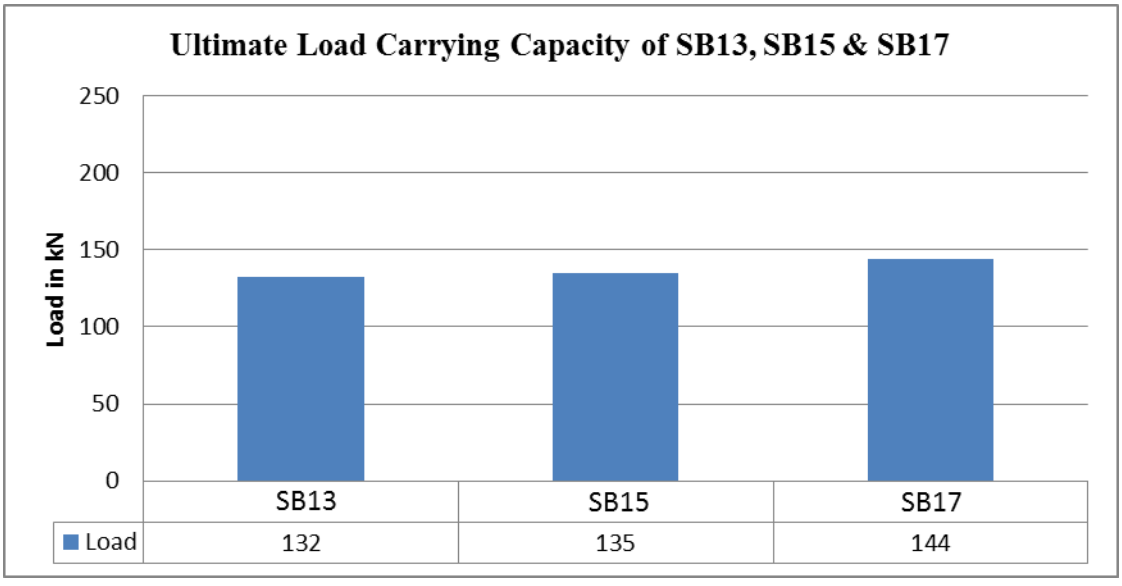

Figure 4.70 Ultimate load carrying capacity of beams SB13, SB15 and SB17

A comparison in ultimate load carrying capacity is drawn among the beams SB14 (strengthened with four layers continuous U-wrap with 90^0 fiber direction with circular shape web opening with end anchorage), SB16 (strengthened with four layers continuous U-wrap with 90^0 fiber direction with rectangular shape web opening with end anchorage) and SB18 (strengthened with four layers continuous U-wrap with 90^0 fiber direction with square shape web opening with end anchorage) and is given in Figure 4.71. It is observed that the ultimate load carrying capacity of SB18 is 1.23% higher than the beam SB14 and is 6.49% higher than the beam SB16.

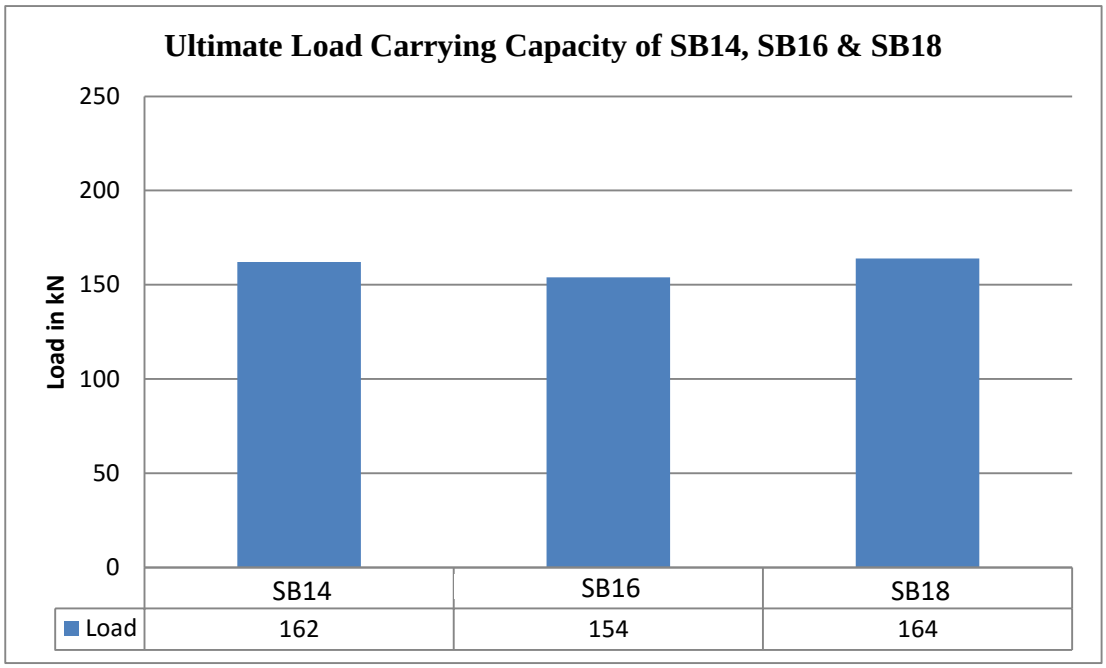

Figure 4.71 Ultimate load carrying capacity of beams SB14, SB16 and SB18

From the above comparisons, it is observed that the shear capacity of the beams strengthened with BFRP sheets/strips is higher than the beam without FRP strengthening. There is an appreciable increase in the ultimate shear carrying capacity of the beam with the introduction of new anchorage system. There is also a considerable improvement in the shear capacity observed for the beams with web opening by using the end anchorage. The ultimate load carrying capacities of all the beams along with the nature of failure are summarized in Table 4.1. The ratio of ultimate load carrying capacity of strengthened beam to control beam are computed for Series A & B and presented in Table 4.1. From the Table, it is observed that the ratio is highest for the beam SB11 (strengthened with four layers continuous U-wrap with end anchorage) in Series A.

The crack patterns and failure modes have been observed for all the beams. It is observed that all the tested beams predominantly failed in shear exhibiting a wider shear crack. The bending-shear crack pattern has not been observed in any tested beams.

It is observed from the curves 4.56-4.62 that, the percentage increase in the load carrying capacity is within 25%. This is due to the premature failure of the BFRP sheets i.e. due to the debonding of the BFRP sheets from the concrete surface, hence full strength of the BFRP has not been utilised. But, it is observed from the curve 4.63-4.69 that the increase in the load carrying capacity is within 62%. This effect is due to the use of anchorage system, which prevents the debonding of the BFRP sheets from the concrete surface. From the curves 4.70-4.71, it is noticed that, the percentage increase in load carrying capacity is within 10%. This is due to the effect of different shapes of the transverse holes.

In the cited literature [43], shear strengthening of RC T-beams using woven GFRP sheets with circular web openings have been studied. From the literature it has been observed that by using woven GFRP sheets provided with anchorage system the percent increase in the ultimate load carrying capacity is only 8.60% as compared to the beam with GFRP sheets without anchorage system. In the present study, different types of transverse web openings have been studied, such as circular, rectangular and square. For circular web opening, it is observed that, there is 22.67% increase in the load carrying capacity for the beam strengthened with BFRP sheets with anchorage system as compared to the beam strengthened with BFRP sheets without anchorage system. But, in the present research work, unidirectional BFRP sheets have been used throughout the experiment. Hence, it cannot be compared with the cited literatures in which woven GFRP have been used.

In the present research work circular, rectangular and square shape transverse holes having same cross-sectional area have been considered. The diameter of the circular hole is 7cm and the size of the rectangular and square holes are 8cmx4.8cm and 6.2cmx6.2cm respectively. Since circular hole has a greater depth as compared to the other shapes of holes, it is more susceptible to failure and the load carrying capacity of the beams with rectangular and square holes is higher than the beam with circular hole. The load carrying capacity of beam with a rectangular hole is lower than that of the beam with a square hole as the edge of the rectangular opening is closer to the support.

Table 4.1 Ultimate load and nature of failure for various beams

Beam ID	Nature of Failure	P_u (kN)	$\lambda = \frac{P_u(Strengthened\ Beam)}{P_u(Control\ Beam)}$
CB	Shear failure	158	-
SB1	Splitting and Debonding of BFRP + Shear failure	178	1.13
SB2	Splitting and Debonding of BFRP + Shear failure	167	1.06
SB3	Debonding of BFRP + Shear failure	170	1.08
SB4	Debonding of BFRP + Shear failure	163	1.03
SB5	Splitting and Debonding of BFRP + Shear failure	200	1.27
SB6	Splitting and Debonding of BFRP + Shear failure	175	1.11
SB7	Debonding of BFRP + Shear failure	185	1.17
SB8	Debonding of BFRP + Shear failure	166	1.05
SB9	Debonding of BFRP + Shear failure	192	1.21
SB10	Tearing of BFRP + Shear failure	219	1.39
SB11	Tearing of BFRP + Shear failure	232	1.47
SB12	Tearing of BFRP + Shear failure	200	1.27
CB1	Shear failure	100	-
SB13	Debonding of BFRP + Shear failure	132	1.32

SB14	Tearing of BFRP + Shear failure	162	1.62
CB2	Shear failure	114	-
SB15	Splitting and Debonding of BFRP + Shear failure	135	1.18
SB16	Tearing of BFRP + Shear failure	154	1.35
CB3	Shear failure	120	-
SB17	Splitting and Debonding of BFRP + Shear failure	144	1.2
SB18	Tearing of BFRP + Shear failure	164	1.37

CHAPTER 5

5 ANALYTICAL STUDY

5.1 General

The design approaches proposed by ACI 440.2R-02 and Chen & Teng's model [13, 14] are used for the prediction of the contribution of externally bonded BFRP sheets for the shear resistance of RC T-beams and is presented in this chapter. The shear strength of Reinforced Concrete (RC) T-beams is obtained analytically for varying degree of FRP strengthening and compared with the experimental findings.

5.2 Shear Strength of RC T-Beams Strengthened with FRP Reinforcement using Chen & Teng Model

According to the design approach proposed by ACI 440.2R-02 [1], the nominal shear strength of RC beams strengthened with externally bonded FRP sheets is computed by adding the contribution of the FRP sheet to the contribution of steel (stirrups, ties or spirals) and concrete as given in equation (1).

$$V_n = V_c + V_s + V_{FRP} \quad (1)$$

The design shear strength is expressed as follows.

$$\phi V_n = \phi\,(V_c + V_s + \psi_f V_{FRP}) \quad (2)$$

where, V_c = contribution of concrete; V_s = contribution of shear reinforcement; and

V_{FRP} = contribution of FRP.

ψ_f is an additional reduction factor applied to the shear contribution of FRP sheet. For bond-critical shear reinforcement, an additional reduction factor of 0.85 is recommended. The strength reduction factor (ϕ) of 0.85 is given in ACI 318-95. V_c and V_s are computed as per ACI code guidelines. V_{FRP} is evaluated using the Chen and Teng's models for FRP debonding [13] and rupture [14].

The contribution of FRP to the shear capacity can be expressed as:

$$V_{FRP} = 2 f_{FRP,e} t_{FRP} w_{FRP} \frac{h_{FRP,e}(\cot\theta + \cot\beta)\sin\beta}{s_{FRP}} \quad (3)$$

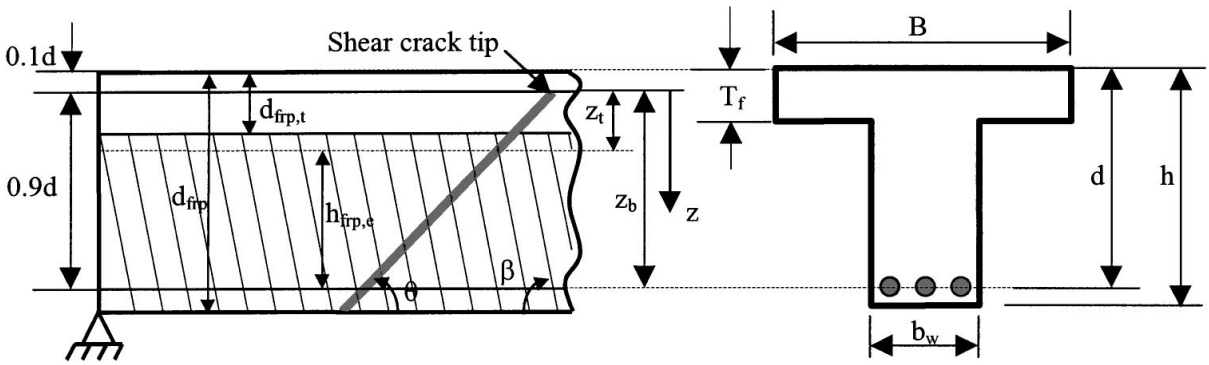

Figure 5.1 Notation for general shear strengthening scheme, Chen and Teng [13, 14]

where, t_{FRP}=thickness of FRP; w_{FRP} =width of each individual FRP strip (perpendicular to fibre orientation); β=angle of fibres in the FRP measured from the longitudinal axis of the beam.

The effective height of FRP on the sides of the beam is calculated from Eq. (4)

$$h_{FRP,e} = Z_{b-}Z_t \tag{4}$$

where, Z_t and Z_b are the co-ordinates of the top and bottom ends of the effective FRP.

Z_t and Z_b may be expressed as:

$$Z_t = \left(0.1d + d_{FRP,t}\right) - 0.1d = d_{FRP,t} \tag{5}$$

$$Z_b = [d_{FRP} - (h - d)] - 0.1d = 0.9d - (h - d_{FRP}) \tag{6}$$

where, $d_{FRP,t}$= distance from the concrete compression face to the actual upper edge of the FRP (thus $d_{FRP,t}$= 0 for wrapping); and d_{FRP} is the distance from the compression face to the lower edge of the FRP ($d_{FRP} = h$ for U jackets).

For unidirectional continuous FRP plates/sheets:

$$S_{FRP} = \frac{w_{FRP}}{\sin\beta} \tag{7}$$

5.2.1 Effective or average stress in the FRP (FRP Debonding)

The effective or average stress in the FRP intersected at the ultimate limit state, $f_{FRP,e}$ can be defined as

$$f_{FRP,e}=D_{FRP}\sigma_{FRP,max} \tag{8}$$

where,

$$D_{FRP} = \begin{cases} \frac{2}{\pi\lambda}\frac{1-\cos\frac{\pi}{2}\lambda}{\sin\frac{\pi}{2}\lambda} & \text{if } \lambda \leq 1 \\ 1-\frac{\pi-2}{\pi\lambda} & \text{if } \lambda>1 \end{cases} \tag{9}$$

Eq. (9) is applicable to both U jackets and side strips/plates.

and

$$\sigma_{FRP,max} = min\begin{cases} f_{frp} \\ 0.427\beta_w\beta_L\sqrt{\frac{E_{frp}\sqrt{f_c'}}{t_{frp}}} \end{cases} \quad (10)$$

where, β_L reflects the effect of bond length and β_w the effect of FRP-to-concrete width ratio of the shear test specimen.

The bond length coefficient β_L can be expressed as

$$\beta_L = \begin{cases} 1 & \text{if } \lambda \geq 1 \\ \sin\frac{\pi\lambda}{2} & \text{if } \lambda < 1 \end{cases} \quad (11)$$

in which the normalized maximum bond length λ is defined as

$$\lambda = \frac{L_{max}}{L_e} \quad (12)$$

where, L_e is the effective bond length and can be expressed as

$$L_e = \sqrt{\frac{E_{frp}t_{frp}}{\sqrt{f_c'}}} \quad (13)$$

The maximum bond length L_{max} is given by

$$L_{max}\begin{cases} \frac{h_{frp,e}}{\sin\beta} & for\ U\ jackets \\ \frac{h_{frp,e}}{2\sin\beta} & for\ side\ plates \end{cases} \quad (14)$$

The strip width coefficient β_W can thus be expressed as

$$\beta_W = \frac{2-w_{FRP}/(s_{FRP}h_{frp,e})}{1+w_{FRP}/(s_{FRP}\sin\beta)} \quad (15)$$

5.2.2 Effective or average stress in the FRP (FRP Rupture)

The effective or average stress in the FRP intersected by a shear crack at the ultimate limit state, $f_{FRP,e}$ is only a fraction of the tensile strength f_{FRP}

$$f_{FRP,e}=D_{FRP}f_{FRP} \quad (16)$$

where, D_{FRP} is defined as the stress (or strain) distribution factor.

The FRP strain increases linearly from zero at the crack tip to a maximum at the lower end.

The strain distribution factor is defined by the equation (17).

$$D_{FRP} = \frac{1+\zeta}{2} \quad (17)$$

where, $\zeta = \frac{Z_t}{Z_b}$ =coordinate ratio of the upper edge to the lower edge of the effective FRP.

For strengthening schemes in which FRPs are bonded over the full height of the sides (e.g. wrapping), $\zeta = 0$ so $D_{FRP} = 0.5$

5.3 Analytical Calculations

The shear strength of the control beam and two strengthened beams (one failed by debonding while other failed by rupture) are computed and presented below.

Control Beam (CB):

The shear contribution of the concrete and steel are given below.

$$V_c = \frac{\sqrt{f_c'}}{6} b_w d = \frac{\sqrt{18.48}}{6 \times 1000} \times 150 \times 140 = 15.05kN$$

$V_s = \frac{A_s f_y d}{s} = 0$ (For no shear reinforcement in the beam)

$V_n = V_c + V_s = 15.05 + 0 = 15.05kN$

$\emptyset V_n = 0.85(15.05) = 12.79kN$

Strengthened Beam failed by debonding (SB5):

The shear contribution of the concrete and steel are given below.

$$V_c = \frac{\sqrt{f_c'}}{6} b_w d = \frac{\sqrt{22.4}}{6 \times 1000} \times 150 \times 140 = 16.565kN$$

$V_s = \frac{A_s f_y d}{s} = 0$ (For no shear reinforcement in the beam)

Shear contribution of the FRP:

The effective height of FRP on the sides of the beam,

$h_{FRP,e} = Z_b - Z_t$

$Z_t = d_{FRP,t} = 50mm$

$Z_b = 0.9d - (h - d_{FRP}) = 0.9d = 126mm$ ($d_{FRP} = h$ For U jackets)

$h_{FRP,e} = Z_b - Z_t = 76mm$

For continuous vertical oriented ($\beta = 90^0$)

$S_{FRP} = \frac{w_{FRP}}{\sin\beta} = 1000mm$

Effective or average stress in the FRP (FRP Debonding)

Maximum bond length, $L_{max} = \frac{h_{frp,e}}{\sin\beta} = 76mm$ (For U jackets)

$E_{frp} = 11.920GPa \quad t_{frp} = 0.56mm$

Effective bond length, $L_e = \sqrt{\frac{E_{frp}t_{frp}}{\sqrt{f_c'}}} = 37.55mm$

Normalized maximum bond length $\lambda = \frac{L_{max}}{L_e} = 2.02$

β_L=1 for $\lambda \geq 1$

β_w=$\frac{\sqrt{2}}{2} = 0.707$ For continuous sheets/plates

$D_{FRP} = 1 - \frac{\pi - 2}{\pi\lambda}$ if λ>1

$= 0.82$

$$\sigma_{FRP,max} = min\begin{cases} f_{frp} \\ 0.427\beta_w\beta_L\sqrt{\frac{E_{frp}\sqrt{f_c'}}{t_{frp}}} \end{cases}$$

$$= \min\begin{cases} 328 \\ 0.427 \times 0.707 \times 1\sqrt{\frac{11920\times\sqrt{22.4}}{0.56}} \end{cases}$$

$= 95.83MPa$

$f_{FRP,e}$=$D_{FRP}\sigma_{FRP,max} = 0.82 \times 95.83 = 78.58MPa$

$V_{FRP} = 2f_{FRP,e}t_{FRP}w_{FRP}\frac{h_{FRP,e}(\cot\theta + \cot\beta)\sin\beta}{s_{FRP}}$

$V_{FRP} = 2 \times 78.58 \times 0.56 \times 1000 \times \frac{76 \times (\cot 0 + \cot 90)\sin 90}{1000}$

$= 6.69kN$

$\emptyset V_n = 0.85(16.565 + 0) + 0.7(6.69) = 18.76kN$

<u>Strengthened Beam failed by rupture (SB10):</u>

The shear contribution of the concrete and steel are given below.

$V_c = \frac{\sqrt{f_c'}}{6}b_w d = \frac{\sqrt{22.664}}{6 \times 1000} \times 150 \times 140 = 16.66kN$

$V_s = \frac{A_s f_y d}{s} = 0$ (For no shear reinforcement in the beam)

Shear contribution of the FRP:

The effective height of FRP on the sides of the beam,

$h_{FRP,e} = Z_{b-}Z_t$

$Z_t = d_{FRP,t} = 50mm$

$Z_b = 0.9d - (h - d_{FRP}) = 0.9d = 126mm$ ($d_{FRP} = h$ For U jackets)

$h_{FRP,e} = Z_{b-}Z_t = 76mm$

Effective or average stress in the FRP (FRP Rupture)

$$D_{FRP} = \frac{1+\zeta}{2}$$

Where, $\zeta = \frac{Z_t}{Z_b}$ = 0.397

$$D_{FRP} = \frac{1+\zeta}{2} = 0.698$$

$f_{FRP,e} = D_{FRP} f_{FRP} = 0.698\ X\ 328 = 228.94MPa$

$$V_{FRP} = 2 \times 228.94 \times 0.56 \times 1000 \times \frac{76 \times (\cot 0 + \cot 90) \sin 90}{1000}$$

$$= 19.49kN$$

$\emptyset V_n = 0.85(16.66 + 0) + 0.7(19.49) = 27.804kN$

In the similar way, the shear strength of the remaining beams can be calculated and the shear contribution of FRP for all the strengthened beams is given in Table 5.1 along with the failure modes. It is observed from the Table 5.1 that end anchored U jacketing appeared to be the most efficient method of strengthening scheme compared to other schemes. U jacketing is more effective than side bonding. In shear strengthening inclined U-strip is more effective than horizontal and vertical strip.

Table 5.1 Contribution of FRP to the shear capacity (V_{FRP})

Specimen	FRP Thickness t_{FRP} (mm)	FRP Effective height $h_{FRP,e}$ (mm)	Stress distribution factor D_{frp}	Effective FRP stress $f_{frp,e}$	Strengthening scheme	V_{FRP} (kN)	Mode of failure
SB1	0.56	76	1	13.86	Horizontal continuous sheet U jacketing	1.18	Splitting + Debonding
SB2	0.56	41	1	13.86	Horizontal continuous sheet side bonded	0.636	Splitting + Debonding
SB3	0.56	76	1	13.86	Horizontal strip U jacketing	1.18	Debonding
SB4	0.56	41	1	13.86	Horizontal strip side bonded	0.636	Debonding
SB5	0.56	76	0.82	78.63	Vertical continuous sheet U jacketing	6.693	Splitting + Debonding
SB6	0.56	41	0.532	37.84	Vertical continuous sheet side bonded	1.738	Splitting + Debonding
SB7	0.56	76	0.817	76.935	vertical strip U jacketing	6.549	Debonding

SB8	0.56	41	0.531	36.238	Vertical strip side bonded	1.664	Debonding
SB9	0.56	76	0.873	58.304	Inclined strip U jacketing	7.02	Debonding
SB10	0.56	76	0.698	228.94	Vertical continuous sheet U jacketing with anchorage	19.49	Rupture
SB11	1.07	76	0.698	228.94	Vertical continuous sheet U jacketing with anchorage	37.23	Rupture
SB12	0.56	76	0.698	228.94	Vertical strip U jacketing with anchorage	19.49	Rupture

5.4 Comparison of experimental results with analytical predictions:

The shear strength of the beams strengthened with BFRP sheets obtained from the experimental study is compared to the design shear strength predicted analytically. Different nomenclatures used in Table 5.2 are explained below for clarity.

$V_{n,test}$ = Total nominal shear strength by test,

$V_{c,test}$ = nominal shear strength provided by concrete obtained from test,

$V_{s,test}$ = nominal shear strength provided by steel shear reinforcement obtained from test,

$V_{f,test}$ = nominal shear strength provided by shear reinforcement obtained from test,

$V_{n,ana}$ = nominal shear strength calculated analytically,

$V_{c,ana}$= nominal shear strength provi1ded by concrete analytically,

$V_{s,ana}$= nominal shear strength provided by steel shear reinforcement analytically,

$V_{f,ana}$ = nominal shear strength provided by BFRP shear reinforcement analytically.

The nominal and design shear strength of all the strengthen beams and control beam along with the experimental results are tabulated in Table 5.2.

Table 5.2 Comparisons of experimental and predicted shear strength results

Specimen	Experimental Results					Predicted analytical Results			
	Load at failure	$V_{n,test}$ (kN)	$V_{c,test}$ (kN)	$V_{s,test}$ (kN)	$V_{f,test}$ (kN)	$V_{c,ana}$ (kN)	$V_{f,ana}$ (kN)	$V_{s,ana}$ (kN)	$\phi V_{n,ana}$ (kN)
CB	158	79	79	0	-	15.05	-	0	12.792
SB1	178	89	79	0	10	15.737	1.18	0	14.202
SB2	167	83.5	79	0	4.5	15.55	0.636	0	13.663
SB3	170	85	79	0	6	15.44	1.18	0	13.95
SB4	163	81.5	79	0	2.5	15.13	0.636	0	13.306
SB5	200	100	79	0	21	16.565	6.693	0	18.765
SB6	175	87.5	79	0	8.5	16.21	1.738	0	14.995
SB7	185	92.5	79	0	13.5	15.98	6.549	0	18.167
SB8	166	83	79	0	4	15.48	1.664	0	14.323
SB9	192	96	79	0	17	16.57	7.02	0	18.998
SB10	219	109.5	79	0	30.5	16.66	19.49	0	27.804
SB11	232	116	79	0	37	16.83	37.23	0	40.366
SB12	200	100	79	0	21	16.565	19.49	0	27.723

It is observed from the literature [41, 43] that the analytical model using ACI guidelines predicts over conservative results. Similar observations are also made in the present study as illustrated in Table 5.2.

CHAPTER 6

6 CONCLUSIONS

6.1 Summary

The main objective of the present investigation is to study the contribution of basalt fiber reinforced polymer (BFRP) composites on the shear capacity of the T-shaped cross-section RC beams externally strengthened with BFRP composites with and without transverse web openings and also to study the effect of a new mechanical anchorage system comprising of BFRP laminated composite plates with nuts and bolts arrangement on the shear capacity of RC T-beams. Twenty two numbers of beams divided into two Series (A and B) are tested under four-point static loading system up to failure. The first series of tests, series A, discusses about the shear strengthening of the RC T-beams without transverse openings. The second series B, focuses on the shear strengthening of the RC T-beams with transverse openings of different shapes. In each series, one beam is not strengthened with BFRP and considered as control beam, whereas all other beams are strengthened with externally bonded unidirectional BFRP sheets in the shear zone of the beams. The effect of various test parameters such as fiber amount and distribution, bonded surface, number of layers, fiber orientation, different shape of transverse web openings and end anchorage on the shear capacity of RC T-beams externally strengthened with BFRP composites are investigated.

6.2 Novelty of the present work

A good number of studies have been carried out on the shear strengthening of RC T-beams using glass and carbon fibres but no work has been reported on the shear strengthening of RC beams with T-section using externally bonded Basalt Fiber Reinforced Polymer sheets/strips. Basalt fiber is a relatively new fiber introduced in the construction industry and its cost is comparable with that of glass fiber. It exhibits high corrosion resistant and chemical durability. It has also higher thermal stability as compared to glass fibers.

To accommodate essential services like electricity cables, natural gas pipes, water and drainage pipes, air-conditioning, telephone lines, and computer network, the transverse web openings are necessary in modern building construction. Works on potential use of FRP strengthening RC T-beams with web openings are scanty in the open literature. The potential

use of FRP composite in strengthening the RC T-beams with web openings is explored in the present study.

The debonding failure of the FRP strengthened beam is a major issue for the research engineers. Due to debonding failure, the full strength of the FRP is not utilized. Hence, an attempt has been taken in this study to prevent premature failure of the FRP sheets. Steel plates can be used as end anchorage to prevent the debonding, but it is susceptible to corrosion. So, the laminated composite plate is used as end anchorage in place of the steel plate in this study.

6.3 Conclusions

Based on the experimental investigation and analytical study of shear strengthening of RC T-beams with externally bonded unidirectional BFRP composites, the following conclusions are drawn:

- The shear capacity of RC beams with T-shaped cross-section can be enhanced significantly by using BFRP composites as an external reinforcement.
- The initial cracks in the strengthened beams are formed at a higher load compared to the ones in the control beams.
- Strengthening with BFRP composites bonded to webs only are most susceptible to debonding with premature failure.
- The beam strengthened with BFRP sheets is found to have more shear capacity than the beam strengthened with BFRP strips.
- Strengthening of beams using U-wrap configuration is found to be more effective than the side-wrap configuration.
- Among all the BFRP strip configurations (i.e., horizontal strips, vertical strips and strips inclined at 45^0), the U-strip with 45^0 fiber orientations is more effective.
- The performance of externally bonded BFRP composites can be improved significantly by using adequate anchoring system.
- A proportional increase in the shear capacity with the increasing BFRP amount cannot be achieved when debonding is not prevented.
- Anchorage system prevents the debonding of BFRP sheets/strips from the concrete surface, eliminating the premature failure, which consequently results in a better utilization of the full strength of the BFRP sheet/strip.

- Formation of crack gets delayed due to the use of BFRP sheets and also by introduction of end anchorage.
- U-wrap with end anchorage is found to be the most effective configuration among all the configurations.
- The load carrying capacity of the strengthened beams are found to be greater than that of the control beams, thus the externally bonded BFRP composites enhances the load carrying capacity.
- The shear strength of the T-beam strengthened with the U - wrap is found to be more in case of the beam without transverse web openings.
- The T-beam with transverse web openings strengthened with anchored U-wrap performs superior than the beam without anchorage.
- Among different shapes of transverse web openings, square hole is found to be more effective as compared to other ones.
- The analytical model based on ACI guidelines and Chen and Teng's model predicts conservative results compared to experimental ones.
- Finally, BFRP composite is proven to be a promising material for shear strengthening of RC T-beams with or without opening.

6.4 Recommendations for Future Studies

Based on the finding and conclusions of the present study, the following recommendations are made for further research in FRP shear strengthening:

- Study of the bond mechanism between BFRP composite and concrete substrate.
- FRP strengthening of RC T-beams using carbon and aramid composites.
- Strengthening of RC T-beams using woven basalt fiber.
- Strengthening of RC L-section beams with FRP composites.
- Strengthening of RC L-section beams with transverse web openings.
- Effect of transverse web openings of different shape and size on the shear behaviour of RC L-section beams.
- Effects of shear span to effective depth ratio on the shear capacity of beams.
- Numerical modelling of RC T & L-beams strengthened with FRP sheets with end anchorage.

REFERNCES

1) ACI 440.2R-02, "Guide for the Design and Construction of Externally Bonded FRP Systems for Strengthening Concrete Structures", Reported by ACI Committee 440.
2) Ahmed A., Fayyadh M. M., Naganathan S., and Nasharuddin K. (2012), "Reinforced concrete beams with web openings: A state of the art review", Materials and Design, 40, 90-102.
3) Al-Amery R., and Al-Mahaidi R. (2006), "Coupled flexural-shear retrofitting of RC Beams using CFRP straps", Construction and Building Materials, 21, 1997-2006.
4) Alex L., Assih J., and Delmas Y. (2001), "Shear Strengthening of RC Beams with externally bonded CFRP sheets", Journal of Structural Engineering, 127(4), 20516.
5) Balamurali krishnan R., and Jeyasehar C. A. (2009), "Flexural behaviour of RC beams strengthened with Carbon Fiber Reinforced Polymer (CFRP) fabrics", The Open Civil Engineering Journal, 3, 102-109.
6) Bousselham A., and Chaallal O. (2006), "Behaviour of Reinforced Concrete T-beams strengthened in shear with carbon fiber-reinforced polymer –An Experimental Study", ACI Structural Journal, 103(3), 339-347.
7) Bukhari I. A., Vollum R. L., Ahmad S., and Sagaseta J. (2010), "Shear strengthening of reinforced concrete beams with CFRP", Magazine of Concrete Research, 62(1), 65-77.
8) Cao S. Y., Chen J. F., Teng J. G., Hao Z., and Chen J. (2005), "Debonding in RC Beams Shear Strengthened with completely FRP wraps", Journal of Composites for Construction, 9(5), 417-428.
9) Ceroni F. (2010), "Experimental performances of RC beams strengthened with FRP materials", Construction and Building materials, 24, 1547-1559.
10) Chaallal O., Nollet M. J., and Perraton D. (1998), "Strengthening of reinforced concrete beams with externally bonded fibre-reinforced-plastic plates: design guidelines for shear and flexure", Canadian Journal of Civil Engineering, 25(4), 692-704.
11) Chajes M. J., Januszka T. F., Mertz D. R., Thomson T. A., and Finch W. W. (1995), "Shear strengthening of Reinforced Concrete beams using externally applied composite fabrics", ACI Structural Journal, 92(3), 295-303.

12) Chen C. C., Li C. Y., and Kuo M. C. (2008), "Experimental Study of Steel Reinforced Concrete Beams with Web Openings", The 14th World Conference on Earthquake Engineering, 14WCEE.

13) Chen J. F., and Teng J. G. (2003), "Shear capacity of FRP-strengthened RC beams: FRP debonding", Construction and Building Materials, 17, 27-41.

14) Chen J. F., and Teng J. G. (2003), "Shear capacity of Fiber-Reinforced Polymer-strengthened Reinforced Concrete Beams: Fiber Reinforced Polymer Rupture", Journal of Structural Engineering, ASCE, 129(5), 615-625.

15) Deifalla A., and Ghobarah A. (2010), "Strengthening RC T beams subjected combined torsion and shear using FRP fabrics: Experimental Study", Journal of Composites for Construction, ASCE, 301-311.

16) Dias S. J. E., and Barros J. A. O. (2010), "Performance of reinforced concrete T beams strengthened in shear with NSM CFRP laminates", Engineering Structures, 32, 373-384.

17) Duthinh D. and Starnes M. (2001), "Strengthening of RC beams with CFRP: Experimental results versus prediction of codes of practice", Journal of Composites for Construction, 16,185-195.

18) Esfahani M. R., Kianoush M. R., and Tajari A. R. (2007), "Flexural behaviour of reinforced concrete beams strengthened by CFRP sheets", Engineering Structures, 29, 2428–2444.

19) Ghazi J. A. S., Alfarabi S., Istem A. B., Mohhamed H. B., and Bader N. G. (1994), "Shear Repair for Reinforced Concrete by Fiberglass Plate Bonding", ACI Structural Journal, 91(4), 458-464.

20) Hadi M. N. S. (2003), "Retrofitting of shear failed reinforced concrete beams", Composite Structures, 62, 1-6.

21) Islam M. R., Mansur M. A., and Maalej M. (2005), "Shear strengthening of RC deep beams using externally bonded FRP systems", Cement & Concrete Composites, 27, 413–420.

22) Kachlakev D., and McCurry D. D. (2000), "Behaviour of full-scale reinforced concrete beams retrofitted for shear and flexure with FRP laminates", Composites: Part B, 31, 445-452.

23) Khalifa A., and Antonio N. (2002), "Rehabilitation of rectangular simply supported RC beams with shear deficiencies using CFRP composites", Construction and Building Materials, 16(3), 135-146.

24) Khalifa A., Belarbi A., and Antonio N. (2000), "Shear performance of RC members strengthened with externally bonded FRP wraps", 12WCEE.

25) Khalifa A., Gold W. J., Nanni A., and Aziz A. (1998), "Contribution of externally bonded FRP to shear capacity of RC flexural members", Journal of Composites for Construction, 2, 195–201.

26) Khalifa A., Lorenzis L. D., and Nanni A. (2000), "FRP composites for shear strengthening of RC beams", Proceedings, 3rd International Conference on Advanced Composite Materials in Bridges and Structures, 137-144, 15-18 Aug.

27) Khalifa A., and Nanni A. (2000), "Improving shear capacity of existing RC T-section beams using CFRP composites", Cement & Concrete Composites, 22, 165-174.

28) Kim G., Sim J., and Oh H. (2008), "Shear strength of strengthened RC beams with FRPs in shear", Construction and Building Materials, 22, 1261–1270.

29) Lee H. K., Cheong S. H., Ha S. K., and Lee C. G. (2010), "Behaviour and performance of RC T-section deep beams externally strengthened in shear with CFRP sheets", Composite Structures, 93(2), 911-922.

30) IS: 456-2000, "Plain and Reinforced Concrete - Code of Practice ", Bureau of Indian Standards.

31) IS: 383-1970, "Specification for Coarse and Fine Aggregates from natural sources for Concrete", Bureau of Indian Standards.

32) IS: 1786-1985, "Specification for high strength deformed steel bars and wires for concrete reinforcement", Bureau of Indian Standards.

33) Maaddawy T. E., and Sherif S. (2009), "FRP composites for shear strengthening of reinforced concrete deep beams with openings", Composite Structures, 89, 60–69.

34) Mansur M. A. (1998), "Effect of openings on the Behaviour and Strength of RC Beams in Shear", Cement and Concrete Composites, 20, 477-486.

35) Mansur M. A. (2006), "Design of reinforced concrete beams with web openings", Proceedings of the 6th Asia-Pacific Structural Engineering and Construction Conference (APSEC 2006), Kuala Lumpur, Malaysia, 104-120.

36) Martinola G., Meda A., Plizzari G. A., and Rinaldi Z. (2010), "Strengthening and repair of RC beams with fiber reinforced concrete", Cement & Concrete Composites, 32, 731–739.

37) Mosallam A. S., and Banerjee S. (2007), "Shear enhancement of reinforced concrete beams strengthened with FRP composite laminates", Composites: Part B, 38, 781-793.

38) Norris T., Saadatmanesh H., and Ehsani M. R. (1997), "Shear and Flexural strengthening of RC beams with carbon fiber sheets", Journal of Structural Engineering, 123, (7).

39) Obaidat Y. T., Heyden S., Dahlblom O., Farsakh G. A. and Jawad Y. A. (2011), "Retrofitting of reinforced concrete beams using composite laminates", Construction and Building Materials, 25, 591–597.

40) Ozgur A. (2008), "Strengthening of RC T-section beams with low strength concrete using CFRP composites subjected to cyclic load", Construction and Building Materials, 22, 2355–2368.

41) Panda K. C., Bhattacharyya S. K., and Barai S.V. (2011), "Shear strengthening of RC T-beams with externally side bonded GFRP sheet", Journal of Reinforced Plastics and Composites, 30(13), 1139–1154.

42) Panda K. C., Bhattacharyya S. K., and Barai S.V. (2012), "Shear behaviour of RC T-beams strengthened with U-wrapped GFRP sheet", Steel and Composite Structures, 12(2).

43) Panigrahi A. K., Biswal K. C., and Barik M. R. (2014), "Strengthening of shear deficient RC T-beams with externally bonded GFRP sheets", Construction and Building Materials, 57, 81-91.

44) Pannirselvam N., Nagaradjane V., and Chandramouli K. (2009), "Strength behaviour of fiber reinforced polymer strengthened beam", ARPN Journal of Engineering and Applied Sciences, 4(9), ISSN 1819-6608.

45) Pimanmas A. (2010), "Strengthening R/C beams with opening by externally installed FRP rods: Behaviour and analysis", Composite Structures, 92, 1957–1976.

46) Priestley, M., Seible, F., and Calvi, G. (1996), Seismic Design and Retrofit of Bridges, John Wiley and Sons, New York, N.Y.

47) Rabinovitch O. and Frostig Y. (2003), "Experimental and analytical comparison of RC beams strengthened with CFRP composites", Composites: Part B, 34, 663-677.

48) Saadatmanesh H., and Ehsani M. R. (1992), "RC beams strengthened with GFRP plates: experimental study", Journal of Structural Engineering, 117(11), ISSN 0733-9445/91/0011, Paper No. 26385.

49) Saafan M. A. A. (2006), "Shear strengthening of Reinforced Concrete beams using GFRP wraps", Czech Technical University in Prague Acta Polytechnica, 46(1), 24-32.

50) Santhakumar R., Chandrasekaran E., and Dhanaraj R. (2004), “Analysis of Retrofitted concrete shear beams using Carbon fiber composites”, Electronic Journal of Structural Engineering, 4, 66-74.

51) Serbescu A., Guadagnini M., and Pilakoutas K. (2008),"Applicability of Basalt FRP in strengthening of RC beams”, Fourth International Conference on FRP composites in Civil Engineering (CICE2008).

52) Shanmugamt N. E., and Swaddiwudhipongt S. (1988), “Strength of fiber reinforced concrete deep beams containing openings”, The International Journal of Cement Composites and Lightweight Concrete, 10(1).

53) Siddiqui N. A. (2009), “Experimental investigation of RC beams strengthened with externally bonded FRP composites”, Latin American Journal of Solids and Structures, 6, 343-362.

54) Sheikh S. A., DeRose D., and Mardukhi J. (2002), “Retrofitting of concrete structures for shear and flexure with fiber-reinforced polymers”, ACI Structural Journal, 99(4), 451-459.

55) Sheikh S. A. (2002), “Performance of concrete structures retrofitted with fiber reinforced polymers”, Engineering Structures, 24, 869-879.

56) Spagnuolo D. M., Napadensky E., Sano T., and Wolbert J. P. (2011), “Investigation of Basalt Woven Fabrics for Military Applications”, Army Research Laboratory.

57) Sundarraja M. C., and Rajamohan S. (2009), “Strengthening of RC beams in shear using GFRP inclined strips - an experimental study”, Construction and Building Materials, 23, 856-864.

58) Taljsten B. (2003), “Strengthening concrete beams for shear with CFRP sheets”, Construction and Building Materials, 17, 15-26.

59) Tanarslan H. M., and Altin S. (2009), “Behaviour of RC T-section beams strengthened with CFRP strips, subjected to cyclic load”, Materials and Structures, DOI 10.1617/s11527-009-9509-8.

60) Teng J. G., Lam L., and Chen J.F. (2004), “Shear strengthening of RC beams with FRP composites”, Programme Structural. Engineering Material, 6, 173–184.

61) Triantafillou T. C. (1998a), “Shear strengthening of Reinforced Concrete Beams using Epoxy-Bonded FRP Composites,” ACI Structural Journal, 95(2), 107-115.

62) Varastehpour H., and Hamelin P. (1997), “Strengthening of concrete beams using fiber reinforced plastics”, Materials and Structures, 30, 160-166.

63) Gang W., Jia-Wei S., Wen-Jun J., and Zhi-Shen W. (2013), "Flexural Behaviour of Concrete Beams Strengthened with New Prestressed Carbon-Basalt Hybrid Fiber Sheets", American Society of Civil Engineers, 10.1061/(ASCE)CC.1943-5614.0000452.

64) Gang W., Yi-Hua Z., Zhi-Shen W., and Wu-Qiang F. (2013), "Experimental Study on the Flexural Behaviour of RC Beams Strengthened with Steel-Wire Continuous Basalt Fiber Composite Plates", American Society of Civil Engineers, (ASCE) CC. 1943-5614.0000328.

65) Sahu S. (2014), "Strengthening of Reinforced Concrete Beams using Glass Fiber Reinforced Polymer (GFRP) composite", M.Tech Thesis, NIT, Rourkela.

List of Publications

- S. Routray and K.C. Biswal, "Use of Basalt Fiber as a Strengthening Material: A Review", International conference on Sustainable Civil Infrastructure (ICSCI-2014), (ASCE), 17th & 18th October, 2014 IIT, Hyderabad.
- Routray S., Biswal K.C. and Barik M.R., "Effect of Fiber Orientation on the Mechanical Properties of Fabricated Plate Using Basalt Fiber", Research Journal of Recent Sciences, ISSN 2277-2502, Vol. 4, 202-208 (2015).
- S. Routray, K.C. Biswal and M.R. Barik, "Experimental and Analytical Studies on the Shear Strengthening of RC T-beams using BFRP sheets" (to be communicated).
- S. Routray, K.C. Biswal and M.R. Barik, "Shear Behaviour of RC T-beams with Web openings Strengthened with BFRP composites" (to be communicated).

APPENDIX-I

Design guidelines for shear strengthening of RC beams with FRP

A-1 GENERAL

The strengthening or retrofitting of existing reinforced concrete beams to resist higher design loads is being traditionally carried out using conventional materials and construction techniques such as concrete jacketing, externally bonded steel plates and post tensioning techniques. Recently, the fibre-reinforced polymers (FRP) have emerged as an alternative to conventional materials due to its several superior properties such as lightweight, noncorrosive, high specific modulus, high specific strength.

FRP systems are used to strengthen or restore the strength of a deteriorated RC beam. The field engineers should access the existing load-carrying capacity of the beam and the design load to be taken by the strengthened beam must be determined before application of the FRP strengthening schemes.

The nominal shear strength of RC beams strengthened with externally bonded FRP sheets is given by;

$$V_n = V_c + V_s + V_{FRP} \quad (1)$$

The design shear strength is expressed as;

$$\phi V_n = \phi\,(V_c + V_s + \psi_f V_{FRP}) \quad (2)$$

where, V_c and V_s are the shear capacity of concrete and contribution of shear reinforcement and can be obtained using any standard codes. ψ_f is an additional reduction factor applied to the shear contribution of FRP sheet. The shear to be resisted by the FRP (V_{FRP}) is computed from the equation (2).

The thickness of FRP can be computed from the equation (3);

$$V_{FRP} = 2 f_{FRP,e} t_{FRP} w_{FRP} \frac{h_{FRP,e}(\cot\theta + \cot\beta)\sin\beta}{s_{FRP}} \quad (3)$$

Where, t_{FRP} = thickness of FRP; w_{FRP} =width of the FRP; S_{FRP} = spacing of the FRP strip;

For unidirectional continuous FRP plates/sheets:

$$S_{FRP} = \frac{w_{FRP}}{\sin\beta}$$

β = angle of fibres in the FRP measured from the longitudinal axis of the beam.

$h_{FRP,e}$ = effective height of FRP on the sides of the beam = $Z_{b-}Z_t$.

Z_t = co-ordinates of the top end of the effective FRP = $\left(0.1d + d_{FRP,t}\right) - 0.1d = d_{FRP,t}$.

Z_b = co-ordinates of the bottom end of the effective FRP

= $[d_{FRP} - (h - d)] - 0.1d = 0.9d - (h - d_{FRP})$.

A-2 Effective or average stress ($f_{FRP,e}$) in the FRP (Debonding)

The effective or average stress in the FRP, $f_{FRP,e}$ can be expressed as

$f_{FRP,e}=D_{FRP}\sigma_{FRP,max}$

For U jackets and side strips/plates D_{FRP} is given by;

$$D_{FRP} = \begin{cases} \frac{2}{\pi\lambda}\frac{1-\cos\frac{\pi}{2}\lambda}{\sin\frac{\pi}{2}\lambda} & \text{if } \lambda \leq 1 \\ 1 - \frac{\pi-2}{\pi\lambda} & \text{if } \lambda > 1 \end{cases}$$

$$\sigma_{FRP,max} = min\begin{cases} f_{frp} \\ 0.427\beta_w\beta_L\sqrt{\frac{E_{frp}\sqrt{f_c'}}{t_{frp}}} \end{cases}$$

Where, β_L = effect of bond length = $\begin{cases} 1 & \text{if } \lambda \geq 1 \\ \sin\frac{\pi\lambda}{2} & \text{if } \lambda < 1 \end{cases}$

β_w = effect of FRP-to-concrete width ratio = $\frac{2-w_{FRP}/(s_{FRP}h_{frp,e})}{1+w_{FRP}/(s_{FRP}\sin\beta)}$

$\lambda =$ normalized maximum bond length = $\frac{L_{max}}{L_e}$

L_e = effective bond length = $\sqrt{\frac{E_{frp}t_{frp}}{\sqrt{f_c'}}}$

L_{max} = maximum bond length = $\begin{cases} \frac{h_{frp,e}}{\sin\beta} & for\ U\ jackets \\ \frac{h_{frp,e}}{2\sin\beta} & for\ side\ plates \end{cases}$

A-3 Effective or average stress in the FRP (Rupture)

The effective or average stress in the FRP, $f_{FRP,e}$ can be expressed as

$f_{FRP,e}=D_{FRP}f_{FRP}$

Where, D_{FRP} = stress (or strain) distribution factor = $\frac{1+\zeta}{2}$

$\zeta =$ coordinate ratio of the upper edge to the lower edge of the effective FRP = $\frac{Z_t}{Z_b}$.

The nomenclatures used are defined in the chapter 5.